PEROXYNITRITE AND MITOCHONDRIAL CYTOCHROMES

by

Elisenda Lopez-Manzano

Licenciatura en Quimica, Universitat de Barcelona, Spain, 2003

Submitted to the Graduate Faculty of

The Graduate School of Public Health in partial fulfillment

of the requirements for the degree of

Doctor of Philosophy

University of Pittsburgh

2011

UNIVERSITY OF PITTSBURGH

GRADUATE SCHOOL OF PUBLIC HEALTH

This dissertation was presented

By

Elisenda Lopez-Manzano

It was defended on

March 15th 2011

and approved by

Dissertation Advisor: James Peterson, PhD, Associate Professor, Department of Environmental and Occupational Health, Graduate School of Public Health, University of Pittsburgh

Linda L. Pearce, PhD, Assistant Professor, Department of Environmental and Occupational Health, Graduate School of Public Health, University of Pittsburgh

Bruce R. Pitt, PhD, Professor and Chairman, Department of Environmental and Occupational Health, Graduate School of Public Health, University of Pittsburgh

James P Fabisiak, Ph.D., Assistant Professor, Department of Environmental and Occupational Health, Graduate School of Public Health, University of Pittsburgh

Mark T. Gladwin, MD, Division Chief Director, Division of Pulmonary, Allergy and Critical Care Medicine, School of Medicine, University of Pittsburgh

Michael P. Hendrich, Ph.D., Professor, Department of Chemistry, Carnegie Mellon University

PEROXYNITRITE AND MITOCHONDRIAL CYTOCHROMES

Elisenda Lopez-Manzano, PhD

University of Pittsburgh, 2011

Mitochondrial dysfunction, particularly in relation to electron transport chain (ETC) derived oxidative stress, is widely held to be important in numerous pathologies. However, mitochondrial levels of the bioenergetically critical small inorganic molecules are still debatable or unknown. Nevertheless, investigation of the behavior of the ETC components, individually and collectively, in response to varying the levels of these species is still of considerable importance. This dissertation investigated the reaction of the reduced forms of isolated bovine complex III, cytochrome *c* and complex IV with peroxynitrite in the presence and absence of CO_2. The presence of CO_2 significantly modulates the mechanisms and extent of the cofactor oxidations. The characteristics of peroxynitrite-modified ferricytochrome *c,* prepared in the presence and absence of CO_2, was examined by a variety of spectroscopic methods. In the absence of CO_2, oxidation of the methionine 80 axial heme ligand to methionine sulfoxide results. During complex IV turnover by native ferrocytochrome *c* at low ionic strength increased rates were observed when the peroxynitrite modified cytochrome *c* is added – indicating preferential binding of the modified cytochrome to a high affinity/low activity electron-entry site on the enzyme, directing native ferrocytochrome *c* to bind to a lower affinity/higher activity site. It is unclear that formation of small quantities of either peroxynitrite-modified cytochrome *c* is proapoptotic.

Since it has been hypothesized that superoxide is the limiting reagent in the formation of peroxynitrite, it is of critical important to quantitate its production in mitochondria and cells. The commonly employed molecular probes for superoxide, hydroethidine, and its mitochondrially-targeted derivative, MitoSox™, were shown to undergo reactions with components of the mitochondrial ETC including reduction of complex IV and partial reduction of complex III. The reaction with complex IV accounts for an oxygen (and hence superoxide), independent fluorescent response of MitoSox™ in cultured endothelial cells. However, the cationic ethidium species formed during oxidation of the probes by the ETC enzymes inhibit the normal turnover of complex IV by blocking transfer of electrons from ferrocytochrome *c* to the oxidase. The inhibition of oxidized MitoSox™ under typical assay conditions was substantial at inhibitor levels comparable to the concentration of substrate cytochrome *c*.

Therefore, this work has special public health relevance since it not only reviews the possible mechanisms for oxidative stress in mitochondria but also reassesses the use of MitoSox™ as it is a net generator of superoxide.

TABLE OF CONTENTS

LIST OF TABLES

LIST OF FIGURES

LIST OF EQUATIONS

ABBREVIATIONS AND NOMENCLATURE

$\bullet NO_2$	Nitrogen dioxide radical
2-OH-E^+	2-Hydroxyethidium
ACS	American Chemical Society
ADP	Adenosine diphosphate
Amplex® Red	10-acetyl-3,7-dihydroxyphenoxazine
ANT	Adenine nucleotide translocase
AP	Alkaline Phosphatase
ATP	Adenosine triphosphate
B	Magnetic field
BCA	Bicinchoninic acid
BMPO	5-tert-butoxycarbonyl 5-methyl-1-pyrroline N-oxide
BPAEC	Bovine pulmonary artery endothelial cells
BSA	Bovine serum albumin
CAPS	cyclohexyl-3-aminopropanesulphonic acid
CCCP	Carbonyl cyanide m-chlorophenylhydrazone
CO_2	Carbon dioxide
$CO_3^{\bullet -}$	Carbonate radical
Complex I	NADH dehydrogenase
Complex II	Succinate dehydrogenase
Complex III	Coenzyme Q – cytochrome *c* reductase
Complex IV	Cytochrome *c* oxidase
Complex V	ATP synthase
CT	Charge transfer
Cu	Copper
Cyt	Cytochrome
DCIP	2,6-dichloroindophenol
DHR 123	Dihydrorhodamine 123
DMPO	5,5-dimethyl-1-pyrroline N-oxide
E	Reduction potential
EDTA	Ethylenediaminetetraacetic acid
Em.	Emission
EPR	Electron paramagnetic resonance
ESI	Electrospray Ionization
ETC	Electron Transport Chain

Etd^+	Ethidium
Ex.	Excitation
e^-	Electron
FAD	Flavin adenine dinucleotide
Fe	Iron
Fe_2S_2	Rieske protein
g	Electronic splitting factor (“~~g~~ value”)
h	Planck‘s constant
H_2O	Water
H_2O_2	Hydrogen peroxide
Hb	Hemoglobin
HCl	Hydrochloric acid
HE	Hydroethidine
HEPES	N-2-hydroxyethylpiperazine-N'-2-ethane-sulphonic acid
His	Histidine
HNO_2	Nitrous acid
HRP	Horseradish peroxidase
HUP	Heme undecapeptide
Hz	Hertz
H^+	Proton
IgG	Immunoglobin G
K	Potassium
K_m	Michaelis constant
L-NAME	L-Nitro-Arginine Methyl Ester
MCD	Magnetic circular dichroism
MeOH	Methanol
MES	2-(*N*-morpholino)ethanesulphonic acid
met	Methionine
metHb	Methemoglobin
Mn	Manganese
MS	Methionine sulfoxide
N_2O_3	Dinitrogen trioxide
Na_2CO_3	Sodium carbonate
n-Ac-HUP	N-acetyl heme undecapeptide
NADH	Nicotinamide adenine dinucleotide
$NaHCO_3$	Sodium bicarbonate
NaOH	Sodium hydroxide
$NaONO_2$	Sodium peroxynitrite
NED	N-1-naphthylethylenediamine dihydrochloride
NO	Nitric Oxide
NO_2^-	Nitrite
NO_3^-	Nitrate
NOS	Nitric oxide synthase
NT	Nitrated tyrosine

O_2	Oxygen
O_2^-	Superoxide
OH●	Hydroxyl radical
OH^-	Hydroxyl anion
ONOOH	Peroxynitrous acid
$ONOO^-$	Peroxynitrite anion
Opti-MEM®	Reduced serum media (from Eagle's Minimum Essential Media)
PBS	Phosphate buffer solution
PN	Peroxynitrite
RH 123	Rhodamine 123
rsAPX	recombinant ascorbate peroxidase
S	Sulfur
$S_2O_4^{2-}$	Dithionite
SCN^-	Thyocyanite
SOD	Superoxide dismutase
SPAEC	Sheep pulmonary artery endothelial cells
Tris	Tris(hydroxymethyl)aminomethane
Tyr	Tyrosine
TyrO●	Tyrosine radical
Zn	Zinc
β	Bohr magneton
Δ	Energy splitting
$\Delta\Psi$	Membrane potential
ε	Molar absorptivity
ν_c	Frequency

ACKNOWLEDGEMENTS

This work was supported by NIH: HL61411 (to JP, LLP & Bruce R. Pitt)

and AI068021 (to Joel S. Greenberger, Project 3 to JP and LLP)

I would like to express my deepest gratitude to Dr. Jim Peterson and Dr. Linda Pearce who are responsible for the successful completion of my dissertation. Their superb guidance, commitment, extreme patience and caring helped me greatly in the understanding of the work (even when the results were unexpected) and in the writing of the dissertation. But most importantly, I would like to thank them for being just Jim and Linda. Their warmth, love and closeness have helped me many times to see the light when times were dark. They have not only become mentors, but also second parents.

I would also like to thank the rest of my committee members, Drs. Bruce Pitt, Mark Gladwin, James Fabisiak and Michael Hendrich for finding time for me in their busy schedules, for their suggestions and criticisms that helped me to improve my scientific proficiency.

I want to express my heartfelt thanks to all the members of the Peterson-Pearce group, including those who already left. It has been a privilege to work with such amazing people, able to turn frustrating days in the lab into fun anecdotes. Their huge assistance includes some of the experimental part shown in this dissertation, but most importantly, incommensurable enthusiasm and moral support. Specially, I will never forget them listening to my many rehearsals with a positive attitude and a smile in their face, always pretending that I did not bored them to death

after each talk. For all those precious moments, lunches, spinning proteins while singing and laughters, just let me say thank you.

Also, I owe my most sincere gratitude to all my invaluable network of supportive, forgiving, generous and loving friends who have been cheering me up and offering free babysitting in order to be able to finish my dissertation and defense.

I would like to mention all my friends and family in Spain, specially my parents and my sister, without whom (and new technologies) I could not have survived the process. My parents deserve special mention for giving me all the education that I needed to pursue my career. But mostly, for always giving me unconditional love.

I would like to dedicate this thesis to the person that I admire the most: my husband, Carlos Vallespi-Gonzalez. He is not only my best friend, but has always been encouraging me to pursue my dreams, insisting that I could do whatever I put my mind to and never allowing me to quit anything because it was getting too difficult. His energy, intelligence and spirit of overcomer are an inspiration to me. If mitochondria are the powersource of the cells, he is the powersource of my life.

Lastly, I would like to dedicate some words to my son. Aran, you are the light of my life, my everything. Your daily smiles and joy fueled me to finish this work. And the most important lesson that I learnt is that there is no better degree to have than being ‗mom'.

1.0 INTRODUCTION

1.1 THE MITOCHNDRIAL ELECTRON TRANSFER CHAIN

In recent years an increasing number of groups have devoted their research to the mitochondria. These organelles of eukaryotic cells have long been identified as the energy powerhouses of the cell and responsible for aerobic respiration. It is a fact that mitochondria play key roles in cell function and many studies have shown that mitochondrial dysfunction is the main cause of a wide range of human diseases. Mitochondrial cytopathies actually include more than 40 different identified diseases: e.g. Parkinson‘s disease; Kearns-Sayre syndrome; Leigh syndrome, MELAS (mitochondrial encephalomyopathy, lactic acidosis, and stroke-like episodes). The common factor among these diseases is mitochondrial electron transport chain (ETC) dysfunction. Although there are uncertainties about the exact nature of the defects in this pathway, it is clear that they may have a profound effect on cellular metabolism, leading to neurological disorders and muscular dystrophies. However, despite advances in this field, disorders of the ETC still remain under-diagnosed and not properly treated [1-2].

A satisfactory understanding of the biochemistry of small reactive species that may be produced by the ETC remains a key area of difficulty. The complexes of the ETC are located within the folded inner membrane and are actually a collection of dozens of protein subunits working together in large macromolecular assemblies to produce the catalytic reducing power that generates ATP. These complexes couple the flow of electrons from NADH to molecular

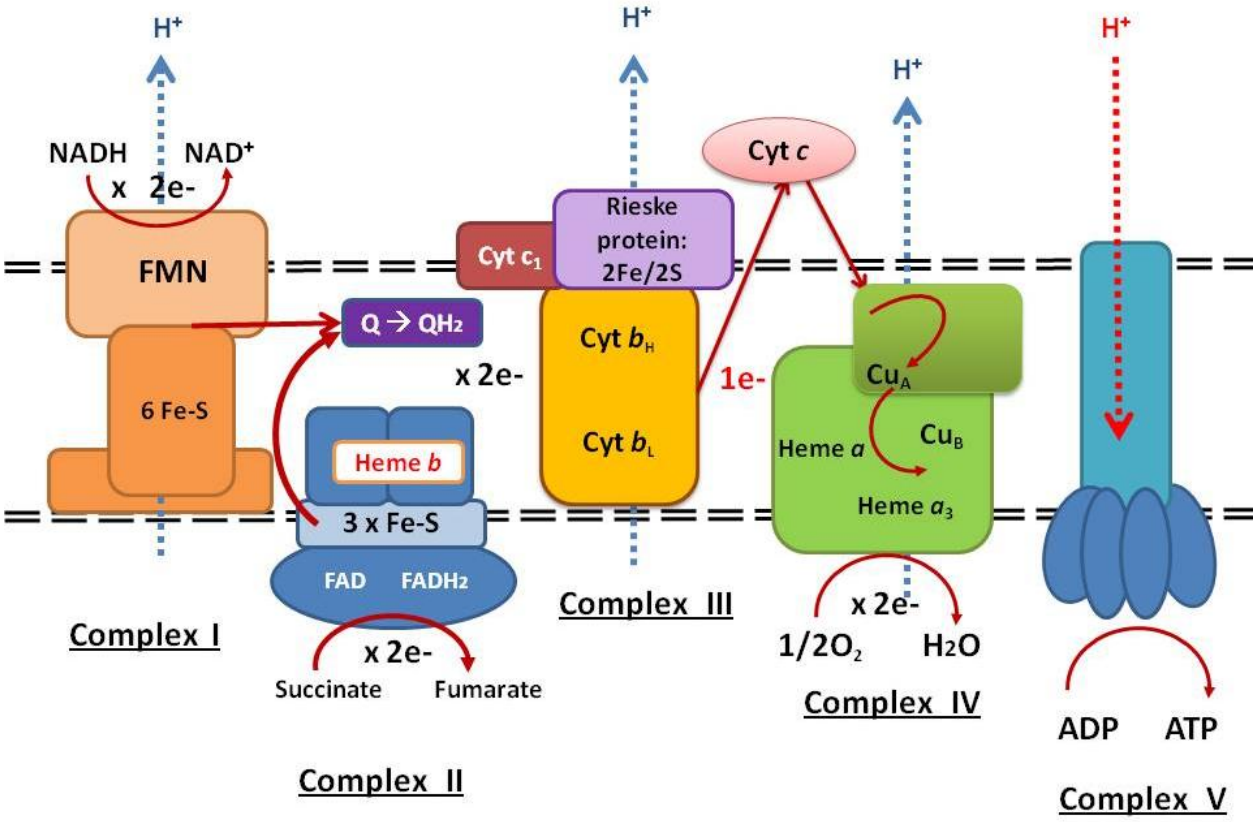

Figure 1. Mitochondrial Electron Transport Chain

Located in the inner mitochondria, the ETC is the responsible of the oxidative phosphorilation. **Complex I** (NADH dehydrogenase) accepts NADH from the citric acid cycle which donates electrons to the chain. **Complex II** (succinate dehydrogenase) accepts electrons from $FADH_2$ and passes them to **Complex III** (cytochrome *c* reducatase) via CoQ 10. The electron is then passed to **Complex IV** (cytochrome *c* oxidase) via cytochrome *c*. All this electron transfer are coupled to proton pumping system which drive the energy to Complex V (ATP synthase) which converts ADP to ATP

oxygen with the transmembrane flow of protons which produce the electrochemical gradient responsible for ATP production (see Figure 1). The electron carriers of the mitochondrial electron transport chain are protein cofactors and include iron-sulfur clusters, hemes, quinones, and flavins.

There are three large protein complexes associated with mitochondrial electron transport, usually called Complexes I, III and IV that also serve to "pump" protons across the membrane to create the proton gradient. Electron transfer between these complexes is accomplished by the mobile coenzyme ubiquinone (in the lipid membrane, from complexes I to complex III) and by cytochrome *c* (in the intermembrane space, from complex III to complex IV). Complex IV (cytochrome *c* oxidase) is the terminal electron acceptor which reduces dissolved oxygen to water. Complex II also transfers electrons (to Complex III via ubiquinone) but does not pump protons. Complex V is the ATP synthase (not normally considered part of the ETC) that utilizes the proton gradient produced by the ETC to promote the phosphorylation of ADP to ATP.

Since one of the main functions of the electron transport chain (ETC) is to become reduced and then, in turn reduce oxygen to water, the presence of large amounts of oxidants could conceivable diminish the amount of ATP produced. Many researchers have suggested that during the transfer of electrons between the various members of the ETC electrons are leaked to molecular oxygen, thus producing superoxide ions (O_2^-). Superoxide is not a particularly strong oxidant itself but reacts in diffusion controlled fashion with nitric oxide (NO) to produce peroxynitrite, a very powerful oxidant. Peroxynitrite is capable of oxidizing members of the ETC once they are reduced and in addition may participate in reactions that further modify these proteins to further reduce the flow of electrons. One of the aims of this work is to investigate the preceding possibility, especially concerning the mitochondrial cytochromes.

Another area of investigation concerning mitochondria is the measurement of superoxide and peroxynitrite produced by the ETC. A number of groups have measured superoxide production using cytochrome *c* reduction in reactions with isolated complexes. However, one would like to know, in a quantitative way, the amount of these species produced in mitochondria or cells. A number of fluorescent compounds have been developed by others toward this end but little attention has been paid to whether or not these compounds actually induce the species they purport to measure. A second aim of this project is to study the oxidation-reduction chemistry of MitoSox™ and rhodamine 123 relevant to their use as indicators of mitochondrially-generated supeoxide.

1.2 MITOCHONDRIAL CYTOCHROMES

For the purpose of this work, only 2 of the main complexes (complexes III & IV) and cytochrome *c* will be studied. The mutual link among these complexes of the electron transport chain is that they all contain cytochromes. Cytochromes are part of a larger group of proteins which contain heme prosthetic groups. The heme group consists of an iron atom coordinated to the four nitrogen atoms of a porphyrin group. Cytochromes were initially described in 1884 by MacMunn [3] as respiratory pigments but it was not until their rediscovery by Keilin in 1925 that they gained their name [4]. The iron atom may then be additionally coordinated by one to two other ligands. The cytochromes that form part of the electron transport chain are as follows:

1. Complex III: cytochromes b_H and b_L ; cytochrome c_1
2. Cytochrome *c*
3. Complex IV: cytochromes *a* and a_3

The axial coordination, usually provided by protein amino acid residues in cytochromes, and the so-called heme –pocket" observed in these proteins is critical to their reactivity. All of the above hemes, with the exception of heme a_3 and cytochrome *c* have bis-histidine coordination. Heme a_3 in cytochrome *c* oxidase is coupled to the Cu_B site. It is at this coupled site where the final transfer of electrons to molecular oxygen occurs. Cytochrome *c* contains histidine and methionine coordination (see Figure 2).

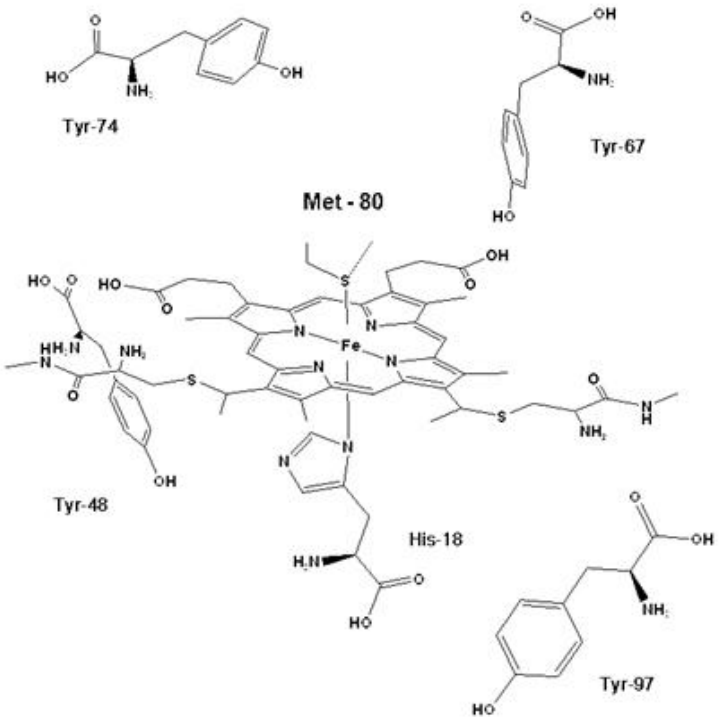

Figure 2. Cytochrome *c* active site structure.

Cytochrome *c* has a hexa-coordinated heme where methionine and histidine are the axial ligands. Also, it contains four tyrosines, 2 of which are internal and the other two are exposed to the environment. The numbering of the amino acid residues refers to the structure of horse-heart cytochrome *c* [5].

The primary function of the majority of cytochromes found in the electron transport chain is to carry out oxidation-reduction reactions, *i.e.* transfer electrons. These reactions are most easily followed through a variety of spectroscopic techniques. In addition, protein modifications causing either ligand exchange or a perturbation of the active site may also be detected. That is, the heme group can be used as an intrinsic spectroscopic probe of reactivity, making the use of indicator dyes unnecessary. In order to carry out the aims of this dissertation a combination of electronic absorption, electron paramagnetic resonance and magnetic circular dichroism spectroscopies will be used and briefly discussed in the following sections.

1.2.1 Electronic absorption spectra of cytochromes

Electronic absorption spectroscopy is a powerful tool for the study of heme proteins. The electronic absorption spectra of heme proteins are quite complicated and dominated by the π-π^* (and n-π^*) transitions of the porphyrin. It is possible, however, to identify some ligand exchanges, as well as changes in oxidation state using electronic absorption spectroscopy in fingerprint fashion (e.g. Figure 3) without the need for any detailed theoretical analysis of the orbitals and transitions involved. In general, hemes exhibit two main bands:

1) A sharp band (the Soret or B band) in the near ultraviolet region (~400 nm). This transition is intense with molar extinction coefficients around 10^5 M^{-1} cm^{-1}. The reduced (Fe^{2+}) cytochromes usually exhibit Soret bands that are red-shifted by ~10 nm with respect to the oxidized (Fe^{3+}) cytochrome.

2) A broad band (the Q bands, often split into multiple bands) of lower intensity is observed in the visible region (450-750 nm), with molar extinction coefficients usually 5-10

times less intense than those for the Soret bands. These transitions are from the first excited state.

Figure 3A illustrates a high-spin ferric heme (metmyoglobin at pH 6) and a low-spin ferric heme (oxymyoglobin) is shown in Figure 3B. In Figure 3C is shown the Q-band spectra of oxidized and reduced cytochrome *c*. Thus, the oxidation (or reduction) of cytochromes can be easily ascertained by electronic absorption spectroscopy, as upon occasion can spin-state changes.

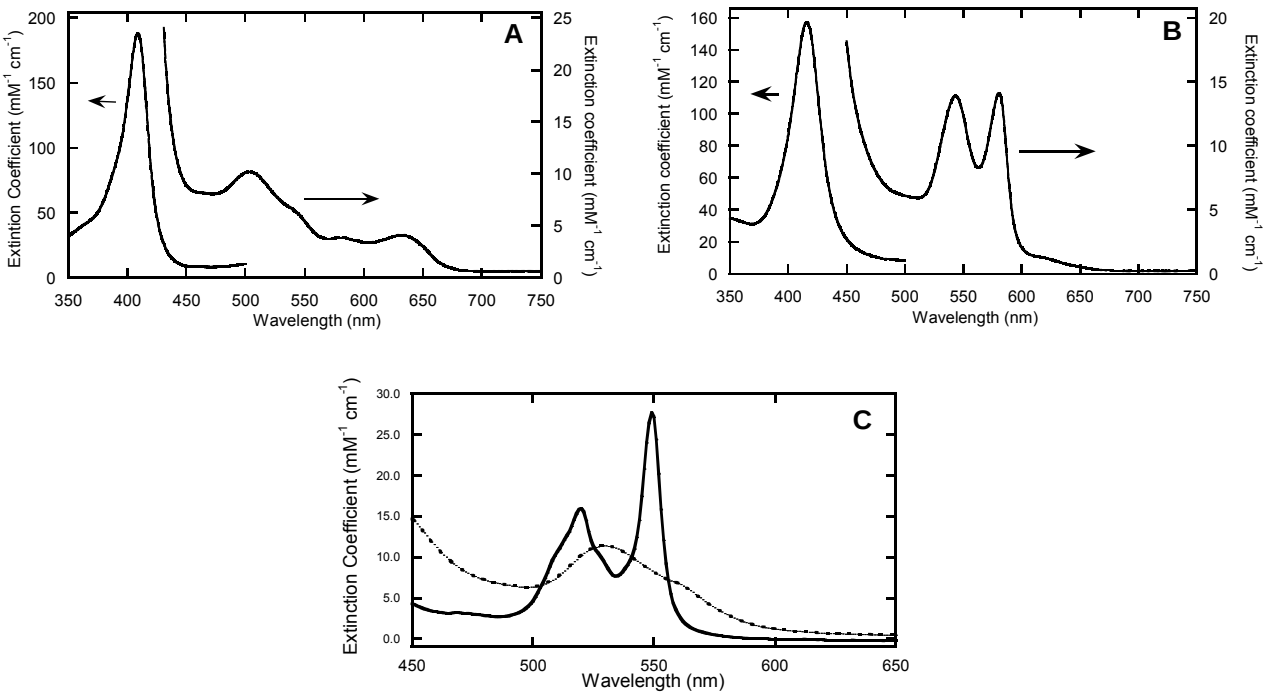

Figure 3. Electronic absorption spectra of myoglobin and cytochrome *c*.

A: Ferric myoglobin at pH 6 (50 mM potassium phosphate), 25°C. B: Oxymyoglobin at pH 6 (50 mM potassium phosphate), 25°C. C: Q-band of ferricytochrome *c* at pH 6 (50 mM potassium phosphate), 25°C.

Cytochromes are classified based on the position of their lowest energy absorption band (α band) in the reduced state, as cytochromes *a* (605 nm), *b* (~565 nm), and *c* (550 nm). Within each class of cytochrome (a, b, or c), the proteins were originally numbered consecutively, *e.g.* cyt *c*, cyt c_1, and cyt c_2. However, the current convention is to assign the cytochrome name by the position of the maximum peak of the α band as in the case of cyt c_{559}.

While oxidation-reduction reactions of cytochromes are quite easy to detect and quantify (see Figure 3C), following axial ligand exchanges can be more challenging. The axial ligands can be more readily ascertained by the ligand-to-metal charge transfer (CT) bands when these are present. These bands can be more difficult to observe as they are often dominated by phorphyrin absorptions and frequently found in the near-infrared region of the spectrum. For example, the CT band associated with methionine coordination in ferric cytochrome *c* (Fe^{3+}←met) is found at 695 nm with an extinction coefficient of ~ 7 mM^{-1} cm^{-1}. Another technique that has been very useful in assigning axial ligands in hemes is near-infrared magnetic circular dichroism (MCD) spectroscopy. While this is a challenging technique to understand, one can take advantage of the reported spectra of various heme model complexes (e.g. heme undecapeptide, HUP - see Figure 4) and proteins with known crystal structures to assign axial ligands in a straightforward fingerprint fashion.

Spin state changes can also be indicative of either ligand changes (low spin to high spin; strong field ligands to weak field ligands) or perhaps perturbation of the heme protein active site (heme pocket). Electronic absorption spectroscopy can be useful in determining these changes also. Frequently CT bands are blue shifted in transitions from low to high spin. In high spin complexes the Soret maxima can be intensified, as well.

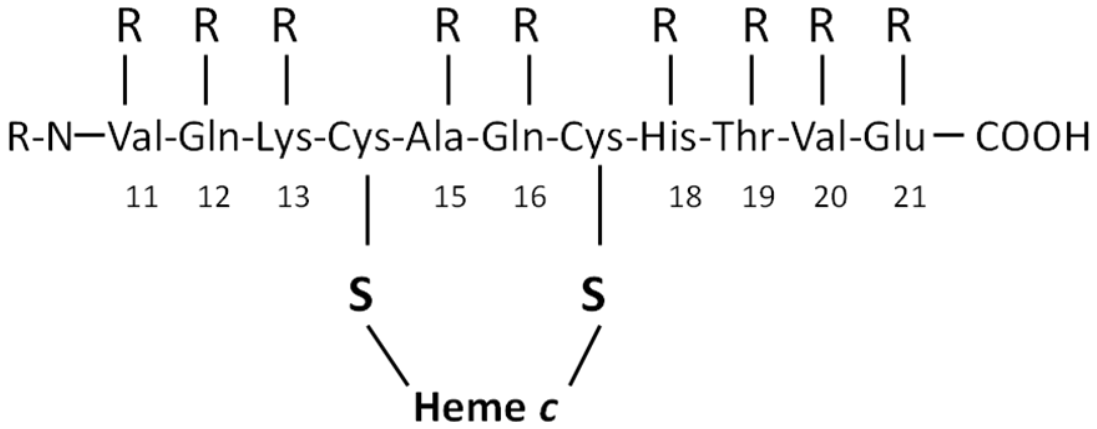

Figure 4**. Schematic representation of the structure proposed for heme undecapeptide HUP .**

R represents different possible residues that can be attached to the heme. The numbering refers to the amino acid sequence of native beef (and/or horse) cytochrome *c*, from which the molecule is derived. The *c*-type heme group is covalently attached to the peptide via two thioether linkages as in other heme peptides and the native cytochrome.

However, one of the most straight forward techniques to determine spin state changes in heme proteins is electron paramagnetic resonance (EPR) spectroscopy. Very briefly, ferric hemes (d^5) have their d shell electrons in either of two configurations; low spin (S = ½, illustrated in Figure 5A) or high spin (S = 5/2, illustrated in Figure 5B). Several factors determine the size energy splitting (Δ) that establishes the spin state but at least one of these is the identity of the axial ligands in hemo-proteins. It is the field strength of the ligand as described by the spectrochemical series which helps determine Δ.

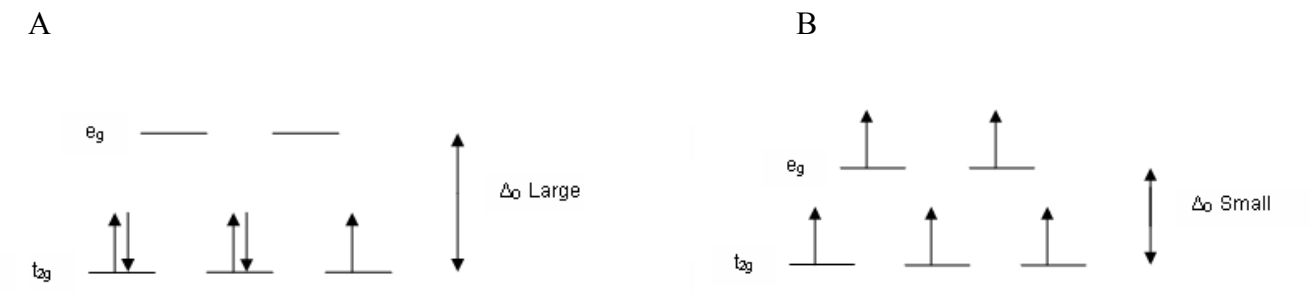

Figure 5. Illustration of high-spin and low spin d shell electron configurations.

A. Low spin crystal field diagram diagram $[Fe(NO_2)_6]^{3-}$. B. High-spin crystal field diagram diagram $[Fe(NO_2)_6]^{3-}$.

1.2.2 Electron paramagnetic resonance spectroscopy of cytochromes

Electron paramagnetic resonance (EPR) spectroscopy is a technique that detects (and allows one to identify) species which have unpaired electrons, such as free radicals and transition metal ions. Thus, ferric hemes (d^5) exhibit EPR spectra due to their unpaired electrons while (in general) ferrous hemes (d^6) do not. There is an extensive literature from decades of studies of EPR spectra of high- and low-spin ferric hemes [6-8]. A typical EPR transition is observed when the magnetic field, **B**, is varied at a fixed frequency, ν_c (typically 9-10 GHz, or ~~"X~~-band"), until a resonance value is obtained (designated B_0). The absorption of energy can be described by the following equation, where β is the Bohr magneton and *g* is the electronic splitting factor (~~"g~~ value"):

$$\Delta E = h\nu_c = g\beta B_0 \qquad [1]$$

Equation 1. Absorption energy for the splitting of the energy levels.

Energy separation of the two spin states increases with the icrease of the applied magnetic field .

A free electron absorbs microwave energy with a frequency of 9-10 GHz in a magnetic field of 330 mT (milli-tesla) or 3300 gauss and has a g-value of 2.0023. Transition metal ions frequently may have g-factors that are anisotropic necessitating more than one g-value to describe the EPR spectrum [9]. In the case of high-spin ferric hemes (S = 5/2), an intense sharp derivative-shaped peak appears at g_{xy} (or $g_{\perp}$) ~ 6 and a less intense and smaller peak at gz (or $g_{\parallel}$) ~2. This axial signal is an indication that the iron center interacts identically with each of the four centers of the

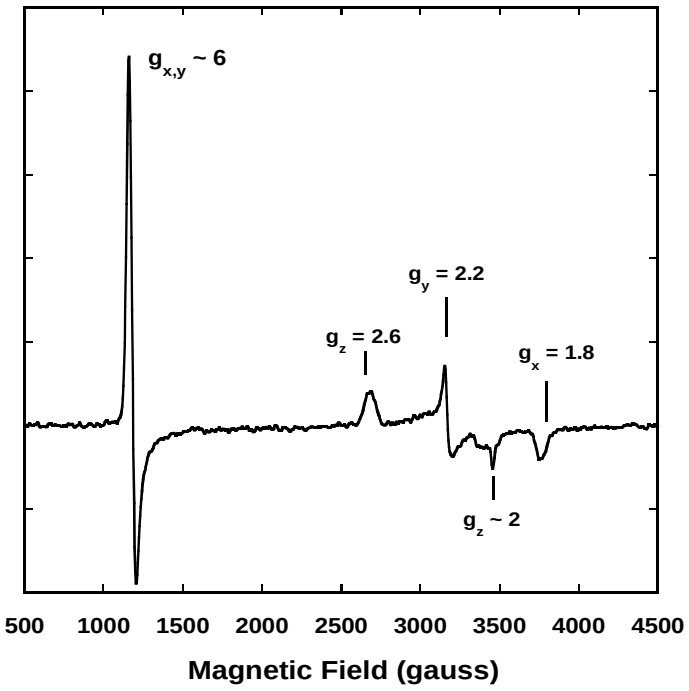

Figure 6. X-band electron paramagnetic resonance spectrum of methemoglobin at pH 7.

Conditions: T, 20 K; power, 63.2 μW; modulation amplitude, 9.8 G.; metHb 200 μM in heme, pH 7.4 in 50 mM HEPES. High-spin signals at g ~6, 2 are due to H_2O:histidine axial coordination of ferric heme and low-spin signals at g = 2.6, 2.2, 1.8 are due to OH^-: histidine coordination.

nitrogen macrocycle [11]. On the other hand, for low-spin (S=1/2) ferric hemes, there are usually three resonances in the ranges of: g_z = 2.4-3.8, g_y = 1.9-2.3, and g_x = 0.7-1.9, indicative of a more asymmetric (rhombic) environment around the heme [12]. The real g-value in each range depends on the axial ligands bound to the iron, therefore, their EPR spectra can give us information on the basic coordination chemistry [13].

The EPR spectrum of metHb (Figure 6) at pH 7.4, shows the normal high-spin component at ~1100 gauss and 3400 gauss due to the aquomet species with the low spin component (2500 to 3800 gauss) caused by the presence of the hydroxide (a strong field ligand) adduct [14]. This is an illustration of a spin-state change induced by a ligand exchange at the iron.

1.3 MITOCHONDRIAL PEROXYNITRITE

It has been hypothesized that mitochondria constitute a primary location for the intracellular formation and reactions of peroxynitrite [15]. Nitric oxide is synthesized by nitric oxide synthases (NOS) and has an important biological function as a smooth muscle relaxer and vasodilator. This small neutral molecule can diffuse freely across membranes, including the mitochondrial inner membrane, and its overproduction (which can be important in endothelial cells) has been associated with many pathological conditions. In addition, it has been long believed that the mitochondrial electron-transport chain (ETC) is a significant source of superoxide and secondary damaging oxidants for the cell as a whole [16] (see Figure 7). In the presence of excess nitric oxide, all the superoxide not converted to hydrogen peroxide by superoxide dismutase reacts in a diffusion limited reaction to form peroxynitrite. The reaction

rate has been determined by Huie *et al.* to be around $6.7x10^9$ $M^{-1}s^{-1}$ [17]. Additionally, mitochondrial peroxynitrite need not only be formed *in situ* but also could diffuse from extramitochondrial compartments into the matrix space [18] within one or two cell diameters (~ 5 – 20 μm) [19].

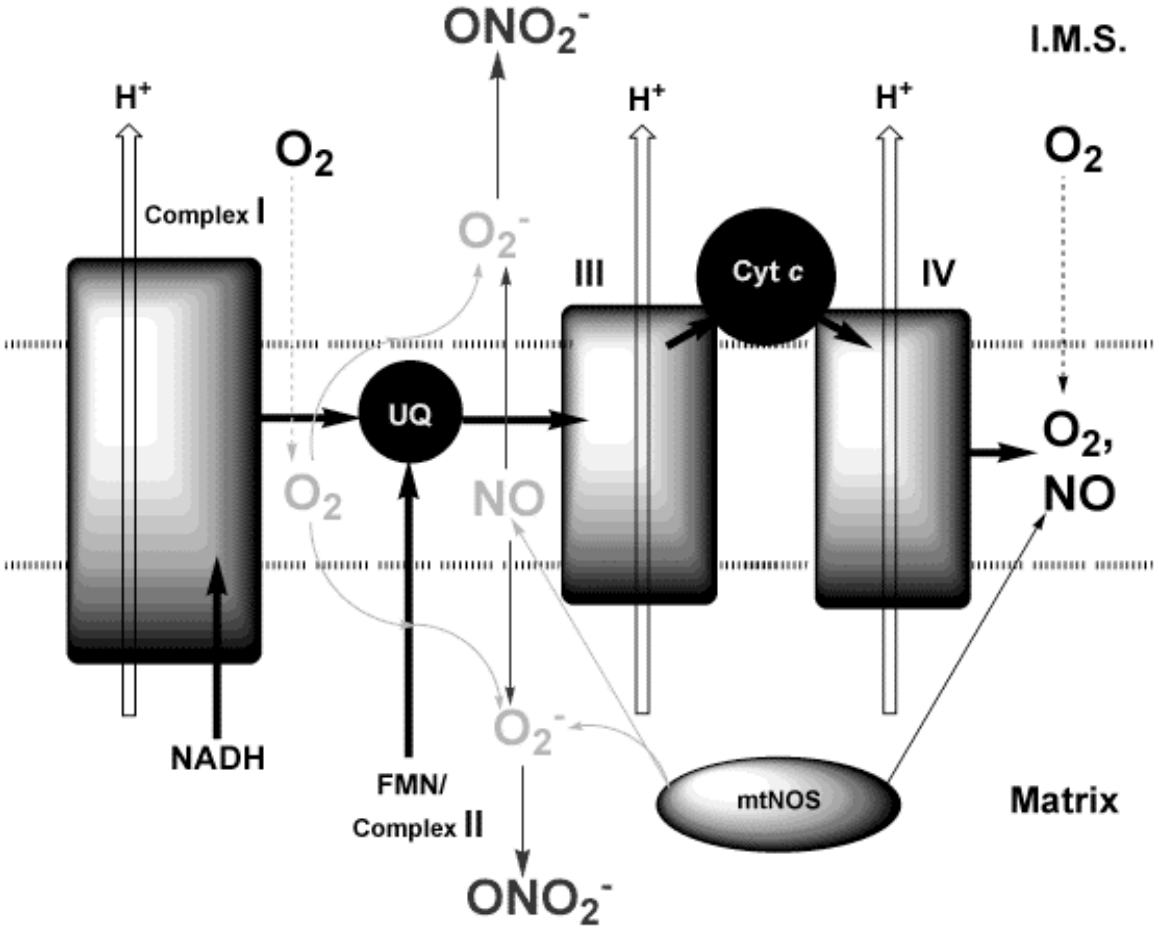

Figure 7. Electron transport chain as a possible source of peroxynitrite production.

Electrons leak from complex I and complex III forming superoxide. Peroxynitrite may reach mitochondria either from extramitochondrial compartments or may be directly produced within the mitochondria by the reaction between $NO^{\bullet}$ made by mitochondrial NOS (mtNOS) and superoxide (O_2^{-}), following the partial reduction of oxygen within the mitochondrial matrix due to the natural leak of electron from the respiratory chain.

Peroxynitrite is a strong oxidant and its reactions with lipids, carbohydrates and proteins have been highly studied [20-23]. Peroxynitrite is considered toxic to cells and assumed to be a potential factor in many different diseases such as vascular endothelial dysfunction, ischemia reperfusion injury, chronic arthritis, inflammatory bowel disease and others [24] . Peroxynitrite can undergo direct and indirect reactions that can result in oxidation, nitration and nitrosation of the elements of the electron transport chain that may alter and/or inhibit its proper function [25]. Proteins, for example, can have their residues modified including for example, tyrosine nitration and methionine oxidation. While the chemistry of peroxynitrite is extensive some of the important reactions will be reviewed in the following paragraphs.

1.3.1 The Chemistry of Peroxynitrite

1.3.1.1 Decomposition of peroxynitrite

The peroxynitrite anion ($ONOO^-$) is formed from the diffusion-controlled reaction between the free radicals •NO and O_2^- ($k \sim 10^{10}\ M^{-1}s^{-1}$). It is difficult to estimate the steady-state concentration of peroxynitrite, but some think it may be in the nanomolar range [26]. Peroxynitrite can be protonated to form peroxynitrous acid with a pK_a of 6.8. While $ONOO^-$ is basically stable, ONOOH has a short half-life (~ 1 s) and decays to nitrate, ~67% [27] via an isomerization reaction. Homolysis of its peroxo bond leads to the formation of hydroxyl (OH●) and nitrogen dioxide (●NO_2) radicals in ~33% yields as shown in the following scheme:

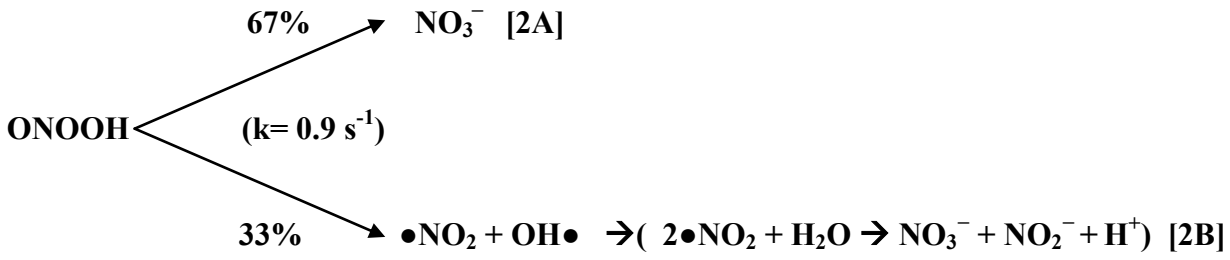

Equations 2. Decomposition of peroxynitrite.

A. Isomerization reaction to nitrate. B. Homolysis of the peroxo bond leads to the formation of hydroxyl (OH●) and nitrogen dioxide radicals

The products of this homolytic fission can rapidly react with the other molecules involved in the formation of peroxynitrite (*i.e.* NO and O_2^-), as described in Figure 8. As the decomposition of peroxynitite at physiological pH is fairly rapid, oxidation of potential substrates by peroxynitrite often occurs indirectly through these products of decomposition.

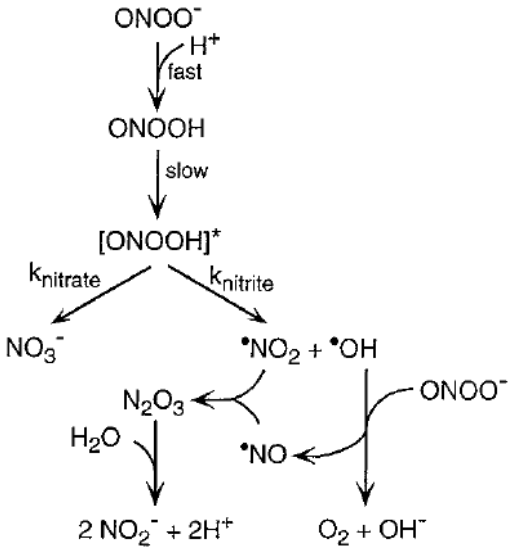

Figure 8. The interplay of binary oxygen-nitrogen molecules.

Reprinted from J Biol Chem, 1997. **272**(6): p. 3465-70 [28] with permission from American Society for Biochemistry and Molecular Biology.

When nitric oxide and superoxide are both present, they may also react with nitrogen dioxide to form N_2O_3 and peroxynitrite. Peroxynitrite decomposes to give nitrite and oxygen, while N_2O_3 can react with thiols to give nitrosothiols or with hydroxide anion to give nitrite. Goldstein et al. [29] showed that peroxynitrite also reacts at a diffusion-limited rate with peroxynitrite to yield two molecules of nitrogen dioxide and one of nitrite. This creates a cycle to generate more nitrogen dioxide when bolus additions of peroxynitrite are added at neutral pH and substantially increases the number of potential reactions occurring. These same reactions will also occur *in vivo*, particularly when nitric oxide is produced faster than superoxide.

The decomposition of peroxynitrite forms nitrate, nitrite and dioxygen, the yields of which vary with pH, temperature and concentration [28]. Below pH 6, nitrate is mainly formed while at and above neutral pH, nitrite and O_2 are produced. The following equation describes the overall decay, the details of which are extensively reviewed in Goldstein and Merényi [30].

$$\mathbf{ONOOH + ONOO^- \rightarrow 2(1-x)NO_3^- + 2xNO_2^- + xO_2 + H^+} \qquad \mathbf{[3]}$$

Equation 3. Overall decomposition of ONOOH.

Reprinted from *The Chemistry of Peroxynitrite: Implications for Biological Activity.* Goldstein S., Methods in Enzymology, 2008. **436**: p. 49-61 [30], with permission from Elsevier B.V.

1.3.1.2 Direct oxidations of peroxynitrite

Peroxynitrite can react directly or indirectly, via secondary radicals formed by its decomposition. Its direct reactions proceed through the peroxynitrous acid molecule and have pH profiles that are consistent with its pK_a (6.8). If direct reactions are involved, peroxynitrite can act as one or two electron oxidant, as illustrated by the following equations [31]:

1 electron process: $ONOOH + H^+ + 1e^- \rightarrow {}^{\bullet}NO_2 + H_2O$ (E/V, pH=7→ 1.6-1.7) **[4A]**

2 electron process: $ONOOH + 2H^+ + 2e^- \rightarrow HNO_2 + H_2O$ (E/V, pH=7→ 1.37) **[4B]**

Equations 4. Direct electron oxidations of peroxynitrite.

Adapted from *The chemistry of peroxynitrite. Reaction mechanisms and kinetics.* Russ. Chem. Rev., 2006. 75(5): p. 375-396, [31] with permission from The Russian Academy of Sciences and Turpion Ltd.

The metalloproteins of the ETC can be considered to be, at least, partly reduced in a low oxygen tension environment. The possible oxidation by peroxynitrite of the metal centers in these metalloenzymes is of considerable interest. In general, most members of the ETC can accept one or two electrons at a time and may be oxidized in a similar fashion. One of the most studied members of the ETC is cytochrome *c*, a one electron acceptor. Thomson *et al.* reported that it reacts in a direct, one electron, reversible oxidation with peroxynitrous acid [32]. Isolated cytochrome *c* oxidase (complex IV) can be oxidized by a direct two-electron process with a rate constant that was estimated to be at least 10^6 M^{-1} s^{-1} [33]. A large excess of peroxynitrite was added to cytochrome *c* oxidase, leads to protein damage and loss of function [34]. Examination of several other proteins in the ETC (Complexes I, II, III and cytochrome *c*) also showed that these proteins can be oxidized with peroxynitrite and then reduced with no loss of function

unless peroxynitrite was added in great excess [25]. However, these later reactions were carried out under ambient CO_2 (~0.5%) and in the presence of 20% oxygen.

1.3.1.3 Bicarbonate and peroxynitrite

In biological systems, the presence of the bicarbonate/carbon dioxide buffer system is undeniable. In mitochondria, CO_2 is produced due to the decarboxylation reactions catalyzed by pyruvate dehydrogenase and in the Krebs cycle. While the exact concentration of CO_2 in mitochondria is not known, reactions of peroxynitrite with CO_2 in the mitochondria have at least some relevance. It has been known for some time that peroxynitrite can react extremely rapidly with CO_2, with a reaction rate of $k \sim 4.6 \times 10^4\ M^{-1}\ s^{-1}$ at 37°C [35]. The reaction of peroxynitrite with CO_2 forms radicals [36] as indicated below:

$$ONOO^- + CO_2 \xrightarrow{67\%} NO_3^- + CO_2 \qquad [5A]_i$$

$$ONOO^- + CO_2 \xrightarrow{33\%} NO_2 + CO_3^{\bullet -} \qquad [5A]ii$$

$$CO_3^{\bullet -} + 1e^- + H^+ \rightarrow HCO_3^- \quad (E/V = 1.8V) \qquad [5B]$$

Equations 5. Relevant reactions between peroxynitrite and carbon dioxide.

5A. Reaction of peroxynitrite with carbon dioxide, leads to the production of carbonate radical with a ~33% yield.

5B. Carbonate radical can later undergo one electron oxidations**.**

1.3.1.4 Peroxynitrite protein modifications

Perhaps among the most well known reactions of peroxynitrite are those responsible for protein modifications. For example, methionine can be converted to the respective sulfoxide by a two electron oxidation. Perrin & Koppenol also report that methionine can be oxidized to methional and ethylene by nitrite, a product and also frequent contaminant in peroxynitrite chemistry [37] .

One of the most studied protein modifications by peroxynitrite is tyrosine nitration. Carbon dioxide promotes the nitration of tyrosine in many proteins by a mechanism involving nitrogen dioxide and carbonate radical [38]. In the presence of excess CO_2, $CO_3^{\bullet -}$ (generated from the reaction with peroxynitrite) reacts with tyrosine to produce tyrosine radical (TyrO$^{\bullet}$). The tyrosine radical can either dimerize to produce dityrosine or react with $^{\bullet}NO_2$ to produce 3-nitrotyrosine as shown in the following Figure 9**:**

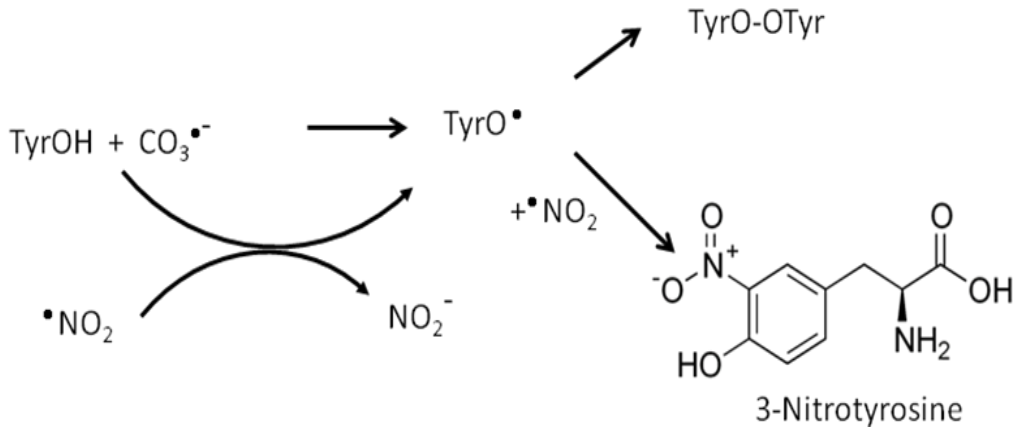

Figure 9. Nitration and oxidation of tyrosine by peroxynitrite.

Reaction rates for the formation of dityrosine and 3-nitrotyrosine are k = 4.5 x 10^{10} $M^{-1}s^{-1}$ and k= 3 x 10^9 $M^{-1}s^{-1}$ respectively. All reaction rates are from condition with excess CO_2 and pH = 7.5 [39]

Several groups have previously shown that peroxynitrite can react with various members of the ETC [34, 40-45]. Indeed, all of the members of the ETC (complex I, III, IV and cytochrome *c*) have been shown to have specific tyrosines nitrated and it has been established that sufficient amounts of 3-nitrotyrosine may lead to protein dysfunction [38, 46-47]. However, some of the details of these reactions have yet to be delineated and, in some cases, corrected. For example, Thomson et al. [32] reported that cytochrome *c* reacted directly with peroxynitrite via a one-electron process and that bicarbonate had no effect on the reaction. This has now been disproved, by Gebicka et al. [48] and by the work contained in Chapters 2 and 3 of this dissertation.

1.4 SUPEROXIDE DETECTION

1.4.1 Superoxide production

Since it has been hypothesized that superoxide is the limiting reagent in the formation of peroxynitrite, it is of some interest to quantitate its production in mitochondria and/or cells. There are two main sites in the respiratory chain where these reactions are believed to occur: complex I [49] and complex III [50] as pictured in Figure 7. There appears to be a growing consensus that inhibition of the electron transfer chain or a back flow of electrons generates an increase in superoxide production. For example, in complex I, the addition of rotenone (a complex I inhibitor) or succinate (an electron donor which passes electrons to complex I through ubiquinone, *i.e.* ~~–b~~ackflow") generates superoxide. Kussmaul and Hirst [51] have determined

that the electron leak to oxygen in isolated complex I involves the flavin moiety and requires a low NADH/NAD^+ ratio. It follows that inhibition of the ETC at any point "downstream" of ubiquinone, may lead to blocking of oxygen turnover at complex IV, consequent electron accumulation ~~u~~pstream" and unavoidable production of superoxide.

1.4.2 Hydroethidine based probes for superoxide detection: false positive?

Much of the evidence for the formation of superoxide in mitochondria has been obtained using oxidant-sensitive dyes of poorly understood specificity, typically in the presence of electron transport chain inhibitors of similarly uncertain additional activities. Hydroethidine (HE, also called dihydroethidium) and MitoSox™ (the mitochondrially targeted version of HE), are fluorescent probes routinely employed as qualitative specific detectors for superoxide anion (Figure 10 and Figure 11)

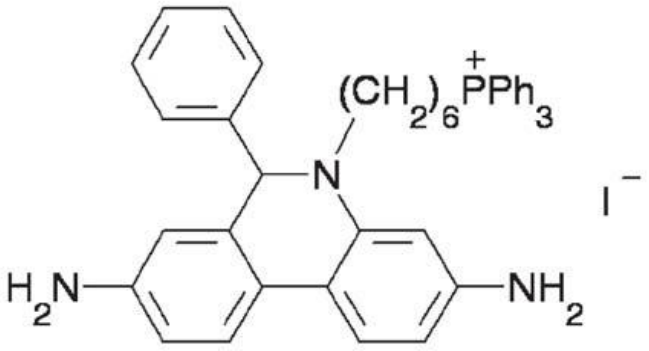

Figure 10. Chemical structure of MitoSox™

It has been shown [52] that a unique product of the oxidation of HE by superoxide, 2-hydroxyethidium (2-HO-E+) (Figure 11) can be detected using selective fluorescence (excitation/emission peaks 480/567nm). Usually when these probes are used, it is under the assumption that all hydroethidine is oxidized to 2-hydroxyethidium. If all the sources of interference can be delineated, it should be possible to equate the measured change in fluorescence intensity due to the oxidized fluorescent species with the net superoxide flux. However, the overall chemistry is complicated [53] and apart from any superoxide that may or may not be formed, there is a surplus of mitochondrial components similarly having the potential to oxidize HE-based probes and consequently produce false positive results. For example, it has been shown that HE can catalyze the dismutation of superoxide to hydrogen peroxide (H_2O_2) and HE can also be oxidized by cytochrome *c* [54]. Herein I examine the possible direct interaction of HE and MitoSox^{TM} with some of the complexes of the ETC.

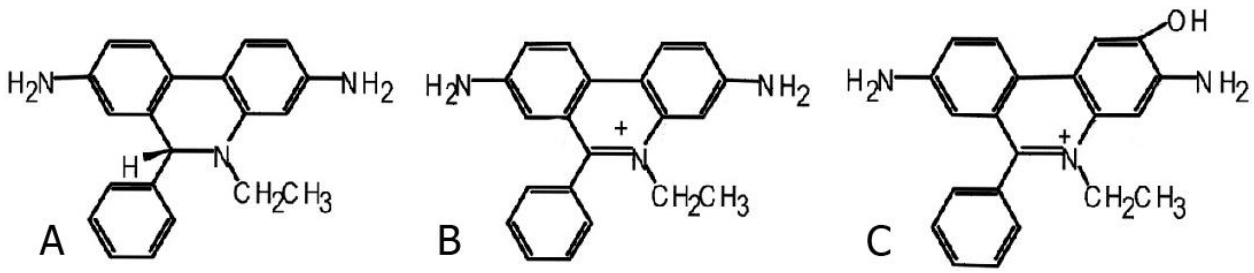

Figure 11. Chemical structure of hydroethidium and its oxidation products.

A. Hydroethidine (HE), B. Ethidium (Etd^+), C. 2-Hydroxyethidium (2-OH-E^+)

1.4.3 Dihydrorhodamine 123

Dihydrorhodamine 123 is another molecular probe that has been used for the detection of oxidant species by following its oxidation to the highly fluorescent product rhodamine 123 (excitation and emission wavelengths of 500 and 536 nm respectively) [55]. Alternately, formation of rhodamine can be followed by absorption spectroscopy at 500 nm (ε_{RH123} = 78,800 $M^{-1}cm^{-1}$) [56].

The first reported study of oxidant detection by DHR 123 was the detection of peroxynitrite [55]. However, further studies showed that the reaction is zero order and it is also depleted by carbon dioxide [57]. Therefore, one way to measure how much peroxynitrite contributes to the oxidation of dihydrorhodamine is to measure its oxidation in the absence of carbon dioxide.

Dihydrorhodamine 123 is possibly a possible better choice for detection of mitochondrial oxidants than MitoSox™ by virtue of the fact that it contains one less positive charge. The mitochondrial inner membrane has a negative charge when intact, attracting any molecule bearing a delocalized positive charge. MitoSox™ has a positively charged triphenyl-phosphonium moiety (Figure 10); the addition of which is a common method of achieving mitochondrial targeting. This moiety is absent the structure of DHR 123 (Figure 12).

For the above reason, it is useful to re-evaluate DHR123 as an alternate probe for reactive oxygen/nitrogen species detection in mitochondria (see section 4.3.1).

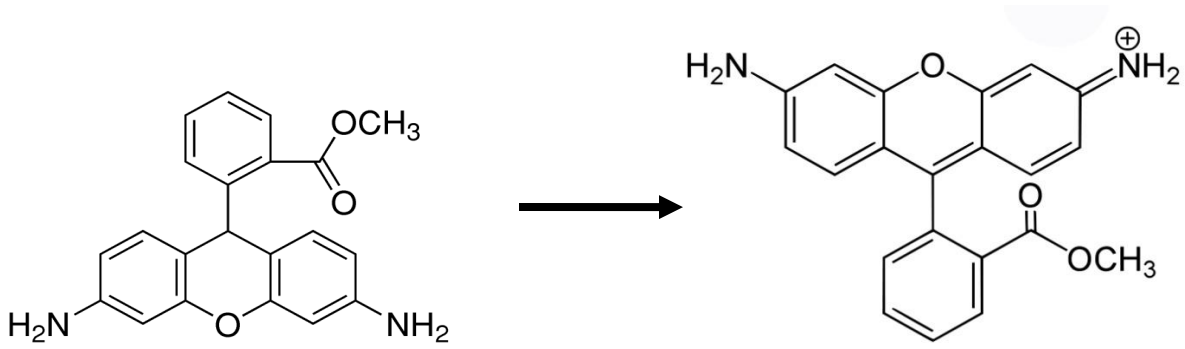

DHR 123 **Rh 123**

Figure 12. Oxidation of Dihydrorhodamine 1,2,3 (DHR 123) to Rhodamine 1,2,3 (RH 123)

1.5 SCOPE OF THE DISSERTATION AND STATEMENT OF HYPOTHESIS

Mitochondrial dysfunction, particularly in relation to electron transport chain (ETC)-derived oxidative stress, is widely held to be important in numerous pathologies. However, mitochondrial levels of the bioenergetically critical small inorganic molecules/ions (O_2, NO, CO_2, O_2^-, $ONOO^-$, H_2O_2, etc) are at best debatable and at worst, unknown. Nevertheless, investigation of the behavior of the ETC components, individually and collectively, in response to varying the levels of these species is still of considerable importance. Understanding the functional consequences of these reactions may then allow us to meaningfully estimate the physiological levels of these small molecules/ions. In order to contribute to these objectives, the Specific Aims covered in this work are the following:

1) Two reactions of the Krebs cycle within the mitochondrial matrix generate CO_2 as a byproduct in the oxidation of isocitrate and the decarboxilation of α-ketoglutarate. Consequently, it is also highly likely that CO_2 is a regulator of mitochondrial bioenergetics. Since CO_2 is known to react rapidly with peroxynitrite (ONO_2^-/ONO_2H), **we hypothesize that CO_2 inhibits the oxidation of ETC cytochromes (complex III, cytochrome *c* and complex IV) by peroxynitrite.** This will be established by functional and spectroscopic assay of isolated mitochondrial cytochromes following reactions with *bona fide* peroxynitrite.

2) Within the mitochondrion, superoxide is almost certainly the limiting reagent in the formation of peroxynitrite from superoxide and nitric oxide. **We propose that the case for the production of superoxide by mitochondria has been overstated due to the tendency of commonly employed fluorescent dyes to inhibit the electron transport chain.** Different experiments will demonstrate that MitoSox™ is a net superoxide generator, due to its tendency to inhibit the ETC at complex IV.

2.0 MATERIALS AND METHODS

2.1 MATERIALS

All reagents used were ACS grade or better and purchased from Sigma-Aldrich and/or Fisher unless otherwise stated. Argon (4.8) and oxygen gases were obtained from Matheson. Lauryl maltoside was obtained from Anatrace. Sodium dithionite (+ H_2O) was obtained from EM Science and (anaerobic) solutions were made using the manufacturer's assay (93% $Na_2S_2O_4$) to calculate dithionite ion concentrations. Stable, hydrogen peroxide-free, alkaline (pH ~12) solutions of sodium peroxynitrite were prepared following the suggestions of Beckman *et al.* [58]. Crystalline bovine cytochrome *c* was obtained from Sigma-Aldrich and further purified by gel-filtration chromatography prior to use as previously described [33]. Peroxynitrite-modified forms of cytochrome *c* were prepared essentially as described by Cassina *et al.* [38, 59] but in the presence or absence of sodium bicarbonate as required.

2.2 INSTRUMENTATION

Electronic absorption measurements were made using Shimadzu UV-1650PC and UV-2501PC spectrophotometers. Fluorescence and chemiluminescence measurements were carried out using either a Fluostar Galaxy plate reader (BMG Labtech) or a Shimadzu RF-5301PC spectrofluorophotometer. Stopped-flow experiments were carried out using an Applied Photophysics LKS.60-SX.1 system.

Cryogenic absorption and MCD spectra were recorded using an Aviv Associates (Lakewood, NJ) 41DS circular dichroism spectrometer in conjunction with a Cryomagnetics Inc. (Oak Ridge, TN) cryomagnet as previously described [45]. For measurements in the near-infrared region of the spectrum (1,000 – 2,000 nm) cytochrome *c* samples were deuterated and glycerol was added to 50%. X-band (9 GHz) EPR spectra were recorded on a Bruker ESP 300 spectrometer equipped with an Oxford ESR 910 cryostat for ultra-low-temperature measurements. The microwave frequency was calibrated by a frequency counter and the magnetic field was calibrated with a gaussmeter. The temperature was calibrated with resistors (CGR-1-1000) from LakeShore. This instrument and the software (SpinCount) to analyze the EPR spectra were graciously provided by Professor Mike Hendrich, Carnegie Mellon University.

Prior to recording mass spectra, native or peroxynitrite-modified bovine cytochrome *c* was diluted into 0.1% acetic acid and analysis was performed by direct infusion into a triple quadrupole ESI mass spectrometer (Quattro II, Micromass UK Ltd., Manchester, England). The sheath flow was adjusted to 5μL/minute and the solvent consisted of 50% acetonitrile containing 0.1% (w/w) acetic acid. The electrospray probe was operated at a voltage differential in the range of +2.3 to +3.5 keV in the positive ion mode and source temperature was maintained at 70 ^{o}C. Scanning was performed in the range of 400-1700 every 3.5 s and individual spectra were summed. Ion series were deconvoluted and converted to molecular (+1 charged) spectra by a maximum entropy algorithm using software supplied by the manufacturer. The absolute standard error in m/z determined thus was ±1.2, but the relative error in comparing the difference between peaks in the same mass spectrum was less than ±0.2.

2.3 METHODS

2.3.1 Enzyme isolations, assays and manipulations

Cytochrome *c* oxidase (complex IV) and cytochrome *c* reductase (Complex III) were isolated from beef hearts obtained from a local slaughterhouse. Beef hearts were chopped and removed of any vasculature, vessels and fat, leaving only red muscle tissue and were frozen before processing for mitochondrial extraction. It should be mentioned that the tissue may be frozen for long term storage prior to extraction of the mitochondrial complexes. Homogenates from beef heart muscle tissue were obtained by mechanical disruption, in order to improve the purity and mitochondrial yield. Mitochondrial fractions were prepared by differential centrifugation of the homogenates obtained. Supernatants from filtrates were treated with different non-ionic detergent extractions as explained in [60]. Using Triton X-114 gives 2 fractions: a red supernatant and a green pellet (red-green split). The green fraction is used to isolate cytochrome *c* oxidase (cytochrome aa_3) by the modified Hartzell-Beinert method [61]. Enzyme concentrations can be determined as total heme *a* using the differential (absorption) extinction coefficient of $\Delta\varepsilon_{604}$ = 12 $mM^{-1}cm^{-1}$ for the reduced minus oxidized spectra. Concentrations throughout are given on a per enzyme concentration basis (NOT per [heme *a*]). Complex III (cytochrome bc_1) was isolated from the red supernatant using a modification of the method originally given by Hatefi [62-63]. Enzyme concentrations could be determined either from the absorption spectra of pyridine hemochromes using the extinction coefficient ε_{554} = 81 $mM^{-1}cm^{-1}$ (2*b* + *c*) or $\Delta\varepsilon_{552\text{-}541}$ (cytochrome c_1) = 17.1 mM^{-1} cm^{-1} and $\Delta\varepsilon_{562\text{-}579}$ (cytochrome *b*s) = 25.6 mM^{-1} cm^{-1}. Complex I was purified using the procedure of Sharpley *et al*. [64]. Note that

cytochrome *c*, complex I and myoglobin may also be obtained, but are discarded as impurities in the isolation of the other complexes of the mitochondrial electron transport chain.

Ferrocytochrome *c*:O_2 oxidoreductase activity was determined employing the high ionic strength method of Sinjorgo *et al.* [65]. Using this assay, we typically obtain a turnover number with respect to cytochrome *c* of 200 - 350 s^{-1} (0.1 M sodium phosphate, 0.1% lauryl maltoside, pH 7.4, 22 ºC) similar to that of the bovine enzyme isolated from a variety of tissues by others [65]. Complex III activity was measured at 37ºC in 50 mM potassium phosphate, pH 7.4, 1 mM EDTA using reduced ubiquinone-2 [60] and monitoring the reduction of 50 μM oxidized cytochrome *c* at 550 nm ($\Delta\varepsilon$= 18.5 mM^{-1} cm^{-1}).

Strongly buffered (100 mM sodium phosphate, pH 7.4) enzyme solutions (5-35 μM) were titrated with concentrated solutions of sodium peroxynitrite (~25 mM) in 0.1M sodium hydroxide (pH 10-11). All quantitative transfers of oxygen gas, sodium peroxynitrite and sodium bicarbonate solutions were made into the reaction cells through rubber septa (Subaseal) using Hamilton gas-tight syringes fitted with new stainless steel needles. At no time were solutions of reagents left standing in contact with syringe needles. Anaerobic conditions were achieved by blowing argon over the top of solutions at room temperature for 10-15 min with mild agitation, or three cycles of evacuation followed by sparging with argon. In experiments where the oxygen concentration was varied, concentrations of dissolved oxygen were usually estimated by calculation (Henry‘s law) and, in a limited number of cases, the oxygen levels were verified using a Clark-type oxygen electrode. The pH of all protein samples was verified at the end of experiments to ensure that conditions had not become significantly more alkaline by additions of peroxynitrite solution. Cytochrome *c* oxidase (or complex III) was reduced

anaerobically by titrating the enzyme with aliquots of sodium dithionite solution before proceeding with oxidation by sodium peroxynitrite.

Aliquots from the titrations of cytochrome *c* in the presence or absence of oxygen and/or sodium bicarbonate were filtered to remove protein through Microcon YM-3 Centrifugal Filter Units tubes (Millipore) and the filtrates used to determine either hydrogen peroxide or nitrite content of samples. Hydrogen peroxide determinations were made using the fluorescent Amplex Red Hydrogen Peroxide/Peroxidase Assay Kit from Molecular Probes (Invitrogen) with Ex: 544 and Em: 590 nm. Nitrite determinations were performed by the Griess method [66] following a standard calibration curve at 550 nm. Formation of 3-nitrotyrosine was measured using nitrotyrosine-assay-kit protocol from Millipore, which is a chemiluminescent method making use of a standard curve employing 3-nitrotyrosine-BSA (bovine serum albumin).

2.3.2 Cell culture and assays in cells

Bovine pulmonary artery endothelial cells (BPAEC) were purchased from Lonza and used at passages 4-8. Cells were grown in Opti-MEM media supplemented with 10% fetal bovine serum, 5 mM glutamate, 100 U/mL penicillin and 100 μg/mL streptomycin under 5% CO_2 and oxygen levels of 3% or 20% (95% air). Cells were grown under defined conditions (*e.g.* 20%, or 3% oxygen) for at least 48 hrs prior to experiments. During irradiation, cells grown under non-atmospheric oxygen levels were placed in gas-impermeable containers, otherwise the cells were minimally handled (~ 10 min) under normoxic conditions. Culture medium was purchased from Invitrogen.

MnSOD plasmids containing a 22-amino acid mitochondrial targeting sequence were a kind gift from Michael W. Epperly [67]. Cells were transfected with MnSOD plasmids using LiopfectaminePLUS (Invitrogen) according to the manufacturer's instructions. Cells were used 24 to 48 h after transfections. Upregulation of MnSOD was confirmed by western blotting and activity assays. MnSOD assays were performed +/- sodium cyanide which inhibits CuZnSOD but not MnSOD) on lysed cells and mitochondrial extracts using a kit from Cayman Chemical Co. as previously described [68].

To assess metabolic activity of cultured cells, BPAEC were incubated with alamarBlue (10% in medium) at 37ºC for 2 hours and subsequently assayed by measuring changes in the fluorescence intensity (ex. 535 nm; em. 590 nm). Mitochondrial membrane polarization ($\Delta\psi$) was determined by measuring JC-1 (Invitrogen) fluorescent changes (ex. 485 nm; em. 535 and 590 nm) using CCCP (carbonyl cyanide *m*-chlorophenylhydrazone) to establish complete depolarization (Invitrogen). Cells (1×10^6) were incubated with 2 μM JC-1 at 37ºC for 10 minutes, washed with PBS, then re-suspended in 2 mL PBS for fluorescence measurements [68]. Dihydrorhodamine-123 (DHR-123) (Invitrogen) was used as a detector of mitochondrial [69] oxidant production as described by Pastorino *et al.* [70]. The dye was incubated with media (control) or cells at a concentration of 10 μM for 1 hour at 37ºC. Cells were then washed twice with PBS prior to fluorescence detection of rhodamine-123 (ex. 500 nm; em. 535 nm). MitoSox™ was used as a mitochondrial detector of superoxide according to the method of Robinson *et al.* [71]. The dye was incubated in media alone (control) or with cells at a concentration of 1.0 μM for 20 minutes at 37ºC. Cells were then washed with PBS and incubation continued for an additional 40 minutes prior to fluorescence measurements (ex. 396 nm; em. 580 nm).

2.3.3 Titration experiments

Oxidation of ferrocytochromes in isolated preparations of bovine complex III, cytochrome *c* and complex IV were examined by titration with peroxynitrite solutions. The reactions were monitored by electronic absorption spectroscopy. Since the relevant extinction coefficients are known, changes in the absorption spectra can be related quantitatively to the extent of oxidation of the individual complexes following each addition of peroxynitrite solution. Therefore, in any given titration, it can be determined if the peroxynitrite behaved as a one-electron, two-electron or non-stoichiometric oxidant.

Prior to any oxidation, cytochrome c was reduced by a few grains of sodium dithionite and then passed through a Sephadex G-25 column to remove excess reductant , using 100 mM potassium phosphate, 1 mM EDTA, pH 7.4, as the elution buffer. The concentration of cytochrome c^{2+} was determined at 550 nm in the same buffer (ε_{550nm}= 28 mM^{-1} cm^{-1}) [72]. Cytochrome *c* oxidase and complex III were previously reduced before their oxidation by sodium peroxynitrite by titrating the enzymes with sodium dithionite before proceeding with the titrations.

Stable, hydrogen peroxide-free, alkaline (pH ~12) solutions of sodium peroxynitrite were prepared as indicated in equation 1, following the recommendations of Beckman *et al. [58]*. Briefly, high yields of peroxynitrite were obtained at room temperature mixing acidified hydrogen peroxide with sodium nitrite; after an appropriate delay (~1 s), the reaction was quenched with strong alkali (sodium hydroxide) and all excess of peroxide was removed by manganese oxide

Presence of carbon dioxide was achieved by adding necessary amount of saturated sodium bicarbonate (~1M) into the enzyme solutions, in order to obtained the required

concentration of bicarbonate (usually 40 mM, except in the case when CO_2 concentrations needed to be varied). Enzyme solutions and saturated bicarbonate were in a closed system with rubber septa in order to prevent CO_2 leakage that could increase the pH.

Enzyme solutions (5-35 μM) were titrated with concentrated solution of sodium peroxynitrite (~25 mM). All quantitative transfers of oxygen gas, sodium peroxynitrite , sodium bicarbonate solutions were made using Hamilton gas-tight syringes fitted with new stainless steel needles into the reaction cell. Samples that required anaerobic conditions were achieved by blowing argon over the top of solutions at room temperature for 10-15 min, with mild agitation. Anaerobic samples were then maintained in glass vessels closed with rubber septa. In the case of sodium dithionite and bicarbonate solutions, water and powders were made anaerobic separately, mixing them afterwards. For variable oxygen concentrations, anaerobic samples were titrated with oxygen by transferring aliquots of oxygen gas. At no time solutions of these reagents were left standing in contact with syringe needles. The pH of all protein samples was verified at the end of the experiments to ensure that the conditions had not become significantly more alkaline by additions of peroxynitrite solution.

2.3.4 Product analyses

Aliquots from the titrations of cytochrome *c* (with presence or absence of oxygen and/or bicarbonate) were assayed for 3-nitrotyrosine, hydrogen peroxide and nitrite. For the latter twom samples were placed in Microcon YM-3 Centrifugal Filter Units tubes (Millipore Inc.) and centrifuged at 14000 rpm for 45 minutes with an Eppendorf Centrifuge 5415 and the filtrates were used to determine their content of hydrogen peroxide and nitrite. In the case of 3-

nitrotyrosine assay, the aliquots were ready to use for the specific assay. Samples, standards and controls were made in duplicate.

2.3.4.1 Hydrogen Peroxide

Hydrogen peroxide content in samples was measured with the Amplex Red®Hydrogen Peroxide/Peroxidase Assay Kit. The instructions provided by the manufacturer were followed. Briefly, The Amplex® Red reagent (10-acetyl-3,7-dihydroxyphenoxazine) reacts with H_2O_2 in the presence of HRP with a 1:1 stoichiometry to form resorufin, the fluorescent product The plate reader was set at 544 and 590 nm for excitation and emission, respectively.

2.3.4.2 Nitrite

Nitrite analysis was performed by following the Griess Assay, which was first describe by Griess [66]. The assay is based on the formation of a transient diazo salt from nitrite and a diazotizing agent (sulfanilamide) under acidic (phosphoric acid) conditions. This short-lived product quickly reacts with N-1-naphthylethylenediamine dihydrochloride (NED) to form a stable colored azo compound. The intense purple color of the product allows the nitrite assay with high sensitivity and can be used to measure nitrite concentration as low as ~0.5 mM level. The absorbance of this adduct at 540 nm is linearly proportional to the nitrite concentration in the sample [73]. Griess reagent was made as one part of 1% of sulfanilamide in 5% phosphoric acid, and one part of 0.1% NED.

2.3.4.3 3-Nitrotyrosine

3-Nitrotyrosine content was assessed using the Nitrotyrosine ELISA Kit (Millipore Inc, cat # 17-376) according to manufacturer‘s instructions. Briefly, high-binding BD Falcon 96 well

plates were incubated with antigen BSA in freshly prepared coating buffer ($Na_2CO_3/NaHCO_3$, 50 mM, pH 9.6). Subsequently, samples, controls and standards were incubated with anti-nitrotyrosine antibody, followed by the incubation of the secondary antibody, the Anti-Rabbit IgG, HRP-conjugate. Formation of 3-nitrated BSA can be measured at 450 nm after treating with the commercial chemiluminescent substract. Moles of 3-nitrotyrosine were calculated by the following equation:

$$1\,\mu M\ Nitrotyrosine = \frac{A\ \mu g(NitroBSA)}{mL} * \frac{10^{-9}\frac{g}{l}}{1\frac{\mu g}{mL}} * \frac{10^{6}\mu mol\ NitroBSA}{68000g} * \frac{5.6\,mol\ Nytrotyrosine}{mol\ NitroBSA} \quad [6]$$

Equation 6. Conversion to nitrotyrosine concentration from moles detected of NitroBSA.

2.3.4.4 Peroxynitrite-modified ferricytochrome *c*

Peroxynitrite-modified forms of cytochrome *c* were prepared essentially as described by Cassina *et al.* [38, 59] but in the presence or absence of sodium bicarbonate as required. Typically, small aliquots of sodium peroxynitrite (~ 0.1 mM in 1mM NaOH) were titrated into cytochrome *c* (0.1 mM in 200 mM sodium phosphate buffer, pH 7.4) by multiple small volume additions. The electronic absorption spectrum was examined for the presence of the 695 nm band and its absence was used as an indicator for the complete reaction of the protein in the absence of bicarbonate. Several such samples were then combined and extensively dialyzed against 50 mM phosphate buffer, pH 7.4, before the protein was passed through a Sephadex G-25 gel-filtration column, concentrated, and then finally dialyzed against the required buffer. The concentration of the peroxynitrite-modified cytochrome *c* samples were determined by a

pyridine hemochrome assay using ε_{550}= 31.2 $mM^{-1}cm^{-1}$ [74]. Structure analysis was performed by EPR. Formation of 3-nitrotyrosine, following the addition of sodium peroxynitrite to cytochrome *c*, was measured as previously described in 2.3.4.3.

2.3.4.5 Mass spectral Analysis

Native or peroxynitrite-modified *bovine* cytochrome *c* was diluted into 0.1% acetic acid and analysis was performed by direct infusion into a triple quadrupole ESI mass spectrometer. The sheath flow was adjusted to 5μL/minute and the solvent consisted of 50% acetonitrile containing 0.1% (w/w) acetic acid. The electrospray probe was operated at a voltage differential in the range of +2.3 to +3.5 keV in the positive ion mode and source temperature was maintained at 70 ^{o}C. Scanning was performed in the range of 400-1700 every 3.5 s and individual spectra were summed. Ion series were deconvoluted and converted to molecular (+1 charged) spectra by a maximum entropy algorithm using software supplied by the manufacturer.

2.3.5 Kinetics experiments

2.3.5.1 Kinetics of the oxidation of cytochrome c by sodium peroxynitrite

A 200 mM phosphate buffer was used as solution media for the enzymes, adjusting pH depending on the required conditions. All solutions of sodium peroxynitrite were made in 1mM sodium hydroxide. All product solutions were checked for pH after each experiment to warrant that conditions had not become significantly more alkaline after additions of sodium peroxynitrite or sodium bicarbonate. On the stopped-flow kinetic experiments, the temperature

of the stopped-flow spectrophotometer reaction chamber and observation cell were maintained constant using a circulating water bath.

2.3.5.2 Effect of pH and temperature

A solution of 10 μM cytochrome *c* was quickly mixed in 1:1 proportion with different concentrations in excess of sodium peroxynitrite solutions (10, 20, 30, 40 and 50 fold in excess relative to cytochrome *c*). Three different pHs were adjusted in the buffer media by means of addition of diluted solutions of NaOH or HCl, getting final pH of 6.0, 7.0 and 9.0, respectively. Two sets of experiments were designed for each pH, working with two different constant temperatures at the observation cell: 25°C and 37°C.

2.3.5.3 Oxygen dependence of the reaction rate

In order to check the dependence on oxygen content, a solution of 10 μM cytochrome *c* was rapidly mixed with a solution of 100 μM sodium peroxynitrite. Two different pHs were checked, pH=6 and pH=8 at the same temperature (25^{o}C) for each condition (aerobicity and anaerobicity).

2.3.5.4 Decomposition of sodium peroxynitrite

Sodium peroxynitrite decay was checked at the 302 nm absorbance band followed in the stopped-flow spectrophotometer, with a time of 10 s. The sample solution was made by having a 1:20 dilution of concentrated $ONOO^-$ (in 200 mM Phosphate buffer (pH=7). Conditions of anaerobicity, 20% and 100% O_2 were tested, all at room temperature.

2.3.5.5 Effect of the the CO_2/HCO_3^- system

Different concentrations of sodium bicarbonate were achieved by adding enough volume of a saturated solution (~1 M) into the cytochrome *c* solution, by means of gas tight Hamilton syringes. Equal quantities of ferrocytochrome *c* (5 μM) and sodium peroxynitrite (46 μM) were rapidly mixed at room temperature and pH=7.

2.3.5.6 Kinetics of the oxidation of cytochrome c oxidase by sodium peroxynitrite

A 5 μM solution of cytochrome *c* oxidase was rapidly mixed with different concentrations of sodium peroxinitrite (as described above). Rate of decrease in absorbance as a result of the oxidation of the cytochrome *c* oxidase by peroxinitrite was monitored using a photodiode array. All kinetic measurements were performed at pH 7 and the temperature of the stopped-flow spectrophotometer reaction chamber and observation cell was maintained at 10°C using a circulating water bath.

2.3.5.7 DHR_{123} kinetics

Concentration of DHR_{123} was monitored spectrophotometrically at 289 nm following the extinction coefficient ε_{289nm}(MeOH) =7,100 $M^{-1}cm^{-1}$ [56]. Hydroethidine concentration was also spectrophotometrically measured as ethidium, using an extinction coefficient ε_{260} =6,600 $M^{-1}cm^{-1}$ [75]. The oxidized enzyme solutions (5-35 μM) were titrated with dihydroethidium (MitoSox™) (~1.8 mM) and dihydrorhodamine 1,2,3 (~1.1 mM). All quantitative transfers and reaction conditions were achieved as previously described in the titrations of the enzymes with peroxynitrite.

Turnover rates with HE will be measured by monitoring the appearance of Etd^+ at 480 nm (ε_{488} = 5.8 x 10^3 M^{-1} cm^{-1}). The electronic absorption spectrum and the fluorescence spectrum of the product of the reaction with cytochrome *c* oxidase can be obtained by quickly removing the enzyme from the reaction mixture using a centricon.

2.3.6 Superoxide spin trapping

Ferrocytochrome *c* 1 mM in 200 mM phosphate buffer, pH 7.4, was combined with 50 mM of the spin trap BMPO (5-tert-butoxycarbonyl 5-methyl-1-pyrroline N-oxide). Controls were prepared as two: one anaerobic solution of 1 mM ferrocitochrome c and an aerobic solution of ferricytochrome *c*, all treated with DMPO with the same approach. After 3 hours, the samples and controls were flash frozen, and analyzed by EPR .

3.0 REACTIONS OF MITOCHONDRIAL CYTOCHROMES WITH PEROXYNITRITE: VARIABLE STOICHIOMETRIES IN ELECTRON TRANSFERS AND CHANGED FUNCTIONALITY OF COVALENTLY MODIFIED CYTOCHROME *C*

Elisenda Lopez Manzano[1@], Daniel E. Winnica[1@], Leah K. Cambal[1], Megan R. Swanson[1], Mai Otsuka[2], Andrew. A. Amoscato[1], Quan Yuan[1] Jim Peterson[1]* and Linda L. Pearce[1]*

[1]Department of Environmental and Occupational Health
University of Pittsburgh Graduate School of Public Health
100 Technology Drive, Pittsburgh, PA 15219 USA
and [2]Department of Chemistry, Carnegie Mellon University
4400 Fifth Avenue, Pittsburgh, PA 15261 USA

*Corresponding Authors: lip10@pitt.edu; jpp16@pitt.edu

3.1 ABSTRACT

The reaction of the reduced forms of isolated bovine complex III (cytochrome *c* reductase) cytochrome *c* and complex IV (cytochrome *c* oxidase) with peroxynitrite have been studied in the presence and absence of CO_2 added as bicarbonate. The presence of CO_2 signifcantly modulates the mechanisms and extent of the observed cofactor oxidations. In the case of ferrocytochrome *c*, where it was practical to perform experiments aerobically, the presence of O_2 was unexpectedly observed to catalyze the oxidation of the cytochrome by peroxynitrite – some residual effect remaining detectable even in the presence of a 160-fold molar excess of bicarbonate over oxygen. It is suggested that all these processes may be important in mitochondria under various circumstances, perhaps in different microenvironments. Also, the characteristics of peroxynitrite-modified ferricytochrome *c,* prepared in the presence and absence of bicarbonate, have been examined by a variety of EPR, electronic spectroscopic and mass spectrometric methods. These data clearly indicate that, unlike the nitrated-tyrosine derivatives obtained if the reaction between peroxynitrite and cytochrome *c* is carried out in the presence of added bicarbonate, in the absence of bicarbonate oxidation of the methionine 80 axial heme ligand to methionine sulfoxide results. The sulphoxide is a weaker ligand than the native methionine and, consequently, under neutral/mildly alkaline conditions, the sixth position of the haem iron is predominantly occupied by one of the available lysines – forms known to exhibit lowered reduction potentials. Neither type of peroxynitrite-modified cytochrome *c* (*i.e.* prepared +/- bicarbonate) can accept electrons from ubiquinone/complex III and thus, they cannot support electron transfer to complex IV. However, significant amounts of either type of modified cytochrome (50%) do not prevent native (unmodified) cytochrome *c* from being reduced by ubiquinone/complex III at a normal rate. During complex IV turnover by native

ferrocytochrome *c* at low ionic strength (10 mM phosphate) increased rates are observed when the modified cytochrome *c* is added – indicating preferential binding of the modified cytochrome to a high affinity/low activity electron-entry site on the enzyme, directing native ferrocytochrome *c* to bind to a lower affinity/higher activity site. It is not clear that formation of small quantities (< 50% conversion) of either peroxynitrite-modified cytochrome *c* need necessarily be proapoptotic.

3.2 INTRODUCTION

It has long been hypothesized that the mitochondrial electron-transport chain (ETC) is a significant source of superoxide and secondary damaging oxidants for the cell as a whole (*e.g.* [76-79]). While this behavior may have been overemphasized with regard to normal physiological circumstances [80-81] there are numerous pathophysiological situations in which mitochondrial generation of superoxide appears significant, including the ionizing radiation-induced apoptosis and inflammation of interest to our group [68, 82]. Particularly when nitric oxide production becomes elevated, peroxynitrite is arguably the most important reactive oxidant formed secondary to superoxide – the diffusion-limited reaction between nitric oxide and superoxide even outcompeting superoxide dismutase for its substrate [83] [24], [47]. Peroxynitrite is a strong oxidant that can reversibly abstract electrons from reductant molecules such as reduced protein cofactors [84], [41], [33]. Alternately, peroxynitrite is able to covalently modify carbohydrates, lipids, nucleic acids and proteins; known modifications to the latter

include tyrosine nitration and methionine oxidation [83], [24], [47]. The preference that peroxynitrite might display towards undergoing one rather than both types of reaction is of interest because while reversible electron transfer might be essentially non toxic, covalent modification can change both molecular recognition characteristics and enzymatic function.

As the mitochondrial ETC is a possible source of superoxide, several groups, including ours, have investigated the reactions of peroxynitrite with members of the ETC. However, to our knowledge, there are no previous reports regarding the effect of carbon dioxide and oxygen on the oxidation of reduced ETC cofactors. In vivo, many tissues exist under relatively low oxygen tensions at which the ETCs are at least partly reduced. Previously, we observed that fully and partially reduced forms of isolated cytochrome *c* oxidase (complex IV) were oxidized by peroxynitrite in a direct two-electron process with a rate constant that we estimated to be at least 10^6 $M^{-1}s^{-1}$ [33]. Subsequent examination of several other complexes of the ETC (I, II, III and cytochrome *c*) also showed that these could be reversibly oxidized and then reduced with no loss of function unless the peroxynitrite was added in great excess [84], [41]. The redox chemistry of peroxynitrite can be quite complicated (see Goldstein [83] for a review). Peroxynitrite, by itself, can react in a direct reaction (with one or two electrons transferred) or in an indirect fashion via degradation products of peroxynitrous acid (see Figure 13 below). Alternately, the peroxynitrite anion can react extremely rapidly with carbon dioxide, leading to some quite different subsequent chemistry (see Figure 13 below):

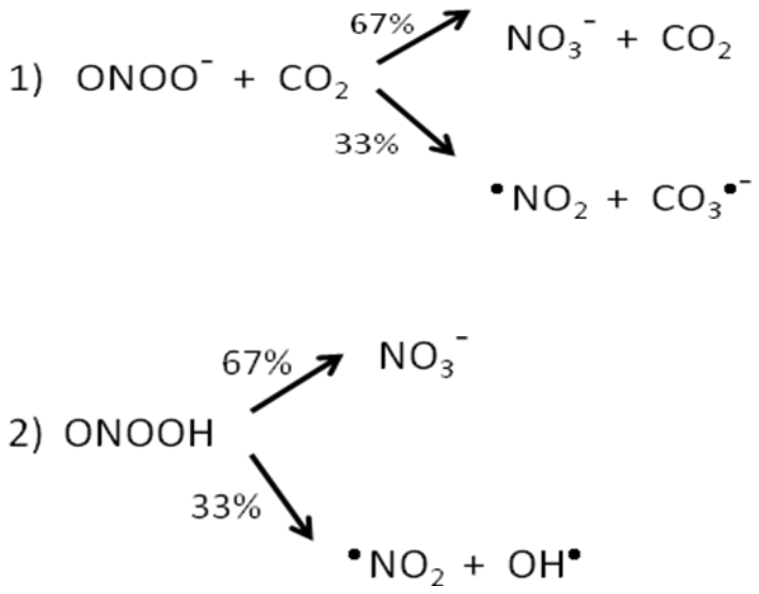

Figure 13. Reaction of peroxynitrite with carbon dioxide.

The reaction of peroxynitrite with carbon dioxide leads to the production of carbonate radical with a ~33% yield. Carbonate radical can later undergo one electron oxidations.

These processes explain, for example, why carbon dioxide promotes the peroxynitrite-dependent nitration of tyrosine in proteins; the proposed mechanism involving abstraction of a hydrogen atom from the phenolic ring by carbonate radical, followed by addition of the nitrogen dioxide radical to the intermediate phenolic radical. Accordingly, we have undertaken an examination of the reactions of reduced forms of several members of the mitochondrial ETC with peroxynitrite in the presence of CO_2 and in one case at variable oxygen tension. Reactions of the cofactors (predominantly hemes) of isolated bovine cytochrome *c*, complex IV (cytochrome *c* oxidase) and complex III (cytochrome *c* reductase) with authentic peroxynitrite are reported with at least two unexpected results.

The product of reactions of (already oxidized) equine and bovine (ferri) cytochromes *c* with peroxynitrite have been reported to be primarily derivatives nitrated at tyrosine 67 that were not reducible by ascorbate and were non-functional in the electron-transport chain when incorporated into mitochondria depleted of native cytochrome *c* [38]. In keeping with the suggestions of others [85] it was argued that peroxynitrite-dependent nitration of cytochrome *c* promotes its release from mitochondria and is therefore pro-apoptotic. The previous studies were performed with peroxynitrite-modified cytochrome *c* prepared in the presence of added sodium bicarbonate (> 20 mM) to promote tyrosine nitration. Here we have undertaken an investigation of the effects of peroxynitrite on bovine cytochrome *c* *both* in the presence and absence of added bicarbonate, but focusing on the latter. The peroxynitrite-modified derivative formed in the presence of bicarbonate we call NT-cytochrome *c* and, for reasons that will become clear, the derivative formed in the absence of bicarbonate we refer to as MS-cytochrome *c*.

Neither of the peroxynitrite-modified cytochromes *c* (MS- nor NT-) seem able to accept electrons from complex III of the ETC and so are non-functional in this respect. However, even in pathophysiological situations, it seems highly unlikely that all the native cytochrome *c* in the functioning mitochondria of a still viable cell could become peroxynitrite modified. Consequently, we have also undertaken an investigation into the effect that the addition of the peroxynitrite-treated cytochromes have on the turnover of isolated preparations of complex III and complex IV in the presence of similar levels of native (unmodified) cytochrome *c*. In view of the results, some possible counterintuitive consequences of the presence of relatively low levels of peroxynitrite-modified cytochrome *c in vivo* are discussed.

3.3 RESULTS

3.3.1 Oxidation of reduced complex III by peroxynitrite

Dilute sodium dithionite solution was titrated into complex III samples (0.2 M sodium phosphate buffer, pH 7.4, 22 ºC) until the cytochromes *b* and c_1 were just fully reduced, as determined by no further increases being observed in the measured absorbances at 553 nm and 562 nm (Figure 14A, main panel). In some cases it was confirmed by EPR measurements that this procedure also resulted in reduction of the Rieske iron-sulfur (2Fe-2S) center (Figure 14A, inset). Re-oxidation of complex III by peroxynitrite during anaerobic titrations was followed by monitoring the visible-region absorption bands (Figure 14B). Absorbance changes at 562 nm reflect oxidation of the 2 *b*-type cytochromes (b_L: lower potential heme; b_H: higher potential heme) and absorbance changes at 552 nm reflect oxidation of the c_1-type cytochome together with the Rieske center. As expected, oxidation of the *b*-type cytochromes was observed initially and followed subsequently by oxidation of the c_1 cytochrome (and Rieske center by implication). Mole-fractions of oxidized cofactors were calculated as $1-[(A-A_{final})/(A_{initial}-A_{final})]$ taking the absorption measurements at both wavelengths indicated above. In the axis legends (Figure 14B) ~~–r~~edox centers" refers to the total metalloprotein oxidation-reduction cofactors present (*i.e.* 1 heme c_1 + 2 hemes *b* + 1 Fe_2S_2). The broken line represents the theoretical relationship predicted for peroxynitrite behaving as a one-electron acceptor (*e.g.* $ONO_2^- + H^+ + e^- \rightarrow NO_2^\bullet + OH^-$). Clearly, the reaction between reduced complex III and peroxynitrite is substoichiometric with respect to the oxidant (■) implying that complex III oxidation is probably carried out by peroxynitrite decomposition products, rather than direct reaction with either ONO_2^- or ONO_2H. An analogous titration was performed, but this time in the presence of 40 mm bicarbonate, in

which case virtually no oxidation of complex III was observed (13B, ●). Consequently, the reaction between peroxynitrite and Complex III must be slower than that between peroxynitrite and CO_2 (k_2 ~2 x 10^4 $M^{-1}s^{-1}$) [83].

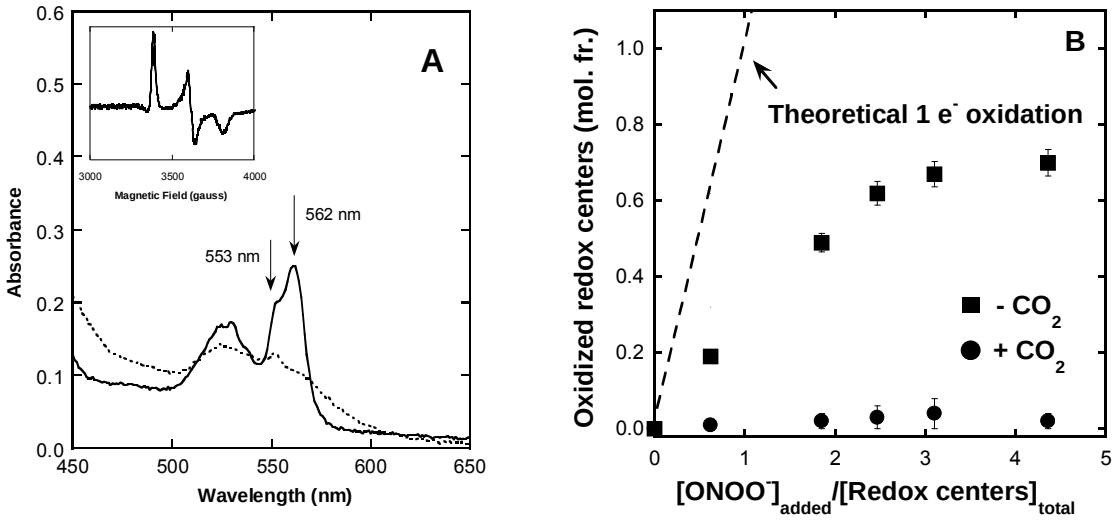

Figure 14. Oxidation of bovine complex III (bc_1, cytochrome *c* reductase) with sodium peroxynitrite.

A: Electronic absorption spectra of oxidized (dotted trace) and sodium dithionite-reduced (solid trace) complex III, 10 μM in 0.1 M postassium phosphate buffer, 0.1 % lauryl maltoside, pH 7.4, 1.0 cm path length, 22 °C. Inset: X-band EPR spectrum of Reiske iron-sulfur center ($[2Fe\text{-}2S]^+$ core) of complex III, 15 K. B: Oxidation of complex III (initially reduced using a minimum of sodium dithionite solution) by sodium peroxynitrite. Reactions were followed spectrophotometrically (see text for further details) at 22 °C. A volume of 3.0 mL of 7.0 μM cytochrome *c* reductase in 100 mM sodium phosphate buffer, 0.1 % lauryl maltoside, pH 7.4 –7.6, was subjected to the addition of 10 μL aliquots of peroxynitrite solution under anaerobic conditions (♦) and anaerobic in the presence of CO_2 (40 mM sodium bicarbonate, ●). The *ordinate* corresponds to the mole fraction of total oxidized metal centers present in individual experiments (*i.e.* 1 heme c_1 + 2 hemes *b* + 1 Reiske Fe-S). The *broken line* represents the theoretical relation for peroxynitrite behaving as a one-electron acceptor.

3.3.2 Oxidation of ferrocytochrome *c* by peroxynitrite

The reaction of ferrocytochrome *c* with peroxynitrite has previously been investigated both by ourselves and other groups. It has been reported [38] that, under aerobic conditions, ferrocytochrome *c* appears to react in a direct fashion with peroxynitrite in a one-electron process with a second order rate constant of 2.3×10^5 $M^{-1}s^{-1}$. Confoundingly, however, the same reaction did not seem to proceed under anaerobic conditions [33]. In the present study, ferrocytochrome *c* has been titrated with peroxynitrite under a greater range of conditions (Figure 15): aerobically, anaerobically, aerobically with CO_2 (added as sodium bicarbonate) and anaerobically with CO_2. Undoubtedly, the aerobic reaction (0.8 (± 0.2) ferrocytochromes oxidized per peroxynitrite added, ■) at least approximates to a one-electron process (broken line) – this result is seemingly uncontroversial. Also, we have again found that removal of oxygen significantly suppresses the reaction (0.20 (± 0.05) ferrocytochromes oxidized per peroxynitrite added, ●).

Cassina *et al.* [59] found that the presence of bicarbonate/CO_2 did not interfere with the reaction between peroxynitrite and ferrocytochrome *c*, but we now find a very significant effect to the contrary. During titrations of ferrocytochrome *c* with peroxynitrite in the presence of added bicarbonate we observed very little oxidation of the cytochrome either in the presence (0.1 ± 0.05 ferrocytochromes oxidized per peroxynitrite added, □) or absence (0.04 ± 0.01 ferrocytochromes oxidized per peroxynitrite added, ○) of oxygen. This observation is consistent with excess bicarbonate (40 mM) reacting rapidly with peroxynitrite and thus suppressing the reaction with ferrocytochrome *c*. The extent of ferrocytochrome *c* oxidation by peroxynitrite was inversely related to the amount of bicarbonate in solution (Figure 16A). A modifying effect of bicarbonate/CO_2 on reaction(s) with peroxynitrite has been shown for a number of other proteins. Interestingly, the ferocytochrome *c* response appeared to be nearly maximal at 10 nM

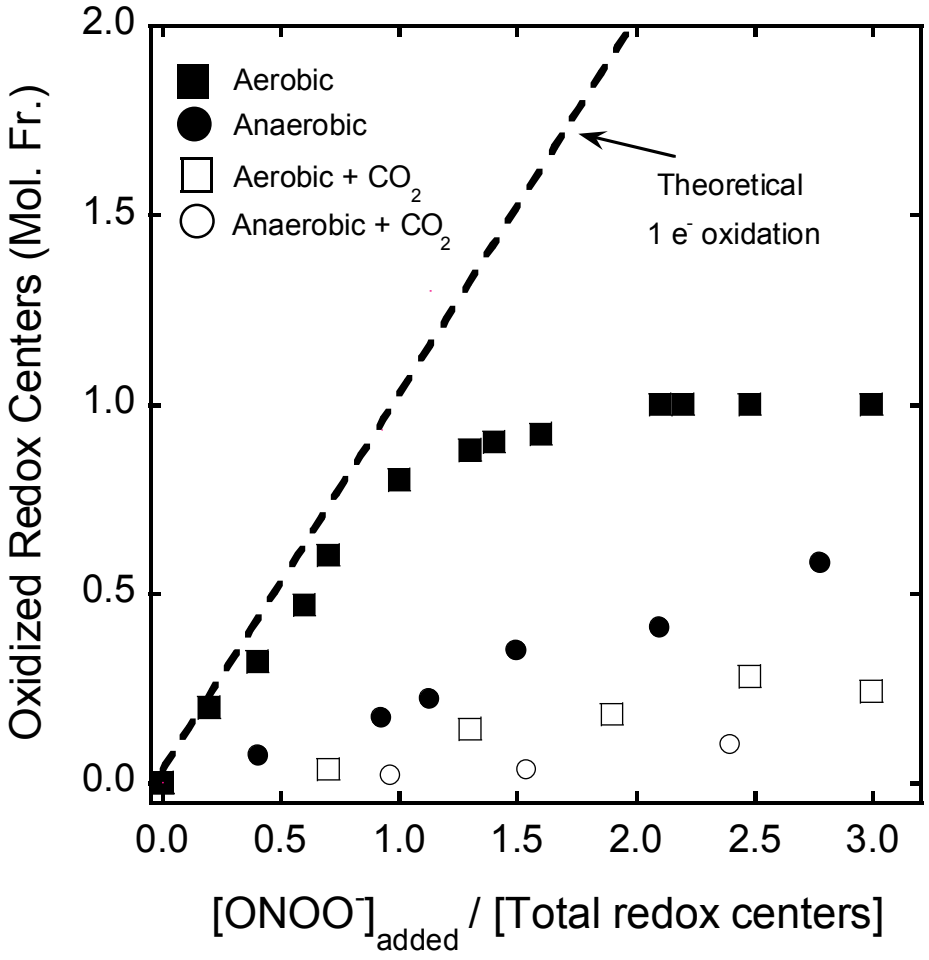

Figure 15. Oxidative titrations with sodium peroxynitrite of bovine ferrocytochrome *c*.

Reactions were followed spectrophotometrically at 550 nm, 22 °C. A volume of 3.0 mL of 35 μM ferrocytochrome *c* in 0.2 M sodium phosphate buffer, pH 7.4 – 7.6, were subjected to the addition of 10 μL aliquots of sodium peroxynitrite solution under aerobic conditions (♦), anaerobic conditions (●), aerobically with 40 mM sodium bicarbonate (□) and anerobically with 40 mM sodium bicarbonate (○). The *broken line* represents the theoretical relation for peroxynitrite behaving as a one-electron acceptor.

added bicarbonate (Figure 16A) close to the bicarbonate concentration thought to exist in the mitochondrion [83]. Subsequent stopped-flow experiments following the oxidation of ferrocytochrome *c* by excess peroxynitrite showed a linear dependence on bicarbonate concentration (Figure 16B) and suggested a pseudo-first order rate constant of 1.9 (± 0.2) x 10^4 $M^{-1}s^{-1}$ at pH 7.4, 25°C. This result is consistent with the oxidation of ferrocytochrome *c* by the products of an initial reaction between peroxynitrite and bicarbonate/CO_2 (k_{11} = 2.9 (± 0.3) x 10^4 $M^{-1}s^{-1}$, 24°C at pH 6.2) [83] – a reasonable finding as reactions of peroxynitrite proceeding via decomposition product(s) are more common than direct reactions of the anion or molecular acid [83].

In the absence of added bicarbonate/CO_2, oxidation of ferrocytchrome *c* by peroxynitrite in titrations at different oxygen levels demonstrated a clear dependence of this chemistry on oxygen concentration (Figure 16C). To rationalize this unexpected observation, possible kinetic explanations were considered. The peroxynitrite anion is quite stable, but the molecular acid form, which predominates at pH < 6.8 is much more reactive [24] and, consequently, peroxynitrite chemistry at pH ~7 usually involves competition between its decomposition and reactions with any other species that may be present. However, while in a series of peroxynitrite decomposition experiments (pH-jump from pH 11 to pH 7.0 by stopped-flow) we did find that the kinetics exhibited some oxygen dependence, the effect was small and, most importantly, there was no significant difference between the results at 21% and ~0% oxygen (Table 1). Therefore, the titration data (Figure 15) cannot be explained on the basis of oxygen somehow stabilizing peroxynitrite thereby allowing more of it to react with ferrocytochrome *c* rather than decompose.

In further stopped-flow experiments, where ferrocytochrome *c* was exposed to excess peroxynitrite, a modest but reproducible dependence of the reaction rate on oxygen concentration was observed (Table 2). This result does suggest an explanation for the titrations, but the argument is a little complicated, as simple inspection of the data (Figure 16) seems to suggest that at 21% oxygen the rate should be about an order of magnitude faster than at the lower end of the oxygen concentration range.

Table 1. Observed rates of decomposition of sodium peroxynitrite with variable oxygen concentrations.

Peroxynitrite (0.5 mM) was rapidly mixed with phosphate buffer (200 mM), pH 7.0 at 25°C and the decay followed at 302 nm.

O_2	k_{obs} (s^{-1})
0%	0.31 ± 0.02
21%	0.30 ± 0.05
100%	0.22 ± 0.03

Table 2. Observed rate constants for the oxidation of ferrocytochrome *c* and excess peroxynitrite under aerobic and anerobic conditions

Ferrocytochrome *c* (final concentration 15 μM) was reacted with a 10-fold excess of peroxynitrite (150-500 μM) at 25°C in 200 mM phosphate buffer, 1 mM EDTA.

O_2	k_{obs} (s^{-1}) pH = 6.0	k_{obs} (s^{-1}), pH = 8.0
21% (aerobic)	47 ± 2	7.0 ± 0.9
0% (anaerobic)	38 ± 3	5.7 ± 0.9

First, we note that in the titration experiments (Figure 16C) ferrocytochrome *c* was always present in excess over added peroxynitrite, whereas the opposite was true in the stopped-flow experiments (Table 2). In this latter case, the levels of peroxynitrite decomposition products, including oxygen [83], can be substantial. Thus, we cannot be particularly confident that the reaction rates measured at nominal 0% oxygen were entirely oxygen-free determinations. Since autoxidations of ferrocytochromes [86-87] as well as other heme proteins [88] are proposed to involve production of superoxide, we suggest that the oxidation of ferrocytochrome *c* by peroxynitrite proceeds as follows:

3) $\text{Cyt } c^{2+} + O_2 \leftrightarrows \text{Cyt } c^{3+}{:}O_2^-$ (where the product is an undissociated ion pair)

4) $\text{Cyt } c^{3+}{:}O_2^- + \text{HOONO} \rightarrow \text{Cyt } c^{3+} + OH^- + O_2 + {}^{\bullet}NO_2$

Consistent with this suggestion, analysis of the products of the reaction mixtures (both in the presence and nominal absence of oxygen) revealed no hydrogen peroxide production and approximately 60 ±5 % nitrite production consistent with ${}^{\bullet}NO_2$ decomposition to roughly equimolar amounts of nitrite and nitrate. The primary electron exit site on the surface of cytochrome *c* contains several lysine residues resulting in a net positive charge at neutral pH [89] that would tend to stabilize the proposed ion pair intermediate. In addition to oxygen, other species present (unavoidable decomposition products of *excess* peroxynitrite) may also be able to act as redox mediators (or otherwise interfere) in the oxidation of ferrocytochrome *c*, leading to an *apparent* decrease in the magnitude of the measured oxygen dependence of the rate. Overall then, there is arguably no inconsistency between the two sets of oxygen dependence data (Figure 16C and Table 2)

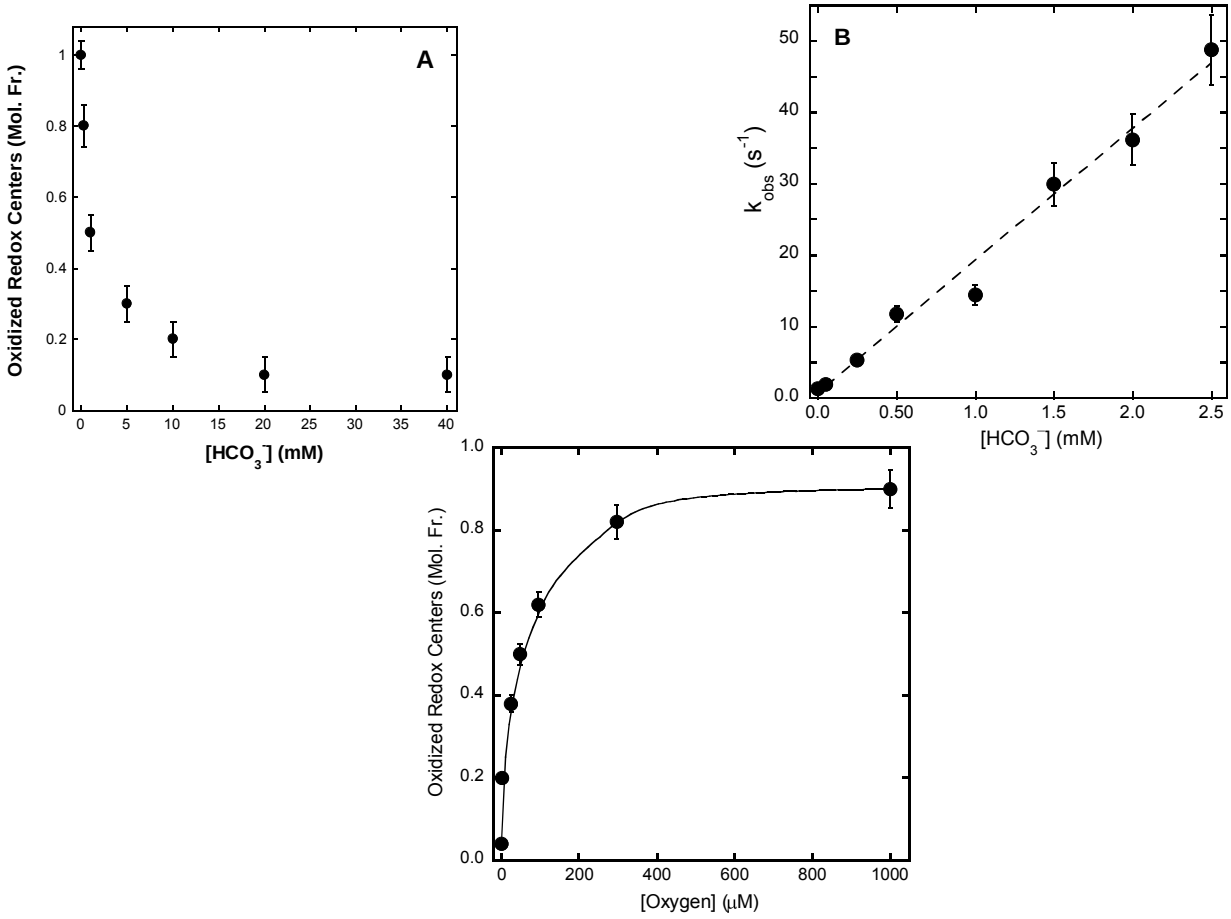

Figure 16. Dependence of the oxidation of reduced cytochrome *c* by sodium peroxynitrite on CO_2 and O_2.

A: Aerobic titrations of ferrocytochrome *c* (35 μM) by sodium peroxynitrite in the presence of sodium bicarbonate (0 - 40 mM), 0.2 M sodium phosphate buffer, pH 7.4 – 7.6 at 22 °C. B: The dependence of the oxidation rate of ferrocytochrome *c* (3.5 μM) by excess peroxynitrite (35 μM) on sodium bicarbonate (0 - 2.5 mM) followed by stopped-flow spectrophotometry at 550 nm. Experiments were carried out in 0.2 M sodium phosphate buffer, pH 7.4 – 7.8 at 25 °C. C: Titrations of ferrocytochrome *c* (35 μM) in 0.2 M sodium phosphate buffer, pH 7.4 – 7.6 at 22°C, by peroxynitrite followed spectrophotometrically at 550 nm in the presence of 0 – 1.0 M oxygen.

3.3.3 Oxidation of reduced complex IV by peroxynitrite

Dilute sodium dithionite solution was titrated into complex IV samples containing 1.5 equivalents of cytochrome *c* (0.2 M sodium phosphate buffer, pH 7.4, 0.1% lauryl maltoside, 22 ºC) until the complex IV and cytochrome *c* were just fully reduced, as determined by no further increases being observed in the measured absorbances at 604 nm and 550 nm (Figure 17A). The presence of cytochrome *c* in these experiments (a potential complication) was unavoidable as complete reduction of complex IV by direct reaction with roughly stoichiometric amounts of dithionite does not occur. Re-oxidation of complex IV and cytochrome *c* by peroxynitrite during anaerobic titrations was followed by monitoring the visible-region absorption bands (Figure 17B). Mole-fractions of ferricytochrome *c* were calculated as $1-[(A-A_{final})/(A_{initial}-A_{final})]$ taking the absorption measurements at 550 nm. Mole-fractions of oxidized complex IV were calculated employing the same general expression, but using absorption changes measured at 604 nm. In the axis legends, ~~–r~~edox centers" refers to the complete set of metalloprotein cofactors present in the mixture of cytochromes (*i.e.* 1.5 heme *c* + 1 Cu_A + 1 heme *a* + 1 heme a_3 + 1 Cu_B). The solid line represents the theoretical relationship predicted for peroxynitrite behaving as a two-electron acceptor (*e.g.* $ONO_2^- + 2H^+ + 2e^- \rightarrow NO_2^- + H_2O$). Clearly, in agreement with previous findings [33], peroxynitrite behaves as a two-electron acceptor towards both ferrocytochrome *c* and reduced complex IV when they are present together in the absence of CO_2. That is, complex IV actually catalyzes the oxidation of ferrocytochrome *c* by peroxynitrite in a facile reaction that is at least faster than the uncatalyzed decomposition rate of peroxynitrite, the half-life of which is estimated to be < 1 s at physiological pH depending upon the particular buffer composition [16, 25].

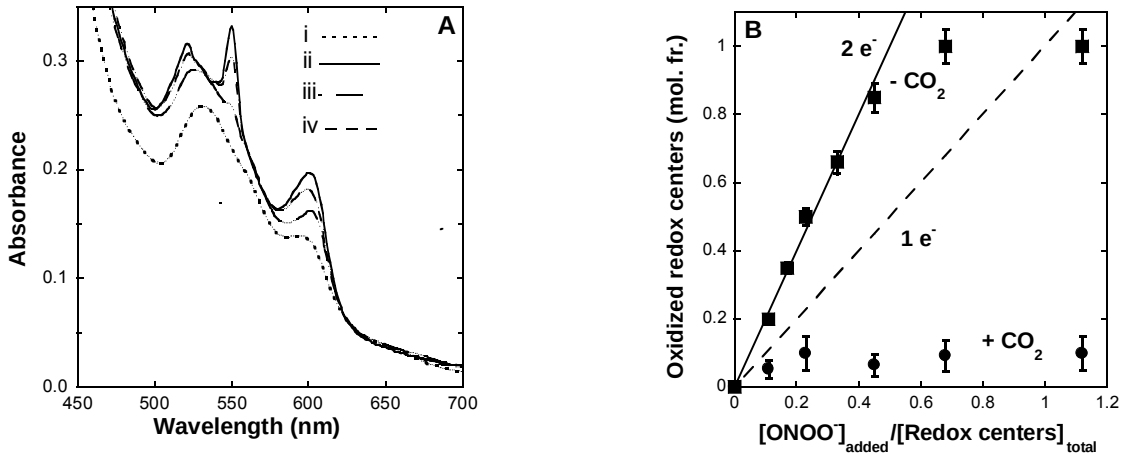

Figure 17. Oxidation of bovine complex IV (cytochrome *c* oxidase) + ferrocytochrome *c* with sodium peroxynitrite.

A: Electronic absorption spectra of oxidized complex IV (7.0 μM) + ferricytochrome *c* (5.0 μM) in the presence of 40 mM sodium carbonate, 0.1 M postassium phosphate buffer, 0.1 % lauryl maltoside, pH 7.4, 1.0 cm path length, 22 °C. Initially oxidized cytochromes as prepared; following reduction using a minimum of sodium dithionite solution; following the further addition of 1 equivalent of sodium peroxynitrite; after 15 min reaction time. B: Oxidative titrations followed spectrophotometrically (see text for further details). 3.0 mL of 7.0 μM complex IV + 5.0 μM cytochrome *c* in 0.2 M sodium phosphate buffer, pH 7.4 –7.8, were subjected to the addition of 10 μL aliquots of peroxynitrite solution under anaerobic conditions (■) and anerobically in the presence of CO_2 (●). The *ordinate* corresponds to the mole fraction of total oxidized metal centers present in individual experiments (*i.e.* 1.5 hemes *c* + 1 Cu_A + 1 heme *a* + 1 heme a_3 + 1 Cu_B). The solid line represents the theoretical relationship for peroxynitrite behaving as a two-electron acceptor and the *broken line* represents the relation for peroxynitrite behaving as a one-electron acceptor.

In an effort to better characterize the kinetics, the reaction of reduced complex IV + ferrocytochrome *c* with excess peroxynitrite was carried out anaerobically by stopped-flow spectrophotometry. A second order rate constant of 1.0 (±0.1) x 10^4 $M^{-1}s^{-1}$ at 25°C was observed (1.0 (±0.1) x 10^4 $M^{-1}s^{-1}$ at 37°C) by monitoring either the 440 nm and 604 nm bands of complex IV, or the 550 nm band of cytochrome *c*. The magnitude found for this rate constant is at least two orders of magnitude lower than anticipated. Previously, based on data similar to that of Figure 17B (■) and the known decomposition rate of peroxynitrite, a lower limit for the relevant rate constant was estimated to be ~10^6 $M^{-1}s^{-1}$ [45]. However, there is a well-known property of complex IV that affords a convenient explanation for this discrepancy. Fully oxidized and fully reduced forms of the enzyme are thought to have "closed" conformations of the active site (binuclear pair) leading to slow reaction with small species such as inhibitory ligands, whereas partially oxidized/reduced forms have "open" active sites. For example, the rate of reaction of complex IV with the inhibitory ligand cyanide is some for orders of magnitude faster in the case of the partially reduced enzyme compared with the fully oxidized and fully reduced forms [90]. During the titration experiments (without CO_2) the enzyme was predominantly present as a mixture of quicker reacting partially reduced forms. On the other hand, in the stopped-flow experiments, not only was the slower reacting fully reduced form of complex IV rapidly mixed with the oxidant, but also, the absorptions at 440 nm and 604 nm are due mainly to the fully reduced enzyme. In essence, these stopped-flow measurements were selective for the properties of a slow reacting form of the enzyme. Very occasionally, when the solutions had been allowed to rest in the drive syringes for ten minutes or more and the stopped-flow kinetics were observed at 550 nm, a much faster reaction (8-fold) was subsequently detected (for one "shot" only). We think that this was due to a slow oxygen leak into the complex IV solution "preparing" a partially

reduced derivative, but disappointingly, were never able to deliberately reproduce this result. The rate-limiting step in the electron-transport pathway from ferrocytochrome *c* through complex IV to oxygen (or whatever other terminal oxidant is provided) is the internal electron transfer to the binuclear pair [91]. Therefore, the rate of any process observed at 550 nm, *before* the rate-determining step, could be significantly slower than the linked process taking place at the binuclear pair where peroxynitrite reacts [33]. It follows that ~10^6 $M^{-1}s^{-1}$ (37 ºC) remains the best estimate available for the lower limit of the rate constant describing the reaction between peroxynitrite and complex IV turnover intermediates.

In the presence of CO_2 (added as 40 mM sodium bicarbonate) reduced complex IV + ferrocytochrome *c* underwent a quite different reaction with peroxynitrite. In titrations there appeared to be very little oxidation of the cytochromes by peroxynitrite (●, Figure 17B) but this presentation masks the underlying complexity. We first observed an initial oxidation upon titrating the reduced cytochromes (Figure 17A ii) with less than 0.25 equivalents (based on a 2-electron process) of peroxynitrite (Figure 17A iii) and then the cytochromes slowly re-reduced over several minutes (Figure 17A iv). The slow reduction of both complex IV and cytochrome *c* continued for over 30 minutes (at least) without the addition of any further reagents. Since no similar slow re-reduction of cytochrome *c* was observed during any experiments when complex IV was absent, we conclude that the slow reduction must be catalyzed by the enzyme. In several independent experiments with partially oxidized/reduced cytochromes, additions of carbonate, nitrite, nitrate or decomposed (by aging) peroxynitrite did not result in any similar slow reduction. A reasonable interpretation of these observations would seem to be that peroxynitrite reacts with CO_2 to form carbonate radical and nitrogen dioxide radical (Figure 13, scheme 1) then subsequently, the carbonate radicals subsequently formed oxidize the cytochromes, while

the more stable nitrogen dioxide radicals slowly re-reduce the cytochromes. Unfortunately, this could not be verified as we were unable to detect any long-lived radicals by EPR either directly, or using spin traps. It is possible that the nitrogen dioxide radical is able to modify one or more of the amino acid residues in the vicinity of the active site and that the side-chain derivative(s) then slowly reduce(s) the cofactors. The practical consequence of this novel reaction is that we were precluded from establishing the stoichiometry of the reaction between peroxynitrite and complex IV in the presence of CO_2.

3.3.4 Modifications of ferricytochrome *c* by peroxynitrite

It has been demonstrated for many proteins that the particular amino acid modifications obtained following peroxynitrite exposure are highly dependent on the prevailing conditions under which the reaction is carried out (*e.g.* buffer, pH, presence of hydroxyl radical scavengers, *etc.*). In this work, bovine MS-cytochrome *c* was prepared in the presence of air by the addition of a large excess of *bona fide* peroxynitrite in multiple small aliquots to the native ferricytochrome *c* – resulting in the quantitative disappearance of the 695 nm absorption band often associated with methionine coordination in the ferric form of the protein. Under these conditions, no significant 3-nitrotyrosine formation as shown by immunoblotting (Figure 18, ■) or mass spectrometry (see below) was detected. In contrast, the presence of sodium bicarbonate added to 40 mM resulted in another derivative, NT-cytochrome *c*, in which the 695 nm band persists to some degree and much larger amounts of 3-nitrotyrosine were formed (Figure 18, ●).

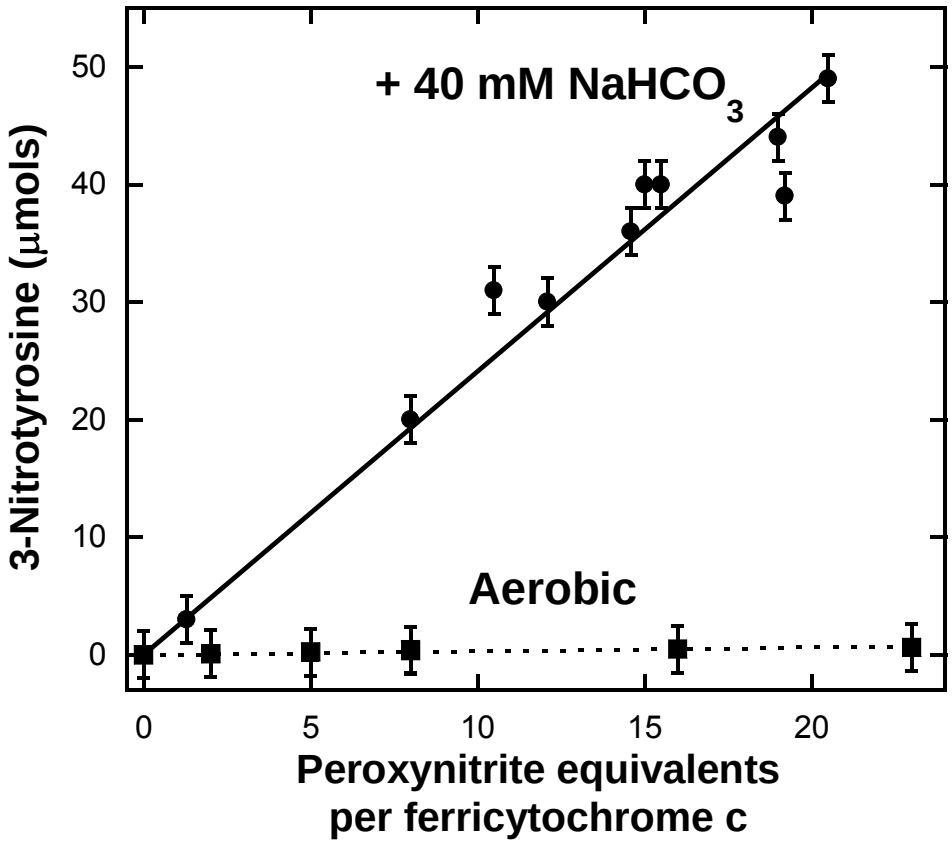

Figure 18. Formation of 3-nitrotyrosine during the reaction of sodium peroxynitrite with ferricytochrome *c* in the presence (●) and absence (■) of sodium bicarbonate.

Ferricytochrome *c* (30 μM) was titrated with small aliquots of concentrated sodium peroxynitrite (35 mM) in the presence and absence of 40 mM sodium bicarbonate in 0.2 M potassium phosphate buffer, pH 7.4. Nitrotyrosine content in samples and standard solutions was measured by chemiluminescence (see Methods for details).

As prepared, MS-cytochrome *c* was reducible with sodium dithionite, but not sodium ascorbate. This is in keeping with observations reported by Cassina *et al.* [38, 59] concerning equine NT-cytochome *c*, suggested by these same authors to be indicative of a more negative mid-point

redox potential (E_m) than that of the native cytochrome. We concur with this argument and, furthermore, unless explicitly stated to the contrary, we adopt the working assumption that the properties of NT-cytochromes *c* from bovine and equine sources are essentially the same. Also, while we presently have no information regarding *equine* MS-cytochrome *c*, we do not expect the properties of this molecule to differ significantly from those of the equivalent *bovine* derivative reported here. Unlike the previous authors, the focus of attention in our project is the peroxynitrite-modified form of bovine cytochrome *c* prepared in the absence of added sodium bicarbonate (*i.e.* MS-cytochrome *c*).

3.3.5 Electronic spectra of peroxynitrite-modified (MS-)cytochrome *c*

We routinely monitored the extent of modification during the peroxynitrite treatment of cytochrome *c* by observing the disappearance of the 695 nm electronic absorption band (Figure 18 A,B). Compared with the absorption features of the native cytochrome, the visible region spectrum of MS-cytochrome *c* at neutral pH exhibits increased absorption intensity at 490 nm and 620 nm (Figure 18B) suggestive of partial conversion of low-spin to high-spin ferric heme [92-94]. However, the spectra of MS-cytochrome *c* samples at pH 5, in which the 620 nm band is more pronounced, show no evidence of any increased intensity at 490 nm (Figure 19A) and, therefore, we conclude that these spectra do not, on balance, support the formation of high-spin ferric heme by loss of the methionine 80 axial ligand. At best, the data (Figure 19B) are ambiguous, but the apparent shift in the 695 nm absorption band of the native molecule to a new

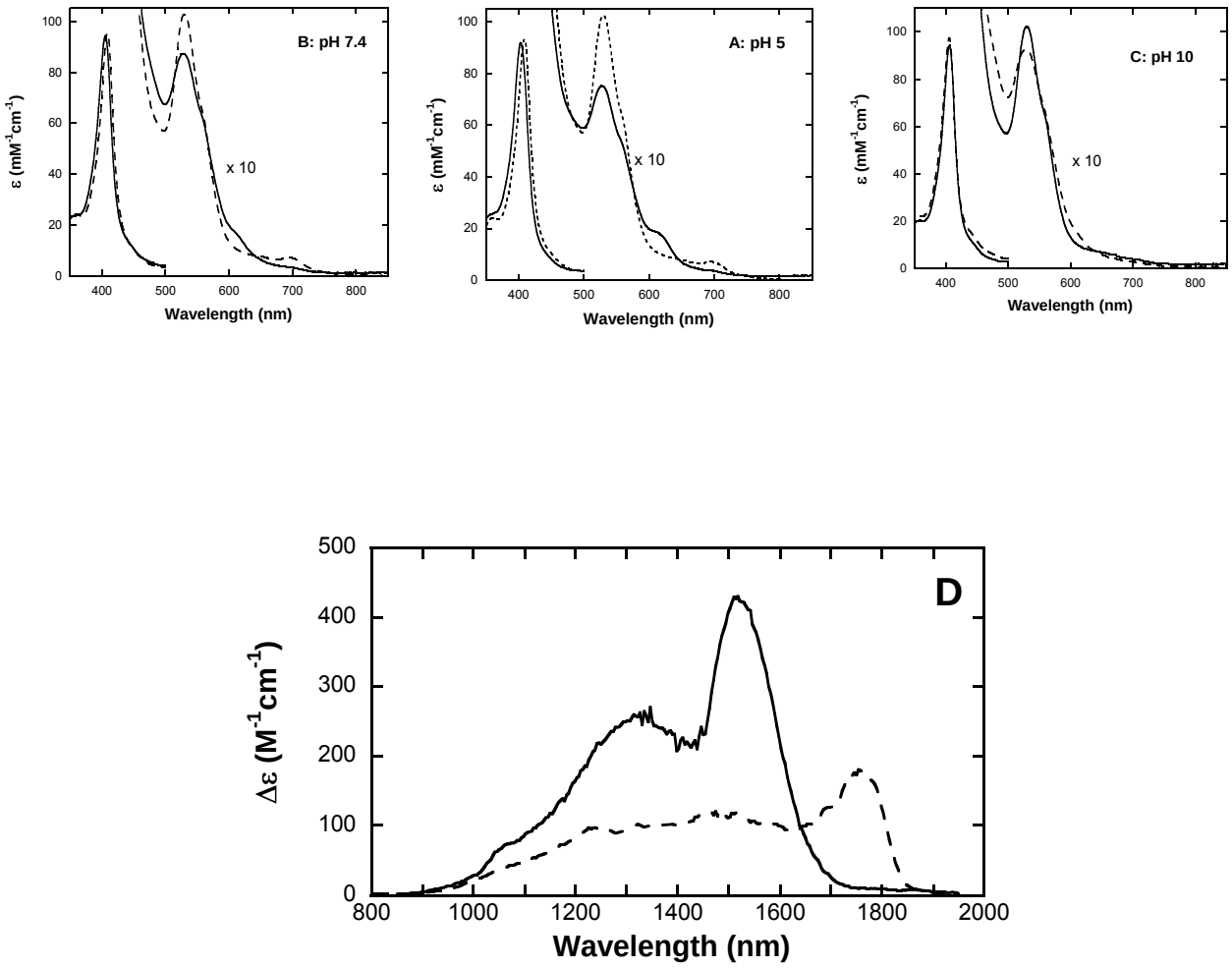

Figure 19. Comparison of the electronic spectra of native ferricytochrome *c* (dashed traces) and MS-cytochrome *c* (solid traces).

Absorption spectra at 22 ºC, 1.00 cm path lengths, 3 – 30 μM heme concentrations: A: 50 mM MES, pH 5.0; B: 50 mM HEPES, pH 7.4; C: 50 mM CAPS, pH 10.0. D: Near-infrared magnetic circular dichroism (MCD) spectra at 4.2 K and 5.0 tesla of native ferricytochrome *c* (0.30 mM, dashed trace) and MS-cytochrome *c* (0.25 mM, solid trace) in 50% glycerol, pD 6.4, 25 mm MES, 0.5 mm path lengths.

position at 620 nm in the spectrum of the derivative (Figure 19A) could indicate a sulfur-donor ligand is still present following the peroxynitrite-dependent modification. At pH 10 the spectra of native and MS-cytochrome *c* are virtually identical, exhibiting no pronounced 620 nm or 695 nm bands (Figure 18C) and, while not definitive, are consistent with the presence of well-known low-spin ferric alkaline forms with histidine-lysine axial coordination [95].

Often, ambiguity in the identification of axial heme ligands can be overcome by application of near-infrared (700 – 2,000 nm) magnetic circular dichroism (MCD) spectroscopy [96-97]. This is because low-spin ferric hemes give rise to porphyrin-to-iron charge-transfer transitions in the near-infrared region which are diagnostic of the axial ligands to the heme; that is, the observed transition energies have been calibrated to known pairs of axial ligands [96-97]. The near-infrared MCD spectrum of native ferricytochrome *c* is typical of a low-spin ferric heme and exhibits a low-energy maximum at 1,760 nm (Figure 19D, dashed trace) indicative of histidine-methionine axial coordination. The spectrum of the MS-cytochrome *c* exhibits a low-energy maximum at 1,550 nm (Figure 19D, solid trace) indicative of histidine-lysine coordination [98] and demonstrating that a significant component of the peroxynitrite-modified derivative is almost certainly one or more of the alkaline forms of the native cytochrome. However, if the 1,760 nm MCD band of the native cytochrome has undergone a blue shift of similar magnitude to the 695 nm absorption band ($695 \rightarrow 620$ nm $\equiv +1{,}740$ cm^{-1}) then there may be at least one unresolved MCD band present at 1,350 nm ($+1{,}740$ cm$^{-1} \Rightarrow 1{,}760 \rightarrow 1{,}350$ nm) in addition to the features arising from the alkaline forms. Despite this remaining potential complication, the MCD spectra do unambiguously confirm that the histidine-methionine axial coordination of the native cytochrome *c* is not present in the peroxynitrite-modified form(s) and, moreover, show clear evidence for the presence of low-spin species as in the absorption spectra.

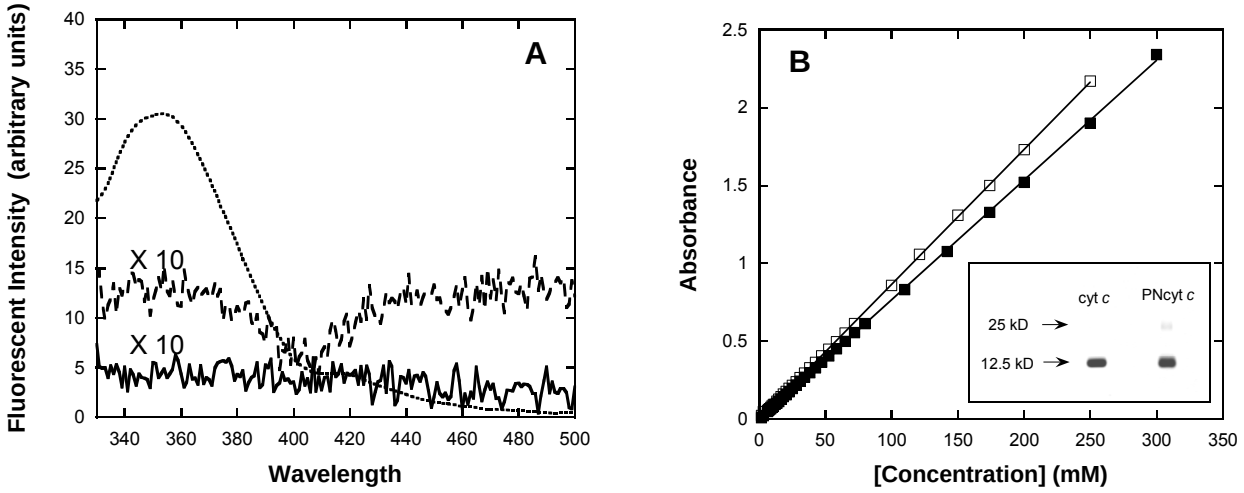

Figure 20. Aggregation state of MS-cytochrome *c*.

A: Fluorescence spectra of native ferricytochrome *c* (solid trace) and MS-cytochrome *c* (dashed trace) at pH 7.4 in 50 mM HEPES buffer, 22 ºC. The addition of guanidine hydrochloride to native cytochrome *c* (2.0 M, final concentration) results in the fluorescence spectrum shown by the dotted trace. Note that the fluorescence intensities of the native and MS-cytochrome *c* samples have been multiplied by ten. B: Concentration dependence of the electronic absorption spectra (λ = 530 nm) of native ferricytochrome *c* and MS-cytochrome *c* at pH 7.0 in 50 mM HEPES buffer, 25 ºC, 1.0 mm path lengths. The solid lines represent extrapolated fits to the data sets in the low (< 60 μM) concentration ranges showing no deviation from Beer's law at higher concentration in either case. Inset: Native-blue-gel electrophoresis of native ferricytochrome *c* and MS-cytochrome *c* demonstrating the lack of any substantial dimerization.

3.3.6 Conformational changes and aggregation state of MS-cytochrome *c*

The question arises as to whether there might be a substantial reorganization of the protein structure in the peroxynitrite-treated molecule compared with the native cytochrome *c*. The fluorescence spectrum of cytochrome *c* is primarily due to the single tryptophan (residue 59) in the molecule, although the four tyrosines present may also contribute to a lesser extent. Furthermore, this type of signal is known to undergo a measurable increase in fluorescence when the structure is unfolded – *e.g.* by the addition of guanidine hydrochloride (Figure 19A, dotted trace). In fact, compared to the native cytochrome *c*, the fluorescence spectrum of MS-cytochrome *c* is hardly perturbed (Figure 20A, *cf.* solid and broken traces) clearly suggesting that the peroxynitrite-dependent modification does not result in any marked changes in the tertiary structure of the protein. The very small changes in the observed tryptophan-tyrosine fluorescence could conceivably be due to either nitration of tyrosine, or some small conformational changes in the vicinity of tryptophan 59.

Peroxynitrite is capable of oxidizing thiols and thus promoting the formation of disulphide bridges. However, native polyacrylamide gels showed that any production of cross-linked (covalently-bonded) dimers in MS-cytochrome *c* samples was minimal (Figure 19B, inset). If concentration-dependent (non-covalent) aggregation of haem-containing systems occurs, this can usually be detected by deviations from Beer‘s law in the intensities of electronic absorption bands [92]. Plots of absorbance at 530 nm versus chromophore concentration of the native ferricytochrome *c* and MS-cytochrome *c* were both found to be linear in the concentration range relevant to the present investigation Figure 20B, main panel).

In summary, we found evidence for only very minor changes in protein structure and essentially no evidence for any aggregation of cytochrome *c* following exposure to peroxynitrite

at levels resulting in abolition of the 695 nm absorption band. These observations place useful constraints on possible axial ligand substitutions responsible for the EPR spectral changes described below.

3.3.7 EPR spectra of peroxynitrite-modified cytochrome *c*

The EPR spectrum of native bovine ferricytochrome *c* at pH 6 exhibits anisotropic, low-spin signals, with $g_z = 3.09$, $g_y = 2.24$ and $g_x \sim 1$ (usually unobserved) (Figure 21A, solid trace) indicative of histidine-methionine axial coordination at the heme. Upon making the conditions more basic (pH > 10) methionine 80 dissociates and the EPR spectrum reveals the presence of at least two new low-spin species ($g_z = 3.33$ and 3.56, Figure 21A, broken trace) [98]. By studying a series of point mutations in the yeast enzyme, Rosell *et al.* (14,31) were able to determine that the signals associated with the minority alkaline form of cytochrome *c* with $g_z \sim 3.5$ arose from lysine 79-histidine 18 coordination to the heme and those associated with the majority $g_z \sim 3.3$ form are due to lysine 73-histidine 18 coordination (where the numbering refers to the *bovine* sequence). The relative amounts of these two alkaline forms do vary somewhat in the presence of ethanediol or glycerol (typical MCD glassing agents) and there is also a slight dependence on the buffer used [98]. The reduction potential of these alkaline forms has been shown to be much lower than that of the native cytochrome *c* [99] resulting in their inability to shuttle electrons between complex III and complex IV.

The EPR spectrum of the alkaline form of bovine MS-cytochrome *c* appears to contain two low-spin species present in roughly equal amounts, with g_z values of 3.48 and 3.27 (observe

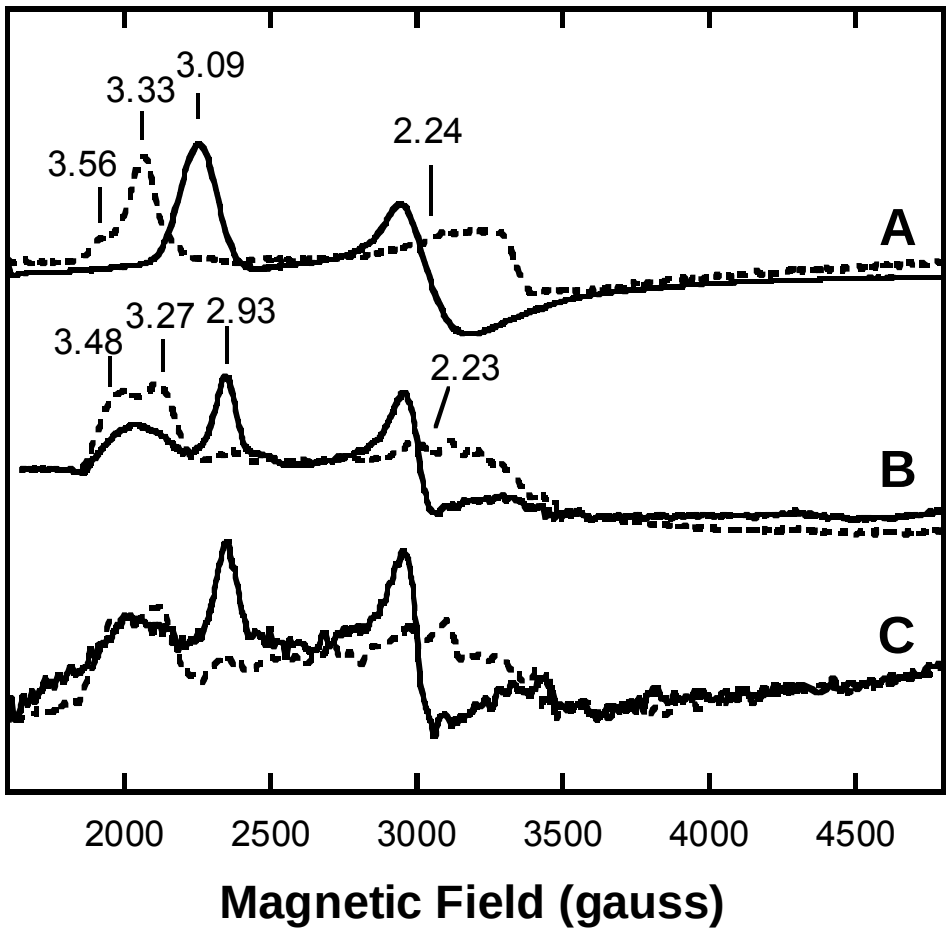

Figure 21. X-band EPR spectra of native bovine ferricytochrome *c* and MS-ferricytochrome *c*.

Conditions: 20 K, 9.8 G modulation amplitude, 200 μW microwave power. A: Native cytochrome *c* (600 μM) in 50 mM MES buffer, pH 6.0 (solid trace); 50 mM CAPS buffer, pH 10.5 (dotted trace). B: MS-cytochrome *c* (500 μM) in 50 mM MES buffer, pH 6.0 (solid trace); 50 mM CAPS buffer, pH 10.5 (dot-dashed trace). C: MS-cytochrome *c* (500 μM) in 25 mM MES buffer, 50% glycerol, pD 6.4 (solid trace); 50 mM CAPS buffer, 50 % glycerol, pD 11 (dashed trace).

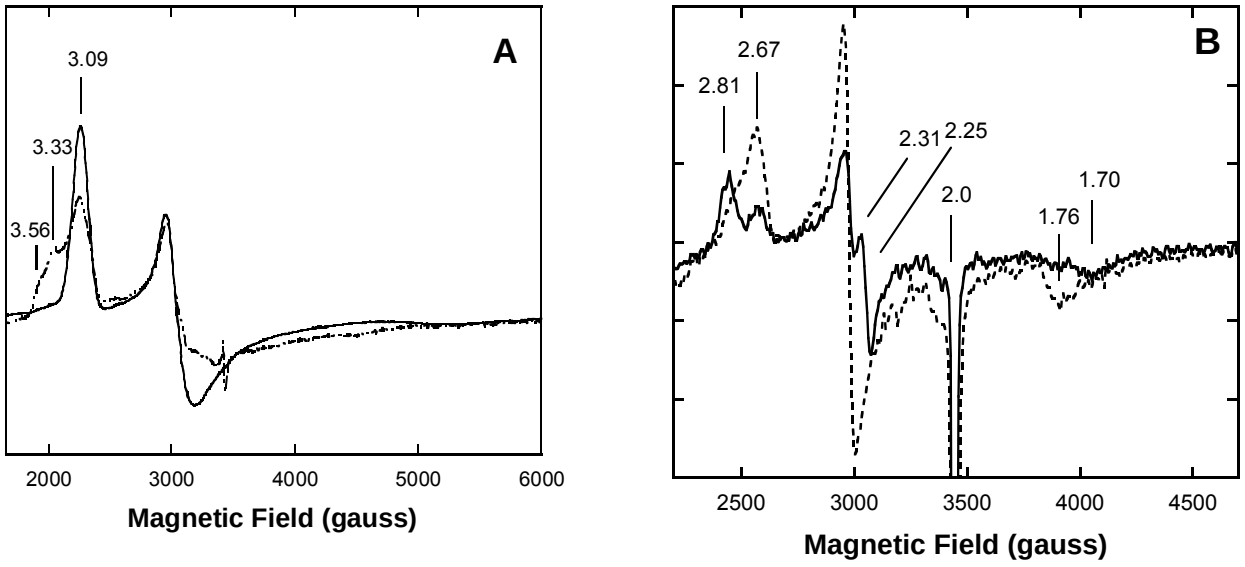

Figure 22. X-band EPR spectra of cytochrome *c* and haem-nonapeptide (20 K, 9.8 G modulation amplitude, 200 μW microwave power).

A: Native bovine cytochrome *c* (600 μM) 50 mM HEPES buffer, pH 7.0 (solid trace) and NT-cytochrome *c* (500 μM, see Methods) 50 mM HEPES buffer, pH 7 (dotted trace) both in the presence of 40 mM $NaHCO_3$. **B:** X-band EPR spectra of haem-nonapeptide: low-spin signals of the peptide as dissolved in ethanol (1.5 mM in heme, dotted line); low-spin signals after the addition of dimethyl sulphoxide to 20% (v/v) (1.2 mM in heme, solid line).

Figure 21Figure 21B, broken trace). A very small amount of high-spin ferric-heme signal at g ≈ 6.0 (as well as some adventitious high-spin Fe^{3+} at g ≈ 4.3) is observed in the MS-cytochrome *c* spectrum (not shown) but this amounts to only a few percent of the total sample. While the majority low-spin signals are slightly shifted relative to those of the native alkaline cytochrome, they are still in the range expected for ferric hemes with histidine-lysine axial ligands (13,18) suggesting that the coordination is probably still through lysine 73 and lysine 79. However, the

spectrum of the acid form of the MS-cytochrome *c* (Figure 21B, solid trace) is quite different from that of the native cytochrome. There is no $g_z = 3.09$ species observed, but a very broad signal with $g_z \approx 3.38$ and another signal with $g_z = 2.93$. The $g_z \approx 3.38$ species is still consistent with amine coordination and the broadness of the signal suggests that the two species observed at higher pH are simply unresolved at lower pH. It is the other signal with $g_{zyx} = 2.93, 2.23, 1.5$ which is more problematic to explain. The addition of glassing agent to the samples did not result in the appearance of different signals in the EPR spectra of either the acid or the alkaline forms of MS-cytochrome *c* (Figure 21C). Therefore, with reference to the MCD spectrum (Figure 19, solid trace) it is clear that the $g_z = 2.93$ signal cannot arise from a histidine-methionine coordinated heme. In general, it is possible that such a signal could arise from *bis*-histidine coordination and the MCD spectrum does not exclude this, but in addition to the known axial ligand, histidine 18, there is only histidine 26 in the structure of *bovine* cytochrome *c*. Since these are close to each other on the same side of the heme, it is difficult to envisage *bis*-histidine coordination without large changes in the structure of the protein, or dimer formation. The fluorescence spectra (Figure 20A) and adherence to Beer‘s law (Figure 20B) argue strongly against such possibilities. Alternately, nitrite anion, formed during the reduction of peroxynitrite, is a potential heme ligand that might be responsible for the $g_z = 2.93$ signal, since nitrite has previously been shown to bind to the ferric form of native cytochrome *c* at pH 5 [100]. However, this possibility can also be excluded as neither the incubation of native cytochrome *c* in 1 M sodium nitrite for several hours, nor extensive dialysis of MS-cytochrome *c* resulted in any significant change in the low-spin ferric signals of samples (not shown) between pH 6 and 11. Mugnol *et al.* have reported an EPR signal with $g_z = 2.90$ for cytochrome *c* in micelles at pH 8.5 [89]. This signal is very similar to those previously reported for *c*-type ferric hemes with

amine-imidazolate ligation, observed only under alkaline conditions [93]. Since the signal we observe at $g_z = 2.93$ is present exclusively under mildly acidic conditions in the absence of any surfactant, the two must arise from distinct species.

In addition, we have also examined the EPR spectrum of the NT-cytochrome *c* – formed in the presence of 40 mM sodium bicarbonate and leading to 3-nitrotyrosine formation (Figure 18). As shown in Figure 22A, the g-values (3.33 and 3.56) observed at neutral pH are consistent with partial conversion to the alkaline form(s) of the enzyme, but persistence of the g = 3.09 signal indicates that a significant portion of the sample (> 50%) retains the native histidine-methionine axial coordination. Abriata *et al.* [59] have recently shown by NMR spectroscopy that tyrosine nitration apparently shifts the pK_a of the alkaline transition so that the lysine-coordinated forms may predominate at neutral pH. The different temperatures at which the EPR (cryogenic) and NMR (ambient) spectra were recorded probably accounts for any quantitative discrepancy here. Importantly, there is no evidence for any high-spin or the new low-spin (g = 2.93) species in the EPR spectra of NT-cytochrome *c* samples.

By far the most straightforward interpretation of the present observations is that, in the absence of added bicarbonate, the principal effect of peroxynitrite has been to modify the axial ligand methionine 80 and it follows that the species yielding the $g_z = 2.93$ signal could be an oxidized derivative of methionine, such as a sulfoxide, which is known to be a likely candidate [37]. The EPR spectrum of heme nonapeptide in ethanol, a model system in which part of the cytochrome *c* polypeptide (including methionine 80, but not histidine 18) has been enzymatically cleaved [101], contains a low-spin ferric signal with $g_z = 2.67$ (Figure 22B, broken trace). This likely represents the heme with either histidine-hydroxide or histidine-ethoxide coordination; but more importantly, following the addition of dimethyl sulphoxide, a new signal with $g_{zyx} = 2.81$,

2.25, 1.7 appears in the EPR spectrum (Figure 22B, solid trace) that is intriguingly similar to the spectral component we seek to identify in the case of the acid form of the MS-cytochrome *c*.

3.3.8 Mass spectra of peroxynitrite-modified (MS-)cytochrome *c*

In comparison with the electrospray-ionization mass spectrum of the native bovine cytochrome *c* (Figure 23A) the mass spectra of MS-cytochrome *c* samples were significantly broadened (Figure 23B) consistent with the formation of multiple minority products. For the +1 ion of the unmodified native cytochrome *c* we find m/z = 12,228.3 which fits the native bovine structure minus the N-terminal N-acetylglycine (m/z = 12,228). The principal derivative detected in the mass spectra of the peroxynitrite-treated samples was m/z = 12,244.3 corresponding to insertion of a single oxygen atom in the native structure, consistent with oxidation of one methionine to methionine sulphoxide. Most importantly, the mass spectra of MS-cytochrome *c* samples did not exhibit any resolved peaks that could reasonably be attributed to the presence of the nitrated forms previously reported by others for NT-cytochrome *c* (9, 37). A single nitro group modification to a tyrosine of cytochrome *c* would be observed at m/z = 12,273 (location show on Figure 23B).

3.3.9 Peroxidatic activity of MS-cytochrome *c*

The peroxidatic activities of native cytochrome *c* and MS-cytochrome *c* were assayed by the guaiacol reaction [92]. The native cytochrome *c* had essentially no activity while that of the

MS-cytochrome *c* was very low, k_1 ~10 $M^{-1}s^{-1}$ at pH 7. This rate is one million times less than that for horseradish peroxidase and about one thousand times less than that for N-acetyl heme undecapeptide, a predominantly high-spin system prepared from cytochrome *c* [92]. In fact, this amount of peroxidatic activity is consistent with the presence of only a tiny quantity (< 1%) of high-spin MS-cytochrome *c* and/or contaminating non-heme iron, in keeping with all the spectroscopic data indicating that the MS-cytochrome *c* exists essentially in low-spin forms only, with histidine-lysine axially coordinated species being the majority forms at neutral pH.

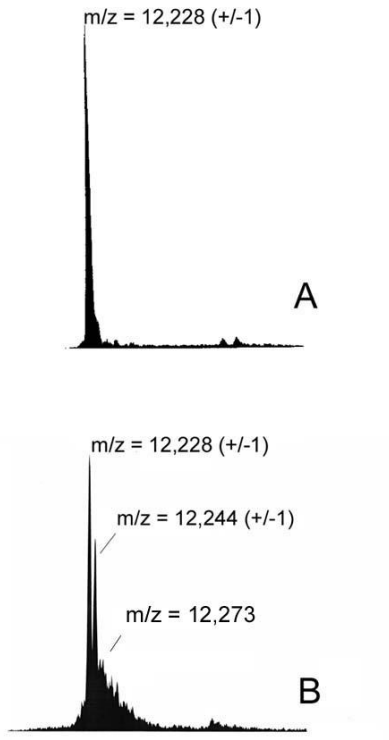

Figure 23. Electrospray-ionization mass spectra of (A) native bovine cytochrome *c* and (B) MS-cytochrome *c*. Samples were diluted into 0.1% acetic acid (in 50% acetonitrile/water) and infused directly into the triple quadrupole electrospray mass spectrometer. The probe was operated at a voltage differential in the range of +2.3 to +3.5 keV in the positive ion mode and source temperature was maintained at 70 ºC. Ion series were deconvoluted and converted to molecular (+1 charged) spectra by a maximum entropy algorithm.

3.3.10 Inhibition of electron-transport chain activity by peroxynitrite-modified cytochromes *c*?

Cytochrome *c* is reduced physiologically by the transfer of electrons from ubiquinone through complex III (ubiquinone:cytochrome *c* oxidoreductase) in the mitochondrial electron-transport chain (ETC). The kinetics of reduction of native ferricytochrome *c* to ferrocytochrome *c* were monitored by the increase in absorbance at 550 nm (Figure 24A, solid trace). Not surprisingly, given the more negative E_m associated with histidine-lysine coordination [102], when this was attempted with MS-cytochrome *c*, no reaction was observed (Figure 24A, dashed trace). In experiments where native ferricytochrome *c* and MS-cytochrome *c* were both present (< 33% MS-cytochrome *c* relative to the native form) the complex III-catalyzed reduction of native ferricytochrome *c* to ferrocytochrome *c* occurred without any apparent inhibition (*e.g.* Figure 24A, □). A more limited set of otherwise analogous observations were made (data not shown) where NT-cytochrome *c* was substituted for MS-cytochrome *c* in the experiments of Figure 24A. Therefore, these results strongly suggest that, *in vivo*, the only kinetic effect that conversion of the native form to either type of peroxynitrite-modified cytochrome *c* is likely to have on electron transfer from complex III will be to lower the concentration of reducible ferricytochrome available to accept electrons.

Interestingly, the question of inhibition of electron transfer between cytochrome *c* and complex IV (cytochrome *c*:oxygen oxido-reductase) is rather more complicated. Clearly, if peroxynitrite-modified cytochromes *c* cannot be reduced by complex III, they are not going to be physiologically active as electron donors to complex IV, but the question of whether they inhibit the oxidation of the native ferrocytochrome remains. The complex IV-catalyzed oxidation of

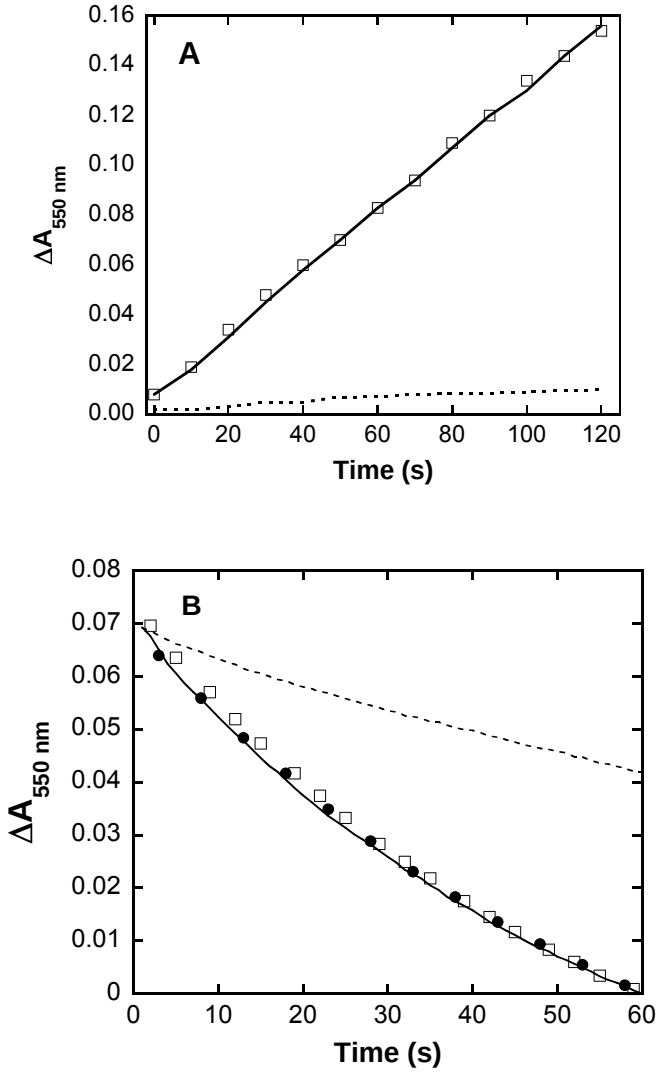

Figure 24. Kinetic traces showing the effect of MS-cytochrome *c* on enzyme turnover (monitoring ferrocytochrome *c* at λ = 550 nm).

A: Reduction of 15 μM cytochrome *c* during turnover of 0.25 nM complex III by 10 μM reduced ubiquinone (solid trace); with 3.0 μM MS-cytochrome *c* added (□) and with 10 μM MS-cytochrome *c* only (dotted trace); 25 mM potassium phosphate buffer, pH 7.4, 0.1 % lauryl maltoside, 25 ºC. **B:** Oxidation of 10 μM cytochrome *c* during turnover of 1.25 nM complex IV in 100 mM sodium phosphate buffer, pH 7.4, 0.05% lauryl maltoside (solid trace); in the presence of 2.5 μM MS-cytochrome *c* (●).Oxidation of 10 μM cytochrome *c* during turnover of 1.25 nM complex IV in 10 mM sodium phosphate buffer, pH 7.4, 0.05% lauryl maltoside (dashed trace) in the presence of 10 μM MS-cytochrome *c* (□).

native ferrocytochrome *c* by molecular oxygen exhibits kinetics that deviate from linearity even at the earliest time points (Figure 24B, solid trace). This is known to be due to competitive product inhibition [103]; that is, the electron transfer from ferrocytochrome *c* to complex IV is increasingly inhibited by the presence of ferricytochrome *c* during the time course of the assay. More intriguingly, however, when MS-cytochrome *c* was added at < 33% of the concentration of native ferrocytochrome *c*, no change in the reaction kinetics was observed (*e.g.* Figure 24B, ●). Thus, under these particular conditions of high ionic strength (pH 7.4, 0.1 M sodium phosphate, 0.1% lauryl maltoside) MS-cytochrome *c* does not effectively compete with either ferro- or ferri-forms of native cytochrome *c* for catalytically relevant sites on complex IV. At low ionic strength (pH 7.4, 10 mM sodium phosphate, 0.1% lauryl maltoside) the complex IV-catalyzed oxidation of native ferrocytochrome *c* by molecular oxygen is slower (Figure 24B, dashed trace). This ionic strength-dependence of the reaction has been reported previously and explained on the basis of the proposition that there are two electron-entry sites on complex IV (26, 27). At the lower ionic strength, ferrocytochrome *c* is thought to bind primarily to a "high affinity" or "regulatory" [104] site that exhibits relatively slow electron transfer from the cytochrome to complex IV. However, at higher ionic strength, it is reasoned that ferrocytochrome *c* must bind to an alternate "low affinity" or "catalytic" [104] site that exhibits faster electron transfer from the cytochrome to complex IV. Surprisingly, addition of MS-cytochrome *c* to the assay mixture at low ionic strength actually led to an increase in turnover, resulting in a kinetic trace equivalent to that obtained at high ionic strength when the MS-cytochrome *c* was present at the same concentration as native ferrocytochrome *c* (Figure 24B, □). This unexpected observation strongly suggests that MS-cytochrome *c* out-competes the native cytochrome *c* for the high affinity (regulatory) site of complex IV, resulting in the displaced native cytochrome *c* binding

primarily to the low affinity (catalytic) site, with a consequent increase in the observed electron transfer rate at low ionic strength.

An investigation into the effect of varying the concentration of either MS-cytochrome *c*, or native *ferri*cytochrome *c*, on the observed complex IV turnover kinetics by *ferro*cytochrome *c* was also undertaken (Figure 25). At high ionic strength both were inhibitory, but the effect of the native ferricytochrome *c* was greater, with K_i for MS-cytochrome *c* calculated to be 117 (± 21) μM versus 20 μM for the native ferricytochrome *c*. In contrast, at low ionic strength, the activity of cytochrome *c* oxidase was increased by the addition of MS-cytochrome *c*, but inhibited by the presence of added native ferricytochrome *c* (Figure 25, inset). We also examined the inhibition kinetics where NT-cytochrome *c* was substituted for MS-cytochrome *c* in the experiments of Figure 25 with essentially similar findings (data not shown, a calculated K_i of 100 (±15) μM was found for NT-cytochrome *c* under conditions of high ionic strength). It follows that if the peroxynitrite-modified forms are only present as a minor component of the total cytochrome *c in vivo*, this will not significantly inhibit the flow of electrons in the ETC and may actually increase the flux. On the other hand, if the majority of the cytochrome *c* present in the mitochondria were to become peroxynitrite modified, electron flow would be severely curtailed and mitochondrial function compromised.

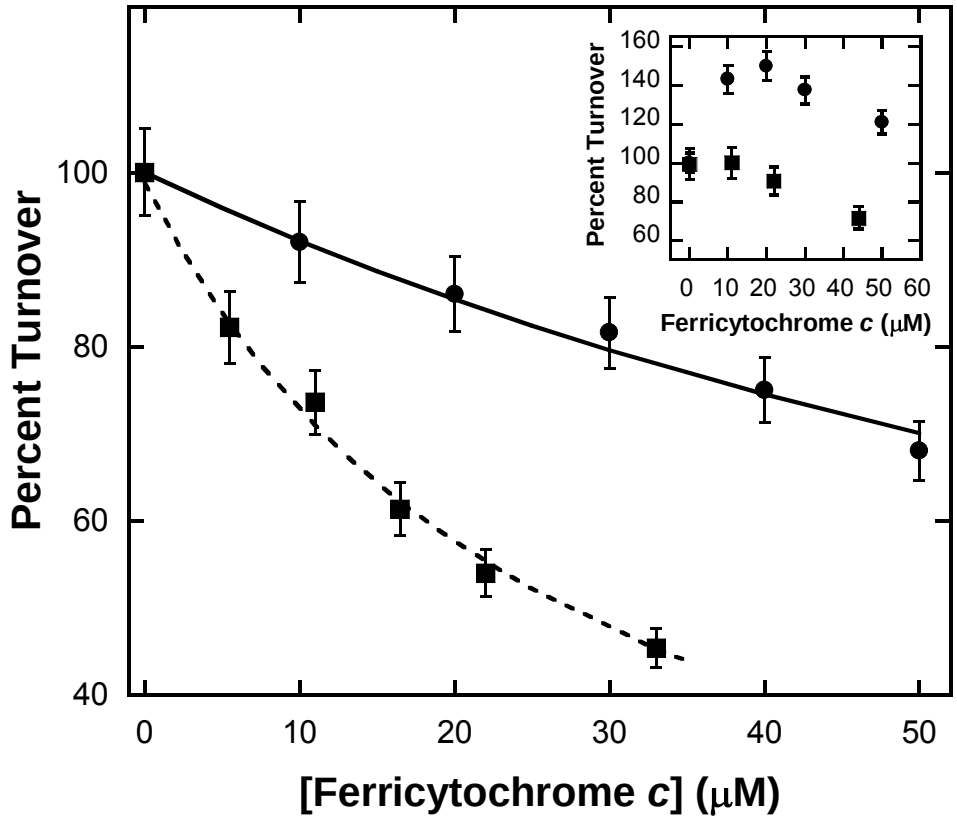

Figure 25. Comparison of turnover inhibition of complex IV by ferrocytochrome *c* due to the presence of native ferricytochrome *c* (■) and MS-cytochrome *c* (●).

Incubation, included 100 mM sodium phosphate buffer (***high ionic strength***), pH 7.4, 0.1 % lauryl maltoside, 25 ºC, 1.25 nM cytochrome *c* oxidase, 10 μM ferrocytochrome *c*. **Inset:** Comparison of the percent turnover of complex IV by *ferro*cytochrome *c* in the presence of native *ferri*cytochrome *c* (■) and MS-cytochrome *c* (●) in 10 mM sodium phosphate buffer (***low ionic strength***), pH 7.4, 0.1 % lauryl maltoside, 25 ºC, 1.25 nM cytochrome *c* oxidase, 10 μM ferrocytochrome *c*.

3.4 DISCUSSION

3.4.1 Combined effect of CO_2 and O_2

"Peroxynitrite" is commonly taken to mean some mixture of the anion ($ONOO^-$) and molecular acid (ONOOH) of unspecified proportion. However, the pK_a of peroxynitrous acid is ~7.8 and, so, at physiological pH, the generally more reactive acid form will predominate. Furthermore, the molecular acid rather than the anion will tend to preferentially partition into non-aqueous phases, like biological membranes. Of course, CO_2 also tends to partition into non-aqueous environments. It follows that within the inner mitochondrial membrane, associated with the ETC complexes, ONOOH and CO_2 may be the dominant species most relevant to the following discussion. However, it is $ONOO^-$ with which CO_2 is known to undergo the facile reaction. Consequently, especially when considering different microenvironments, it is not straightforward to dismiss either scheme 1 or scheme 2 as biologically unimportant and we continue to consider both.

The present results (Figures 13-18) are in agreement with the consensual view [83], [24], [47] that the presence of CO_2 dramatically modulates the interaction of peroxynitrite with biomolecules, but to our knowledge, the observation that oxygen is able to mediate the abstraction of an electron by peroxynitrite (Figure 16) has not previously been reported. While this action could be demonstrated in the oxidation of ferrocytochrome *c*, the susceptibility of the *b*-type hemes in complex III precluded aerobic titrations. However, although difficult to verify in specific cases, it is reasonable to anticipate that the ability of oxygen to mediate redox reactions involving peroxynitrite may extend to other reduced cofactors in the ETC like those of complex III. The possible pathological consequences of such behavior are of interest because of

the widespread therapeutic use of oxygen. Taking any ETC cofactor able to undergo one-electron redox reactions to be given by X/X^+, we may write with reference to Figure 13:

$$ONOO^- + CO_2 + X \rightarrow X^+ + CO_3^{\bullet -} + {}^{\bullet}NO_2 \quad \textbf{[7A]}$$

$$ONOOH + X \rightarrow X^+ + OH^- + {}^{\bullet}NO_2 \quad \textbf{[7B]}$$

Equations 7. Reaction of peroxynitrite with CO_2 and cofactors of the ETC

The present data (Figure 16) shows that oxygen promotes reaction 6 and it follows that this must be at the expense of decomposition (upper pathway in Figure 13-scheme 2, producing nitrate). Thus, at neutral pH the effect of oxygen is predicted to be increased generation of nitrogen dioxide radicals and reduced production of nitrate anions. This mechanism of exacerbating ~~–n~~itrosative stress" under hyperoxic conditions will, of course, be in addition to any elevated nitric oxide production due to increased availability of substrate oxygen to nitric oxide synthases.

3.4.2 Suppression of peroxynitrite-mediated nitrosative/oxidative stress

We have previously shown that peroxynitrite is able to abstract electrons from most reduced cofactors of the ETC component enzymes [84], [41], [33] suggesting that this could be a mechanism for protecting the individual complexes from irreversible inhibition by covalent modification and also, lowering the peroxynitrite flux to which the rest of the mitochondrion might otherwise be exposed. It is clear from the present data (Figures 13-17) that any such protective capability must be greatly ameliorated by the presence of CO_2. Nevertheless, even at 40 mM bicarbonate, closer to cytosolic/plasma rather than mitochondrial levels, there is a

measurable increase in the oxidation of ferrocytochrome *c* by peroxynitrite aerobically (Figure 14, □) compared to anerobically (Figure 14, ○) indicating that the reaction given in equation 6 does not necessarily dominate. Therefore, the redox reactions between peroxynitrite and reduced ETC cofactors probably take place to some extent within the mitochondrion and, especially under hyperoxic conditions, the protection afforded could be significant. Certainly under typical ("normoxic") cell culture conditions the possible importance of these reactions should not be overlooked. However, while peroxynitrite-mediated oxidative stress may be alleviated, any nitrosative stress stemming from $^{\bullet}NO_2$ production (equation 6) must persist. Consequently, the catalytic conversion of NO + O_2 to nitrite + water by complex IV [105-106], thereby avoiding generation of peroxynitrite in the first place, seems to be a much more likely principle mechanism by which the ETC can safely suppress peroxynitrite levels as the "NO oxidase" activity is essentially insensitive to bicarbonate/CO_2.

As noted earlier, the effective physiological concentration of bicarbonate/carbon dioxide in the immediate vicinity of the mitochondrial inner-membrane's outer surface is not really known. Given that this particular surface attracts positively charged species like cytochrome *c*, it must tend to repel negative ions and, therefore, the assumption that the prevailing bicarbonate concentration can be approximated by that of the mitochondrion as a whole is questionable. During the course of what began as routine spectroscopic characterization of MS-cytochrome *c* samples (*e.g.* Figures 14 and 19B) intended for use in kinetic-inhibition studies, it quickly became clear that the prevalent view in the literature concerning the nature of the covalent modification to native cytochrome *c* following exposure to peroxynitrite was probably incomplete. At this time, the most reasonable position would seem to be that in the functioning mitochondrion we should suspect the formation of both MS-cytochrome *c* and NT-cytochrome *c*.

Clearly, in the absence of added bicarbonate, or other potential hydroxyl radical scavengers [83], the primary reaction between the protein moiety and peroxynitrite is almost certainly insertion of an oxygen atom into methionine 80 to form sulfoxide (Figures 13, 15, 18, 21 and 22). This conclusion ought to not prove very controversial, as this particular derivative of cytochrome *c* is quite well known, having originally been obtained following treatment of the protein with methylene blue in the presence of oxygen [107], [108]. Furthermore, methionine residues in other proteins have been found to undergo conversion to their sulphoxides by reaction with peroxynitrite [109]. Also, we note that reversal of this modification could be pointing to a function for the methionine sulphoxide reductase that has been shown to be specifically targeted to mitochondria [110].

From a structure-function perspective, the consequences of peroxynitrite modification on the electron-transfer activity of cytochrome *c* are readily understood. We have shown that MS-cytochrome *c* and NT-cytochrome *c* (Figure 19) exist as multiple low-spin species, but in both cases, the majority forms exhibit histidine-lysine axial coordination, analogous to the alkaline forms of native cytochrome *c* [97, 111]. Such alkaline forms are known to exhibit a lowered mid-point reduction potential compared to the native structure [102], offering a straightforward explanation for the inability of either peroxynitrite-modified cytochrome *c* to support electron transfer between ETC complexes III and IV. It follows that the functional properties of MS-cytochrome *c* and NT-cytochrome *c* in relation to their interactions with the ETC appear to be so similar, that the question of which form may dominate *in vivo* (governed by an unknown effective bicarbonate concentration) may be somewhat moot.

Complex III is able to reduce neither MS-cytochrome *c* nor NT-cytochrome *c*, but unless there has been complete conversion of all the native cytochrome *c* present to the modified forms,

electron flow to the remaining unmodified ferricytochrome can still occur. In fact, the introduction of a substantial amount of MS-cytochrome *c* or NT-cytochrome *c* to the assay mixture fails to inhibit the transfer of electrons from complex III to native cytochrome *c* (Figure 24A). At the next point in the ETC, it appears that the presence of MS-cytochrome *c* or NT-cytochrome *c* could actually increase the rate of complex IV turnover by binding preferentially to the regulatory site, leading to stimulation of electron transfer from unmodified ferrocytochrome *c* at the catalytic site on the enzyme (Figure 24). It is unclear if both cytochrome *c* binding sites on complex IV, as suggested by many turnover experiments with micellar preparations at high and low ionic strengths, are also present *in vivo*. When situated in the mitochondrial membrane, perhaps only one site may be accessible to cytochrome *c*, or they may not show the same ionic strength-dependent behavior as when dispersed in laboratory surfactants. Consequently, it is not possible to assert with confidence whether the presence of peroxynitrite-modified cytochromes *c* should be expected to inhibit or stimulate ETC activity. However, even in extreme pathological circumstances, it is very difficult to envisage the majority of the cytochrome *c* present in a still viable mitochondrion becoming peroxynitrite modified. Thus, it is probably unlikely that formation of MS-cytochrome *c* and/or NT-cytochrome *c in vivo* will have a significant impact on electron transfer or inner membrane potential while the ETC is still functioning.

It has been suggested that NT-cytochrome *c* may either increase [112] or decrease caspase activity [113]. Certainly, given we find that under turnover conditions the modified forms exhibit 5-to-6-fold decreased affinity for complex IV compared with the native ferricytochrome *c*, it could be argued that during apoptosis either one should be lost more readily from the mitochondrion than the unmodified native molecule. However, this argument rests on the assumption that the low affinity site (catalytic) for cytochrome *c* on complex IV dominates *in*

vivo – a questionable position since the ETC complexes do not in general need to exhibit maximal turnover rates in the functioning mitochondrion. In our view, because of the large excess of peroxynitrite required to form significant amounts of either derivative, these reactions are probably secondary to compromised ETC function; that is, formation of MS-cytochrome *c* and/or NT-cytochrome *c* is unlikely to be an upstream apoptotic signal for the initial cytochrome *c* release and ensuing changes in mitochondrial function.

4.0 HYDROETHIDINE-BASED FLUORESCENT PROBES BOTH REDUCE AND INHIBIT THE MITOCHONDRIAL ELECTRON TRANSPORT CHAIN

Elisenda Lopez Manzano, Elizabeth A. Ungerman, Oscar S. Benz, Sandra Martinez-Bosch, Patrick P. Kerr, Linda L. Pearce* and Jim Peterson*

Department of Environmental and Occupational Health

University of Pittsburgh Graduate School of Public Health

100 Technology Drive, Pittsburgh, PA 15219 USA

*Corresponding Authors: lip10@pitt.edu; jpp16@pitt.edu

Keywords: BPAEC, Complex III, complex IV, cytochrome oxidase, cytochrome reductase, endothelial cells, superoxide

Supported by NIH: NS063732 (to JP, LLP & Bruce R. Pitt) and AI068021 (Joel S. Greenberger PI, Project 3 to JP and LLP)

4.1 ABSTRACT

The commonly employed molecular probes for superoxide hydroethidine and its mitochondrially-targeted derivative (MitoSox™), are shown to undergo reactions with components of the mitochondrial electron-transport chain (ETC) including reduction of complex IV (cytochrome *c* oxidase) and partial reduction of complex III (cytochrome *c* reductase). The reaction with complex IV accounts for an oxygen (and hence superoxide) independent fluorescent response of MitoSox™ in cultured endothelial cells. False-positive detection of superoxide due to such interfering reactions can be avoided by adherence to either of two previously reported methodologies for specifically quantifying the superoxide-indicating 2-hydroxyethidium produced ([71] and [114]). However, the cationic ethidium species formed during oxidation of the probes by the ETC enzymes inhibit the normal turnover of complex IV, almost certainly by blocking transfer of electrons from ferrocytochrome *c* to the oxidase. In the case of oxidized MitoSox™, the observed inhibition under otherwise typical assay conditions is substantial (~ 90%) at inhibitor levels comparable to the concentration of substrate cytochrome *c*. For those situations where the ETC is intact and supplied with reducing equivalents, inhibition of complex IV must unavoidably result in upstream accumulation of electrons resulting in increased superoxide generation. Therefore, if MitoSox™ is used to detect mitochondrial superoxide, inhibition of complex IV by the oxidized probe can lead to superoxide production that the remaining reduced probe will then detect – *i.e.* in the worst possible case, none of the superoxide detected would necessarily have been generated in the absence of the probe.

4.2 INTRODUCTION

In view of the probable role played by reactive oxygen species in some cell-signaling pathways and the observation that oxidative stress is often a significant factor in many biomedical and experimental circumstances [78, 115], there is an ongoing interest in developing better methods for detecting and imaging superoxide production. For example, Wang *et al.* have reported [114] a mitochondrially-targeted protein indicator seemingly able to image transient bursts of superoxide from individual mitochondria within cardiomyocytes. The specificity for superoxide displayed by this detection system is particularly impressive. A viable alternative superoxide imaging protocol based upon fluorescent dyes has also been demonstrated [71]. Nevertheless, the problem of reliably quantifying the levels of superoxide production in biological samples, particularly in sub-cellular locations, remains a crucial difficulty. Hydroethidine (HE, also called dihydroethidium) is a routinely employed fluorescent probe for the detection of superoxide ion, for which if all sources of interference can be delineated, it should be possible to equate measured change in fluorescence intensity with net superoxide flux. It has been shown [52] that a unique product of the oxidation of HE by superoxide, 2-hydroxyethidium (2-HO-E^+) can be detected using selective fluorescence excitation. However, the overall chemistry is complicated, resulting in a non-fluorescent two-electron oxidized product (E^+) and multiple dimeric structures in addition to the superoxide-indicating product (2-HO-E^+) [53, 116].

With few dissenters (*e.g.*[117]) it remains the consensual view that the mitochondrial electron-transport chain is a significant source of superoxide and secondary damaging oxidants for the cell as a whole (*e.g.* [76-79]). Much of the evidence for this, however, has been obtained

using oxidant-sensitive dyes of poorly understood specificity, typically in the presence of electron-transport chain inhibitors of similarly uncertain additional activities. For example, apart from any superoxide that may or may not be formed, there are a plethora of mitochondrial components having the potential to oxidize HE-based probes. In experiments with cultured cells undergoing oxidative stress, we now demonstrate that the majority of the response elicited from the mitochondrially-targeted HE probe MitoSox^{TM} is independent of oxygen and, hence, must not involve superoxide. Seeking a plausible explanation for this finding, we have studied the reactions of HE and MitoSox^{TM} with a selection of the isolated components of the electron-transport chain and found multiple interactions that can potentially lead to false-positive results when attempting to use these fluorescent dyes to detect superoxide production in mitochondria.

4.3 RESULTS

4.3.1 Superoxide Toxicity in BPAEC at 20% versus 3% Oxygen

Using the metabolic indicator alamar Blue to determine cell growth in sub-confluent bovine pulmonary artery endothelial cells (BPAEC) it was apparent (Figure 26A) that cultures grew better in 3% oxygen (approximating systemic levels *in vivo*) compared to 20% oxygen (resulting in oxidative stress). Furthermore, significantly improved growth at 20% oxygen was clearly obtained by over-expression of MnSOD (5-fold increase in activity). These results were verified by cell counting in a subset of the experimental trials (data not shown). Measurements with the potentiometric dye, JC-1, indicated that an increased mitochondrial membrane potential

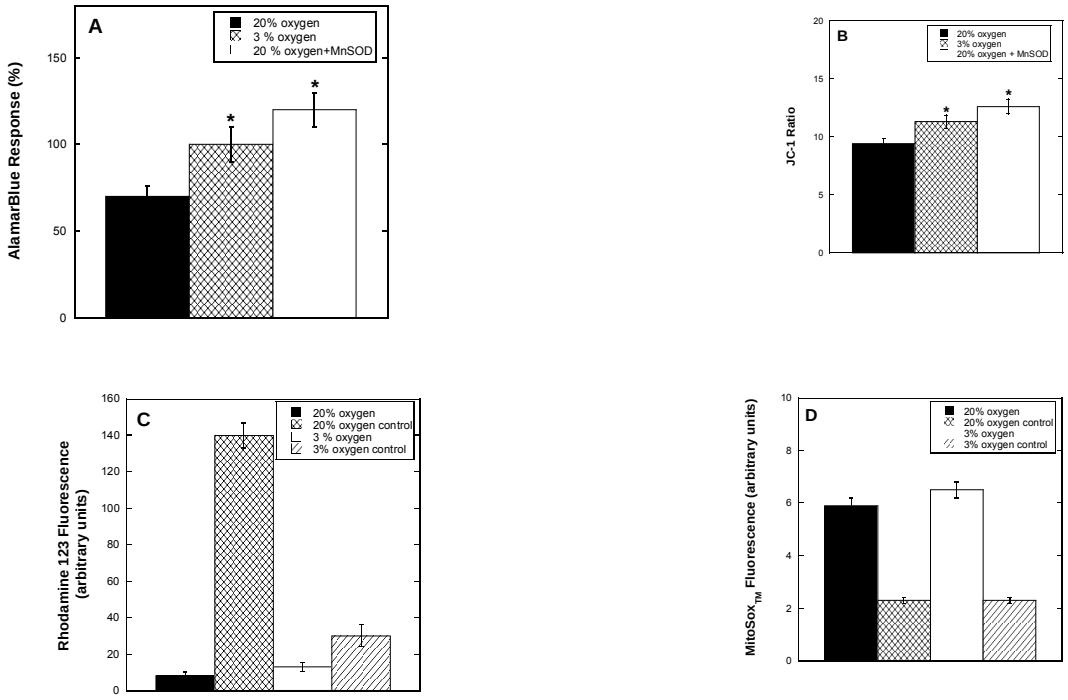

Figure 26. Evaluation of bovine pulmonary endothelial cells (BPAEC) at 20% and 3% oxygen.

Cells were grown at 20% or 3% for 48 hours prior to plating for assays. **A:** BPAEC were seeded at 5 x 10^4 cells per well (6 well plates), grown for 24 hrs and then assayed for metabolic activity using 10% alamar Blue. Values were normalized (arbitrarily set at 100%) to the 3% oxygen condition. Incubating alamarBlue in 3% oxygen and 20% oxygen (without cells) as controls showed no changes in absorbance or fluorescence (data not shown). **B:** BPAEC were seeded at 5 x 10^4 cells per well (6 well plates), grown for 24 hrs and then assayed for mitochondrial function using JC-1. **C:** BPAEC were seeded at 5 x 10^6 cells per plates, grown for 24 hrs and then assayed for oxidant production by DHR-123 (ex. 500 nm; em. 535 nm). Controls were DHR-123 solutions in either 3% or 20% oxygen without cells. **D:** BPAEC were seeded at 5 x 10^6 cells per plates, grown for 24 hrs and then assayed with MitoSox™ (ex. 396 nm; em. 580 nm). Controls were MitoSox™ solutions in either 3% or 20% oxygen without cells.

was obtained at 3% compared to 20% oxygen and over-expression of MnSOD (> 90% localized to mitochondria) led to increased polarization at 20% oxygen (Figure 26B). Together, the results of Figure 26A and B clearly demonstrate that significantly increased (sub-lethally toxic) levels of mitochondrial superoxide are present in BPAEC at 20% compared to 3% (~systemic) oxygen.

The oxidant-indicating dye dihydrorhodamine-123 is sensitive to oxygen dissolved in aqueous buffer, but after loading into the mitochondria [69-70] of BPAEC shows significantly less response and no difference between cells cultured at 20% and 3% oxygen (Figure 26C). That is, in the net reducing milieu of mitochondria, the probe is unable to detect the excess superoxide (or secondary products like peroxynitrite) that it is known must be present from the results of Figure 26A and Figure 26B. Similarly, the more specific indicating probe for superoxide MitoSox^{TM} showed no difference in response between cells cultured at 20% and 3% oxygen (Figure 26D). In this case, however, in addition to failing to detect the increased superoxide present at 20% oxygen, the probe was clearly exhibiting a significant oxygen-independent fluorescence in the presence of cells. Given these results, an examination of the reactions of MitoSox^{TM} (and HE) with various members of the mitochondrial electron transport chain (ETC) was undertaken.

4.3.2 Reaction at Complex I

Oxidation of HE can be monitored by observing an increase in absorbance at 488 nm, or the fluorescent emission of products at 580 nm. Absorption measurements are sensitive to all the known one- and two-electron oxidation products of HE. In fluorescence measurements, using the conventional excitation wavelength of 510 nm leads to the detection of ethidium ion (E^+)

predominantly, whereas an excitation wavelength of 396 nm results in the more specific detection of 2-hydroxyethidium (2-HO-E^+) with only the latter species being an indicator of superoxide [52]. The possible reaction of HE with various mitochondrial two-electron oxidants was investigated by fluorescence at both excitation wavelengths; additionally, the reactions were also studied by absorption spectroscopy at 488 nm in case only non-fluorescent products were formed. When a 200-fold excess of HE was added to NAD^+, or oxidized ubiquinone (UQ-1, UQ-2, or UQ-10) no oxidation of HE was observed during the following 30 minutes (pH 7.4, 22 °C). Similarly, there was no reaction observed following the addition of HE to complex I (NADH dehydrogenase) whether electron acceptors (ubiquinones) were present or absent.

4.3.3 Reaction at Complex III

In contrast to the above findings, the reduction of complex III (cytochrome *c* reductase) by HE was facile. Following the addition of a 10-fold excess of HE to complex III solutions the visible region electronic absorption spectrum of the enzyme exhibited two peaks 524 nm and 553 nm (Figure 27, solid trace) indicative of heme c_1 reduction [118]. Addition of larger excesses (100-fold) did not lead to any detectable reduction of the *b* hemes in the enzyme. However, examination of the EPR spectrum of these samples, revealed the appearance of a signal (Figure 27, inset) attributable to the presence of reduced Rieske iron-sulfur centers [119]. Double integration of the EPR signal suggested more than 80% of the Rieske centers present to be in the reduced form. The mid-point reduction potentials for heme c_1 and the Rieske center are significantly more positive (~ +300 mV) than those of the *b* hemes (< +100 mV) [120]. Therefore, our results are consistent with the propensity for HE to reduce particular sites within

the electron-transport chain to be governed by the mid-point reduction potentials of the individual acceptors. Consequently, it is unremarkable that we do not observe reduction of components upstream of complex III, while others have reported [53] that cytochrome *c*, for example, is susceptible to reduction by HE.

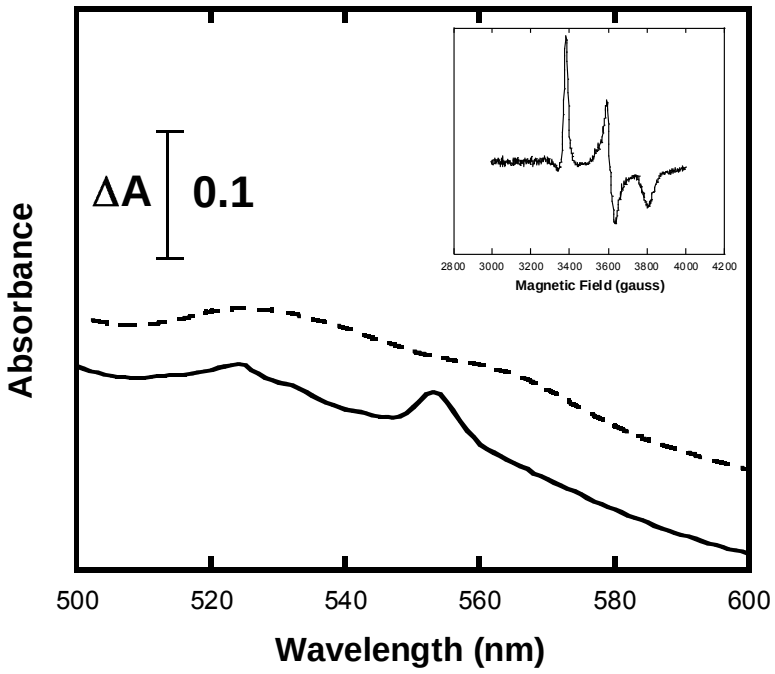

Figure 27. Reduction of complex III (cytochrome *c* reductase) cofactors by hydroethidine (HE) at pH 7.4 in 50 mM potassium phosphate.

Main panel: absorption spectrum showing cytochrome c_1 reduction (solid trace); 6 μM complex III, HE added to 60 μM, 1.00 cm pathlength, 22 ºC. *Inset:* x-band EPR spectrum showing signal from reduced Rieske iron-sulfur center; 30 μM complex III, HE added to 2.4 mM, 40 μW microwave power, 5 G modulation amplitude, 20 K.

4.3.4 Reactions at Complex IV

Addition of HE (or reduced MitoSox^{TM}) to Complex IV under aerobic conditions resulted in excess amounts (over enzyme concentration) of HE being oxidized as determined by the increase in absorbance at 488 nm. The HE was clearly acting as a substrate for complex IV turnover as the extent of HE oxidation per unit time was dependent on the enzyme concentration and Lineweaver-Burk (double-reciprocal) plots of 1/[substrate] against 1/rate were linear (*e.g.* Figure 28A). While the turnover number (mol substrate/s/mol enzyme) for the enzyme by reduced MitoSox^{TM} (~ 4 s^{-1}) is an order of magnitude faster than that for HE (< 0.5 s^{-1}) it is still only 2% of that observed for the native substrate ferrocytochrome *c* (> 200 s^{-1}). After adding a ten-fold excess of HE to complex IV (5 μM) under aerobic conditions, the resulting oxidized dye was separated from the enzyme by ultracentrifugation and the fluorescence spectra of the product obtained using two different excitation wavelengths as suggested by Robinson *et al*. [52]. The fluorescent emission at 580 nm was relatively weak in the case of excitation at 396 nm compared to excitation at 510 nm in keeping with conversion of HE to predominantly ethidium ion (E^+) by a two-electron oxidation. This was confirmed by anaerobic titration of complex IV with HE (Figure 30) where the dye was clearly behaving as a two-electron donor to the enzyme. We are confident there were no confounding (enzyme-independent) photochemical reactions taking place in the spectrometers, because on the timescale of these experiments, we detected no measureable conversion of HE (or MitoSox^{TM}) to oxidized products in the absence of added complex IV. With the benefit of hindsight, it is not surprising that the mitochondrially-targeted MitoSox^{TM} is a better substrate for complex IV than HE. The native substrate, cytochrome *c*, is a strongly positively-charged protein at neutral pH [121] and, consequently, we should expect any

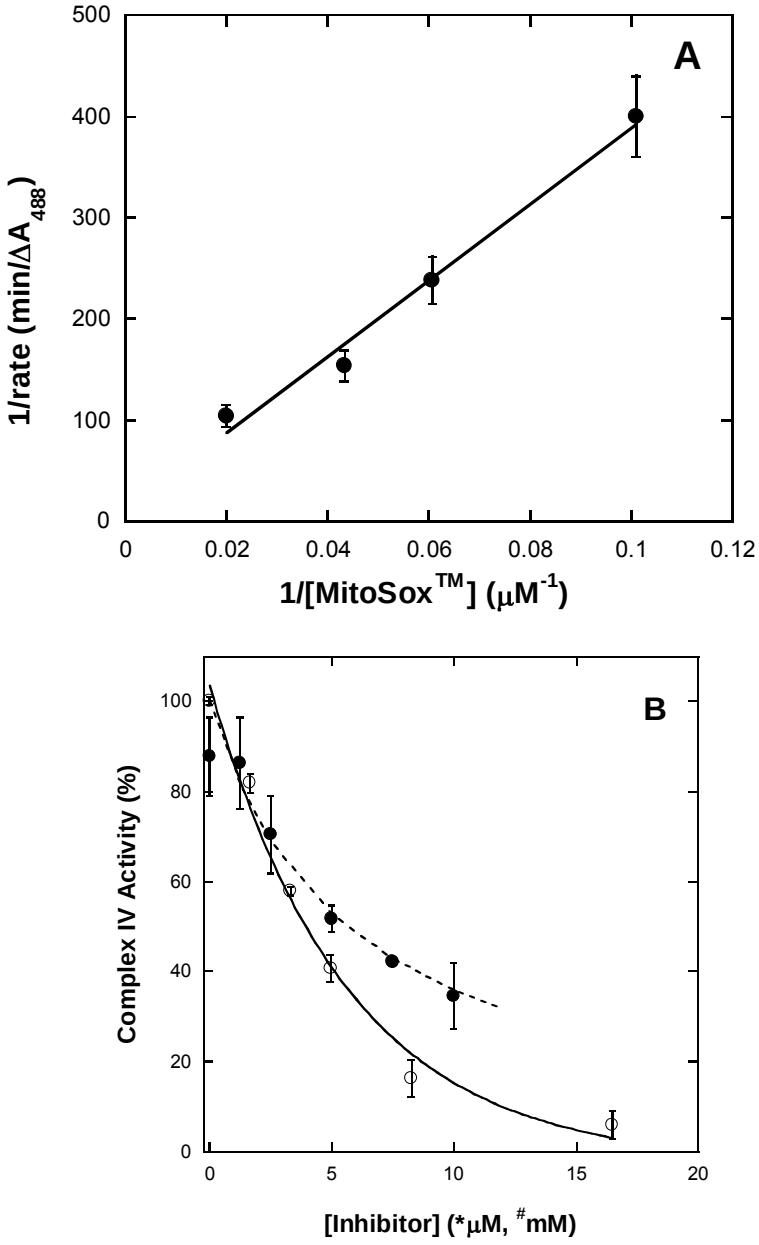

Figure 28. Effect of MitoSoxTM species on steady-state kinetics of complex IV (cytochrome *c* oxidase) at pH 7.4 in 0.1 M sodium phosphate, 0.05% lauryl maltoside, 22 ºC.

Panel A: Lineweaver-Burk plot showing complex IV turnover by reduced MitoSox™, 50 nM enzyme concentration, 0.25 mM oxygen. *Panel B:* Normal turnover (ferrocytochrome *c*:oxygen oxidoreductase activity) inhibition by oxidized ™ (○, **x*-axis μM) and tetraphenyl phosphate (●, *#x*-axis mM) 1.2 nM enzyme concentration, 10 μM ferrocytochrome *c*, 0.25 mM oxygen.

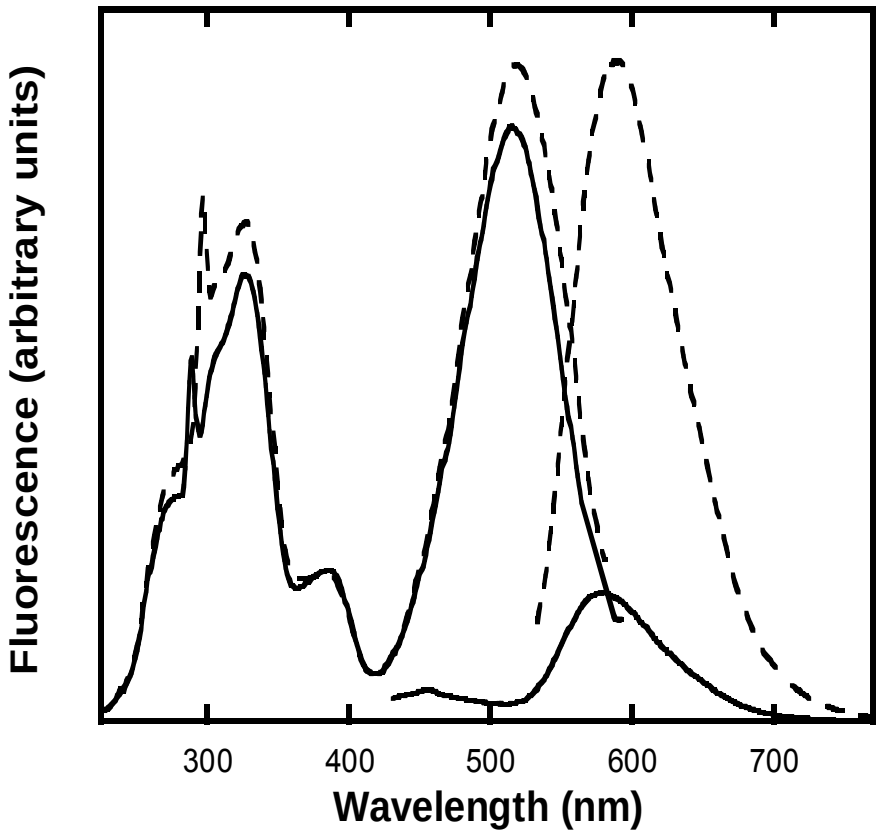

Figure 29. Fluorescence spectra of hydroethidine (HE) oxidation product(s) following reaction with complex IV (cytochrome *c* oxidase).

Excitation at 396 nm showing relatively little fluorescent emission at 580 nm (solid trace) compared with 510 nm excitation (broken trace) indicating the predominant formation of ethidium ion (E^+). Prepared sample (see text) diluted with water to approximately 1 μM in HE-derived species, 3 mm excitation and emission bandwidths, 2 x 1.00 cm cell, 22 ºC.

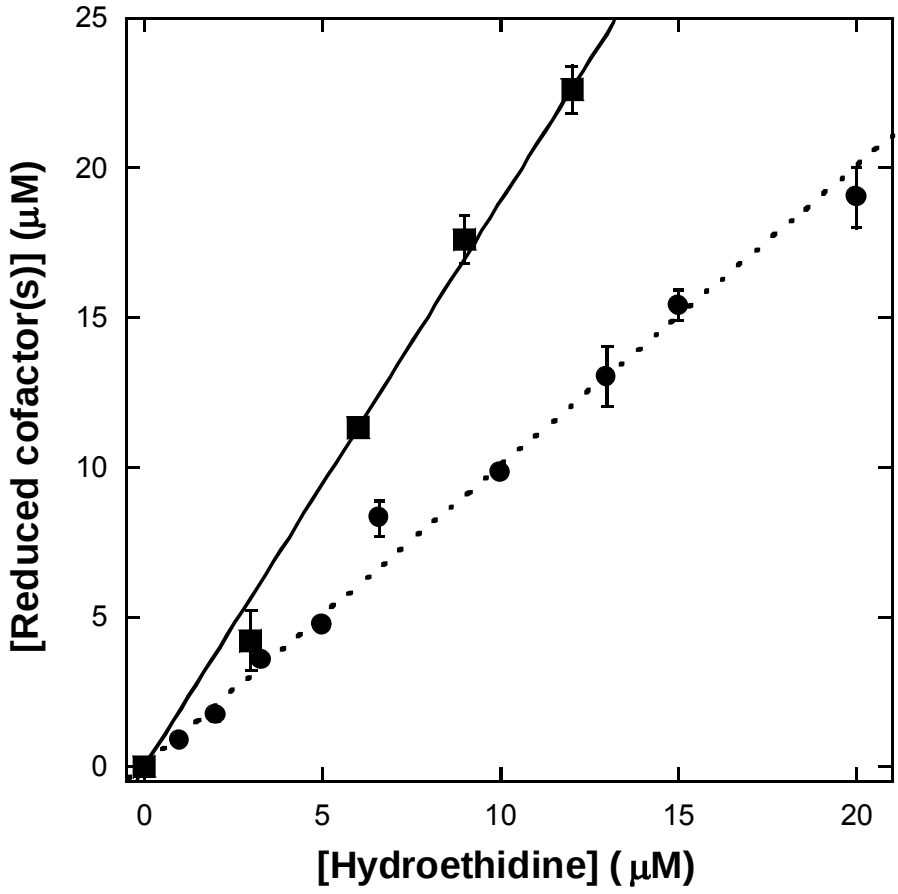

Figure 30. Comparison of the anaerobic titration of hydroethidine (HE) with complex IV (cytochrome *c* oxidase) and cytochrome *c*.

10 μM complex IV (■, 40 μM in total electron-accepting cofactors) pH 7.4 in 0.1 M sodium phosphate, 0.05% lauryl maltoside, 22 ºC, with fit to data (solid line) showing 2.0 (±0.14) electrons donated per molecule of HE consumed, consistent with production of ethidium ion (E^+). 20 μM cytochrome *c* (●, 20 μM in total electron-accepting cofactors) pH 7.4 in 0.1 M sodium phosphate, 22 ºC, with fit to data (dotted line) showing 0.97 (±0.04) electrons donated per molecule of HE consumed, consistent with production of HE-derived dimers.

positively-charged species to be attracted to the electron-entry site on complex IV. Moreover, any positively-charged species may inhibit normal enzyme turnover by blocking the approach of ferrocytochrome *c*, particularly if the species in question has other features likely to increase membrane affinity, such as aromatic rings. Accordingly, we observe that oxidized MitoSox^{TM}, which contains both an E^+ moiety and a mitochondrial-targeting triphenylphosphonium group, does indeed inhibit complex IV turnover (Figure 28B, solid symbols). Further to the same point, the tetraphenylphosphonium ion is also measurably inhibitory (Figure 28B, open symbols) albeit to a considerably lesser degree. In light of these observations, because introduction of something like a positively-charged triphenylphosphonium moiety is a common method of achieving mitochondrial targeting, we are bound to wonder if there is a body of literature in which effects due to inhibition of cytochrome *c* oxidase (complex IV) have erroneously been attributed to other causes.

4.4 DISCUSSION

In extracellular locations and in cell compartments other than the mitochondrion, proposed approaches for detecting superoxide production with HE-based probes, such as the selective fluorescence [52] and HPLC [116, 122] methods may have considerable merit. However, in our opinion, the same is not necessarily true in the case of mitochondrially-localized superoxide. The results of Figure 26 demonstrate, at least in the case of these particular experiments, that levels of superoxide resulting in measurable biological effects (*i.e.* changes in cell growth and mitochondrial membrane polarization) are below the detection capabilities of both dihyrorhodamine-123 and MitoSox^{TM}. Direct reaction of the probes with ETC components

such as complex III and cytochrome *c*, perhaps in addition to other presently unidentified targets is a potential complication. However, reaction of reduced MitoSox^{TM} with complex IV (cytochrome *c* oxidase) leading to a two-electron oxidized fluorescent product (analogous to HE-derived E^+) (Figure 29 and Figure 30) represents an entirely plausible explanation for the oxygen-independent response observed in the BPAEC (Figure 26D).

It has previously been pointed out [123] that interruption (or inhibition) of the electron-transport chain in the vicinity of cytochrome *c* must inevitably lead to accumulation of electrons upstream, with ensuing production of superoxide. That is, if the electron-entry site on complex IV becomes inhibited by something like oxidized MitoSox^{TM} (Figure 28B) increased production of superoxide by the functioning ETC cannot be avoided. It follows that if MitoSox^{TM} is employed to detect superoxide production in mitochondria, it is probably not possible to be sure that any superoxide detected would necessarily have been there in the absence of the probe system. If the objective is to establish whether there has been any change in the level (higher or lower) of superoxide following a given experimental manipulation, then HE-based probes may be used with a well-planned protocol and appropriate controls – for instance, in imaging (by fluorescence) the mitochondrial location of superoxide production [71]. However, being certain that the magnitude of any change observed by this method is biologically significant and not largely due to experimentally introduced artifact remains a perplexing problem. The alternate HPLC-based approach [122] is almost certainly not better in the mitochondrial case as no amount of product analysis overcomes the more fundamental difficulty that the decomposition product(s) of MitoSox^{TM} can induce generation of superoxide by the ETC and, consequently, the ambiguity persists.

5.0 CONCLUSIONS

5.1 FREE RADICALS AND OTHER REACTIVE OXIDANTS IN DISEASE

The study of free radicals and reactive oxidants has been of special importance in Public Health for the past few decades; in fact, many experts believe that free radicals pose one of the greatest single threats to our health as we progress into the twenty-first century [124-127]. Free radicals and other ROS are derived from normally essential metabolic processes in the human body (enzymatic or non enzymatic) and/or from external sources such as exposure to high energy radiation, ozone, cigarette smoking, air pollutants and industrial chemicals [76, 128-130]. The accumulation of oxidants/free radicals in the human body is also influenced by genetics and environmental differences that modulate their damage. In addition, free radicals are thought to exacerbate many serious diseases; for example, cancer and atherosclerosis. Ionizing radiation can initiate endogenous free radical reactions that can lead to DNA damage and subsequent tumor formation [131] and studies on atherosclerosis reveal the probability that the disease may be due to free radical reactions involving diet-derived lipids in the arterial wall [132-133]. Of special importance in Public Health is the contribution from oxidants or free radicals in the increasing incidence of diseases associated with advancing age. For example, free radicals are thought to contribute to Alzheimer‘s disease [134].

However, while molecular and cell biological studies are implicating oxidants in more diverse and complex processes, the underlying chemical mechanisms are not often clear. Even today, it is a great challenge trying to link observable chemistry with a biological phenomenon. Many researchers, however, have produced evidence that mitochondria play a pivotal role in free radical production, signal transduction and disease pathogenesis. The details of these biochemical mechanisms are still emerging and thus the current studies, contained within this dissertation, will add to the accumulating body of evidence for the involvement of oxidants in functional and metabolic alterations of tissues.

This is also the case, in particular, for peroxynitrite; a reactive oxidant (not itself a radical) formed by the combination of two biological free radicals, superoxide and nitric oxide. For a long time it has been proposed that the in *vivo* formation of this molecule could represent a crucial pathogenic step in conditions such as stroke, myocardial infarction, chronic heart failure, diabetes, circulatory shock, chronic inflammatory diseases, cancer, and neurodegenerative disorders [24]. The occurrence of protein tyrosine nitration under disease conditions, mainly arising from peroxynitrite formation, has now been firmly established [47]. However, other oxidative modifications and processes induced by peroxynitrite may be more important than nitration in cellular dysfunction or death. This leads to the work presented in this dissertation that seeks to delineate whether under physiological conditions peroxynitrite could be a key damaging molecule for the heme proteins of the electron transport chain, which are vital for cell function and survival.

5.2 PEROXYNITRITE REACTIONS WITH HEME PROTEINS

While much attention has been focused on the study of biologically adventious metal ions, which may promote Fenton chemistry and the possible involvement of these metal centers with peroxynitrite, there has been less written about the direct (or indirect) interaction of peroxynitrite with heme protein systems. Clearly, this is an issue, since heme proteins are present in biological systems at levels orders of magnitude greater than adventitious metal ions. The heme peroxidases have been the most studied, *e.g.* [135-138]. In mammals, these enzymes are mainly found in white blood cells and are important in the production of oxidants which digest bacteria. Myloperoxidase, lactoperoxidase, horse radish peroxidase, chloroperoxidase were shown to catalyze the destruction of peroxynitrite. Cytochrome p450 only undergoes this type of catalysis at non-physiological pH. These reactions are often pH dependent but have reported second order rate constants of near 10^6 M^{-1} s^{-1}, at 25°C and neutral pH [139]. In the nineties, at least two studies suggested that catalase (a ~~h~~ydroperoxidase") did not catalytically destroy peroxynitrite in the same manner as the other peroxidases had been shown to do. However, a recent study by Gebicka *et al.* showed that catalase was relatively resistant to damage by peroxynitrite and that the enzyme appeared to catalyze the decay of peroxynitrite with concomitant decreases in nitrotyrosine formation (in the presence of an appropriate substrate, see [140]). In addition, others have shown that myeloperoxidase can also catalyze tyrosine nitration from nitrite and hydrogen peroxide [141-142]. Consequently, it will be important to reconsider nitrotyrosine assays in conjunction with peroxidase activities as a method to detect and quantitate levels of peroxynitrite formation.

In addition, both methemoglobin and metmyoglobin (the ferric forms of the proteins) have been shown to react with peroxynitrite and the concomitant nitration of tyrosine residues

has been observed [143-145]. While there have been a number of mechanisms proposed for these heme proteins, most mechanisms involve the binding of peroxynitrite to Fe(III) with subsequent formation of either compound I (oxoferryl porphyrin π-cation radical) or compound II (oxoferryl porphyrin) and $^{\bullet}NO_2$ (which can then undergo disproportionation to nitrite and nitrate). Interestingly, Su et al. [145] have provided evidence that the reaction of peroxynitrite with metmyoglobin proceeded through a [Fe^{IV}=O $^{\bullet}NO_2$] caged radical intermediate leading to preferential nitration of Tyr 103 in horse heart myoglobin. Sui & Groves [146] suggest that the reaction of oxymyoglobin with NO proceeds through the same intermediate and thus while metmyoglobin (or hemoglobin) "may reduce the intracellular concentration of NO, it would not eliminate the formation of $^{\bullet}NO_2$ as a decomposition product."

It can be noted, that the decomposition rate of peroxynitrite by peroxidases and globins is much faster (x 2) than the reaction of peroxynitrite and CO_2. However, as other authors have theorized [139, 147-148] the ability of these proteins to eliminate peroxynitrite will depend on the relative amount of enzyme and CO_2 in the tissues studied as the relative rates are indeed second order in nature.

Finally, a good deal has been written about the interaction of peroxynitrite with cytochrome *c*. [38, 149-152]. Radi and co-workers first described the interaction to be a direct one which did not involve any intermediates. Subsequent studies showed that in the presence of CO_2, the reaction with cytochrome *c* yielded mainly nitrotyrosine and little oxidation of the heme iron occurred [153]. However, the spectroscopy of the nitrated cytochrome *c* was somewhat neglected. This has largely been rectified in this current work. In addition, much has been propounded concerning the capabilities of nitrated cytochrome *c* to carry out peroxidatic chemistry. Firstly, as isolated, the heme peroxidases generally contain an open site where

peroxide (or peroxynitrite) can interact with the heme iron; that is, excluding solvent-derived species, they are five-coordinate rather than six-coordinate. In this work and that of Radi's [151], it was shown that at neutral pH, the heme of nitrated cytochrome c (either in the presence or absence of CO_2, i.e MS- or NT-cytochrome *c*) is not five-coordinate but six-coordinate. While cytochrome *c* is not in its native configuration (methionine as the sixth ligand to the heme) it is partly coordinated by a lysine (as occurs during its alkaline transition) so that there is approximately 50% native configuration and ~50% lysine coordination. Now lysine is not a particularly good ligand to the ferric heme iron atom at neutral pH and, therefore, we suppose that it may briefly become five-coordinate in order to bind substrate when it is acting as a peroxidase. A recent paper studying the effects of a mutation (W41A) of ascorbate peroxidase showed that a histidine became coordinated to the sixth position of the heme iron, but that binding of substrate (hydrogen peroxide) "triggered a conformational change" in which H42 became dissociated from the heme [154]. In addition, these authors found that the reduction of the heme iron also caused the enzyme to become five-coordinate. This mutant, W41A, was shown to have good catalytic activity even though the active site was initially six-coordinate.

Thus, the fact that the nitrated cytochrome *c* is six-coordinate cannot exclude it from being a peroxidase. However, comparison of the peroxidatic activity of cytochrome *c*, nitrated cytochrome *c* with heme peptides (see Section 1) and horse radish peroxidase using the pyrogallol assay shows that even though the N-Ac-HUP (N-acetylated heme undecapeptide) is undoubtedly five-coordinate with respect to cytochrome *c*-derived ligands [155] it has rather indifferent peroxidatic activity compared to horse radish peroxidase as shown in Table 3. Interestingly, none of these proteins/peptides show any catalase activity; the heme moieties are bleached rather quickly by hydrogen peroxide.

Table 3. Pyrogallol assay for peroxidatic activity of several hemes/heme peptides.

Reactions were carried out at pH 7.0 at 20°. [a]Method and data from AC [29]). [b]Carraway *et al.* Inorganic Chem. 35, 1996 [156]. [c]Personnal communication, L. Pearce

Catalyst	H_2O_2 consumption, mmol of H_2O_2 min^{-1} (μmol of heme) $^{-1}$
heme octapeptide	0.9[b]
heme nonapeptide	1.0[b]
heme undecapeptide	1.3[b]
cytochrome *c*	0.09[c]
nitrated cytochrome *c*	3[c]
horse radish peroxidase	170[a]

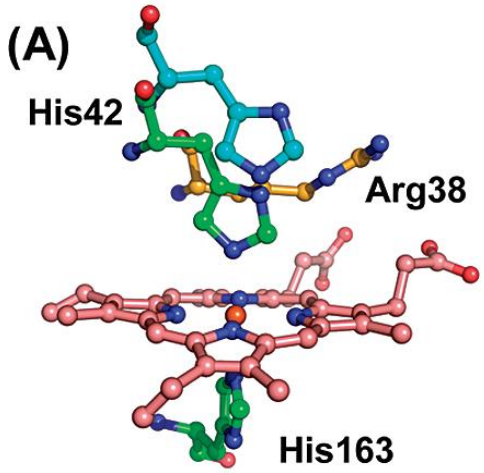

Figure 31. Structural alignment of the active sites of rsAPX (recombinant ascorbate peroxidase) .

Protein Data Bank entry 1OAG (blue) and W41A (green), showing the orientation of H42 in the off and on positions, respectively. Reprinted from [154] with permission from the American Chemical Society.

Another potential alteration of the function of cytochrome *c* by nitration is the ability of the protein to stimulate caspase activity. Nakagawa et al. demonstrated that cytochrome *c*-induced caspase-9 activity could be disrupted depending on which particular tyrosine was nitrated [113].

5.3 MITOCHONDRIAL PEROXYNITRITE: FORMATION AND TARGETS

As previously discussed (see Section 1), there appears to be a growing consensus that inhibition of the electron transfer chain or a back flow of electrons in mitochondria generates an increase in superoxide production. This was precipitated by the evidence that certain effects of NO could not be explained by the direct reactions of NO on cell respiration, but by some NO derived factors [157]. Thus as nitric oxide levels increase and complex IV is inhibited the electron transport chain can become a key producer of superoxide radical (O_2^-) and by extension, peroxynitrite from the rapid reaction of NO with O_2^-.

The biological half life of peroxynitrite has been estimated to be ~10 ms and may be shorter in mitochondria, 3-5 ms, because of the great number of available targets. However, while NO can easily diffuse through biomembranes and so forth, O_2^- diffusion is much more limited. On the other hand, peroxynitrite (both the anion and the acid) can diffuse some distance from the mitochondria or even *into* the mitochondria from the cytosol. Various studies have studies suggested that O_2^- can be formed on both the cytosol and matrix sides of the inner mitochondrial membrane space [35, 158-159]. A mean diffusion distance of 5 μm has been

calculated for peroxynitrite produced in mitochondria [160]. Since mitochondria have a size of ~1 μm, peroxynitrite produced within the mitochondria may diffuse to the cytosol.

In experiments with chemically synthesized peroxynitrite and biologically-induced peroxynitrite in chopped tissue from rat hearts, the oxidation of iron-sulfur clusters (predominatedly complex II and aconitase, data not shown) can be observed (Figure 32). The topical application of norepinephrine to cardiomyocytes elicits the intracellular production of nitric oxide, transiently (~1 s) reaching concentrations of several hundred nanomolar [161-162]. Inhibition of complex III with antimycin A is a convenient way of producing superoxide inside mitochondria of all cells [163]. Interestingly, the same barely significant degree of complex II inhibition in the cardiac tissue was observed whether nitric oxide production was stimulated by norepinephrine, superoxide generation was stimulated by antimycin A, or both norepinephrine and antimycin A were used together to give elevated peroxynitrite [41]. This is good evidence for 1) mitochondrially produced peroxynitrite, 2) evidence for its oxidation of metalloproteins and 3) endogenous CO_2 levels do not appear to suppress oxidation of metalloprotein centers by peroxynitrite. The tissue in question may have had slightly elevated oxygen levels but at the same time (the tissue was rapidly respiring) there was probably somewhat elevated CO_2 levels as the samples were frozen at the bottom of deep (~15 cm) EPR tubes from which CO_2 does not readily escape. This is at least added evidence that mitochondrial/tissue levels of CO_2 (a product of Krebs cycle) do not preclude oxidation of iron-sulfur clusters by peroxynitrite or peroxynitrite decomposition products.

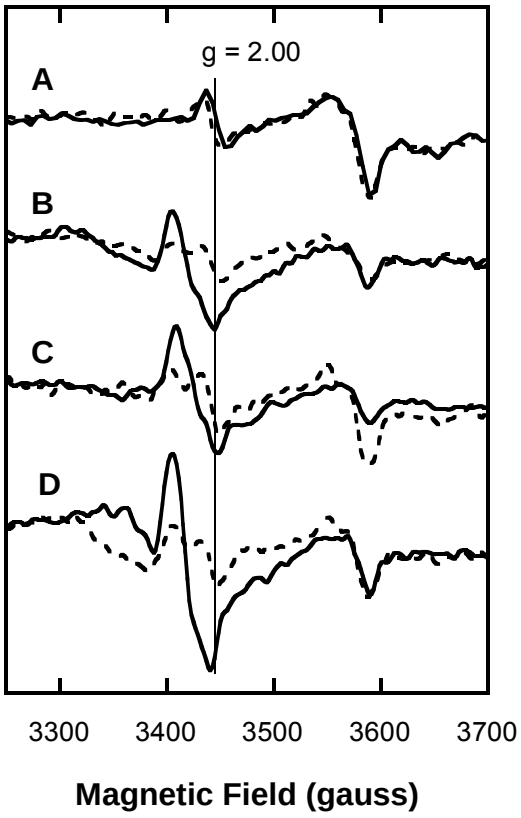

Figure 32. X-band EPR spectra of minced rat-heart myocardium demonstrating the effects of antimycin A, norepinephrine and succinate.

X-band EPR recording conditions: 15 K sample temperature; 4 mm o.d. sample tubes; 9.96 GHz; frequency; 40 μW power; 10 G modulation amplitude; 100 kHz modulation frequency). Myocardium was prepared as described in [41] All samples were frozen within 2 minutes of reagent additions and cryogenically preserved for subsequent introduction to the spectrometer without thawing. **Solid traces:** (**A**) Control sample. (**B**) Norepinephrine (cardiomyocyte stimulant for nitric oxide production) added to 1 μM. (**C**) Antimycin A (specific complex III inhibitor leading to mitochondrial superoxide production) added to 100 μM. (**D**) Antimycin A and norepinephrin added to 100 μM and 1 μM respectively. **Dashed traces:** As above, but samples pre-incubated with sodium succinate (added to 100 μM) for five minutes prior to other additions.

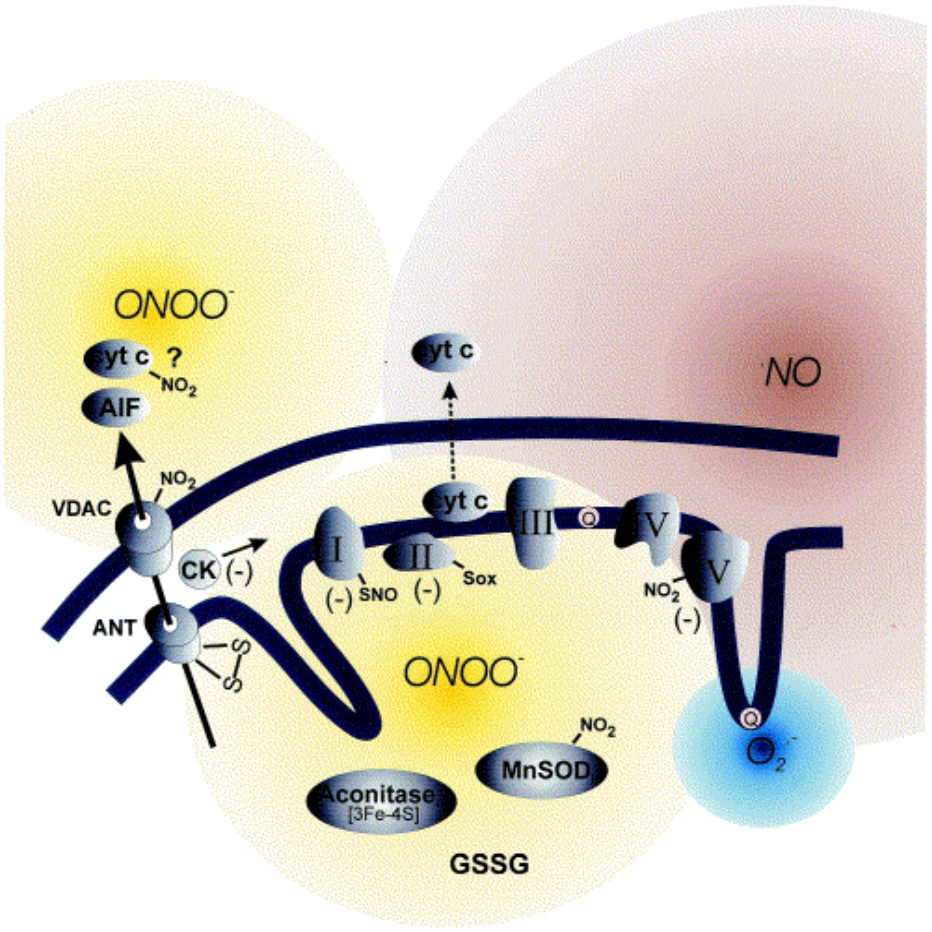

Figure 33. Overview of peroxynitrite formation/reactions in mitochondria.

Nitric oxide can freely diffuse to or be formed in mitochondria, while the Q-cycle is a key source of intramitochondrial O_2^-. Peroxynitrite arising from extramitochondrial sites or formed intramitochondrially undergoes reactions in the different mitochondrial compartments and small amounts may even diffuse to the cytosol. In mitochondria, peroxynitrite can trigger processes that affect mitochondrial physiology, including inhibition in energy metabolism, disruption of calcium homeostasis, and opening of the permeability transition pore (PTP). Reprinted from [164] with permission from Elsevier.

A plethora of mitochondrial proteins have been shown to be damaged by peroxynitrite. Indeed, while much of the evidence for the production of peroxynitrite in tissues is indirect (see above), at least one set of markers does seem consistent: protein nitration and hydroxylation [165]. A mitochondrial marker correlated with the production of peroxynitrite is the site-specific nitration/inactivation of MnSOD, the superoxide dismutase found only in mitochondria. This marker has been detected in animal and human tissues in both chronic and acute inflammatory situations [166-169]. Obviously the inactivation of MnSOD will lead to an increased production of peroxynitrite if superoxide is indeed the limiting reagent. Additionally, another matrix component found to be significantly affected, by oxidative degradation of its constituitive Fe-S cluster, is aconitase (see Appendix B).

Nevertheless, complexes I, II and V, as well as adenine nucleotide translocase (ANT) on the inner mitochondrial membrane have all been shown to also be affected by peroxynitrite. However, it is unclear if certain components of the ETC have simply been slightly impaired due to lessening of the flow of electrons through the ETC or that the proteins have become "permanently" impaired due to nitration, thiol oxidation or other reactions. As shown herein, this depends on the concentration of oxygen, carbon dioxide and perhaps, the location of the protein target within the mitochondrion (see below). For example, oxygen tension within tissues can be as low as 5 μM in working skeletal muscle [170]. Also, the physiological concentrations of HCO_3^- are considered to be around 25 mM (plasma), but these concentrations are probably somewhat lower in the mitochondria (< 9 mM) [83].

In chapter 3.0 it is shown that in the absence of CO_2, peroxynitrite can oxidize cytochrome *c* and cytochrome *c* oxidase, acting as a 1-electron and 2-electron oxidant respectively. Complex III was also oxidized, but indirectly, suggesting that the reaction occurred

via peroxynitrite degradation products. However, in the presence of bicarbonate no oxidation of complex III by peroxynitrite is observed. Cytochrome *c* exhibits only some slight oxidation by peroxynitrite in the presence of bicarbonate (aerobically) but no oxidation of cytochrome *c* is observed in the absence of oxygen (+/- bicarbonate). In addition, we found cytochrome *c* oxidation by peroxynitrite is clearly meditated by oxygen. To our surprise, a remarkable effect was observed in the case of the reaction of peroxynitrite with complex IV in the presence of bicarbonate; that is re-reduction was observed after initial oxidation (see section 3.3.3). This is still a puzzling dilemma that has yet to be resolved. Whether the reaction involves the formation of secondary reductant products or not, what it is significant is the fact that the re-reduction is faster than the oxidation of the enzyme, which will in the end effectively prevent the enzyme from oxidation by peroxynitrite.

To quote Prof. Jan Hoh, Dept. of Physiology, Johns Hopkins University, "One of the primary determinants of cellular activity in the body of an animal is the microenvironment, which is defined by the chemical and physical composition of the material that immediately surrounds the cell." Extending this to subcellular structures, the microenvironment is especially important in mitochondria, which has a very hydrophobic membrane, an alkaline matrix (pH ~ 8) and high reduced glutathione content. The microenvironment either side and within the inner mitochondrial membrane will, therefore, have a large effect on the chemistry we observe. Firstly, non-ionic species accumulate in hydrophobic membranes; *i.e.* NO partitions into membranes ~8-fold higher than in aqueous environments. Thus in the mitochondrial membrane, we should find predominately CO_2 and HOONO rather than HCO_3^- and ^-OONO. Goldstein *et al.* [171] have shown that it is most likely the anion of peroxynitrite that reacts with CO_2 (leading to nitrotyrosine formation) so we then expect that in the highly hydrophobic environment of the

membrane that this reaction would be minimal (Figure 34). The pK_a of the $ONOO^- \leftrightarrow HOONO$ couple is 6.8 and in the alkaline aqueous mitochondrial matrix, the peroxynitrite anion will predominate. Equally, we should find predominately HCO_3^- with only some CO_2 in the matrix. While the exact concentrations of CO_2 and bicarbonate are not known with any precision, we can assume that enough CO_2 is present so that the reaction of the peroxynitrite anion with CO_2 will

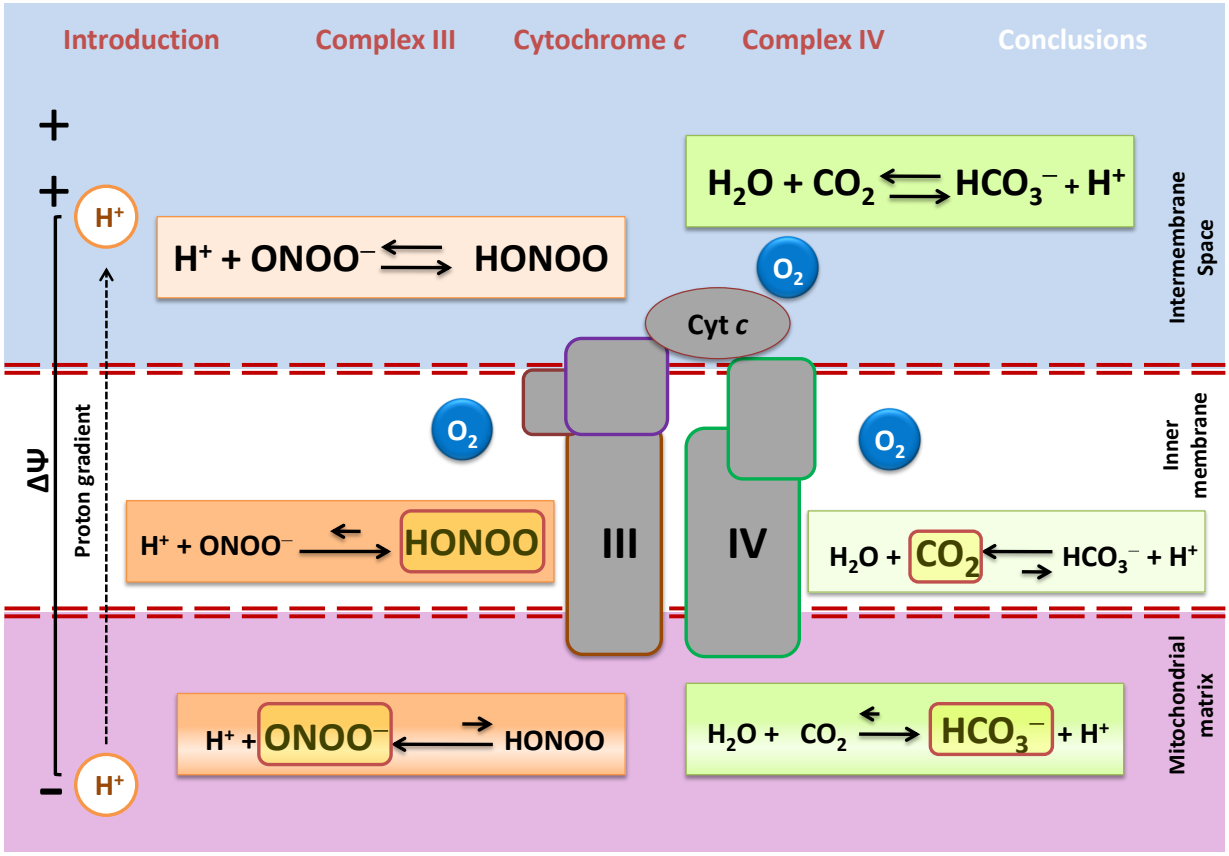

Figure 34. Distribution of biomolecules within the mitochondria.

Biophysical profile of the mitochondria predict that non-ionic molecules tend to rest within the hydrophobic membrane while charged species will tend to partition to the aqueous phase of the mitochondrial matrix.

predominate and thus nitrotyrosine formation will result in the reaction of peroxynitrite with proteins. Within the membrane, direct reactions of HOONO with complexes III and IV (and probably others) will occur. On the other hand, as cytochrome *c* (mediating electron transfer between complexes III and IV) sits at the interface between the aqueous and hydrophobic environments, it is quite likely that some combination of these two extremes will occur.

5.4 FINAL THOUGHTS AND FUTURE STUDIES

Since the mitochondrial electron-transport chain (ETC) consumes > 90% of our oxygen intake, the notion that this apparatus represents the major cellular source of superoxide (by "electron leak") is appealing to common sense. Unfortunately, it can be argued that the majority of the evidence in support of this idea is ambiguous in various ways and it is not at all clear that mitochondria are the main source of intracellular superoxide [81, 117]. The present findings support this minority position and lead us to suggest that, in particular, the case for the viable ETC being a significant source of superoxide has at the very least been overstated (Chapter 4.0). There are certainly other much better superoxide generators in most cells, like the nitric oxide synthase isoforms [172] and NADPH oxidase systems [173], but we do not mean to imply that superoxide generation in mitochondria is never of any pathological consequence. For instance, knocking out MnSOD is a lethal mutation [174], depletion of mitochondrial glutathione is cytotoxic [175-176] and the Krebs cycle enzyme aconitase is highly susceptible to oxidative damage [177]. In *non-apoptotic* pulmonary artery endothelial cells, the inner-membrane potential ($\Delta\Psi$, assessed using the fluorescent reporter JC-1) is decreased by culture in 20% versus 3% oxygen (Figure 26). Furthermore, the effect of 20% oxygen is reversed by over-

expressing MnSOD, confirming protection within the *matrix* microenvironment (where high levels of glutathione and aconitase are found) to be important. Consequently, it appears that we should be more concerned with superoxide generated by the ETC being released on the matrix side of the inner membrane rather than any leaking out into the rest of the cell. Of course, during apoptosis the mitochondria may generate substantial fluxes of superoxide, but this probably occurs only in cells already committed to die and it may be misleading to think of the reactive oxidants produced as causative agents.

It has become clear, that under normal physiological conditions, peroxynitrite can react with a variety of metalloproteins and /or glutathione and be degraded rather quickly. The complexes of the ETC, particularly cytochrome *c* oxidase (complex IV), can certainly be included in this group of peroxynitrite detoxifying systems (Chapter 3.0). The reaction of peroxynitrite with CO_2 is in competition with these processes (mostly in aqueous microenvironments) and probably results in some nitration of proteins. However, as long as the extent of nitration remains small, there will be no drastic consequences for cells; that is, so long as the rate of new protein synthesis remains faster than the rate of damaging nitration. Alternatively, under the acute or even chronic nitrosative/oxidative stress associated with some pathological conditions, the normal defense systems of the cell may begin to be overwhelmed. The most likely scenario for mitochondria involves at least two feed-forward loops. First, the nitration of MnSOD resulting in an inability to rid the matrix of superoxide – hence further elevation in peroxynitrite levels. Second, the Fe-S clusters of aconitase would be degraded to the extent that the enzyme would no longer function, slowing the flow of electrons through the ETC and severely compromising the ability of complex IV to detoxify peroxynitrite. It follows that irreversible inhibition of aconitase is more likely to be the cause of the observed superoxide-

dependent membrane depolarization (Figure 35) than a direct inhibition of any ETC complexes. While it has not been a subject for experimental investigation in this work, the question of whether peroxynitrite and/or its downstream products (*e.g.* nitrated lipids/proteins) might be involved in cell signaling should be addressed in future studies. For example, stimulation of mitochondrial biogenesis has been linked to NO [178-180], but since it is also associated with oxidative stress [181-183] perhaps this is really a peroxynitrite-mediated process.

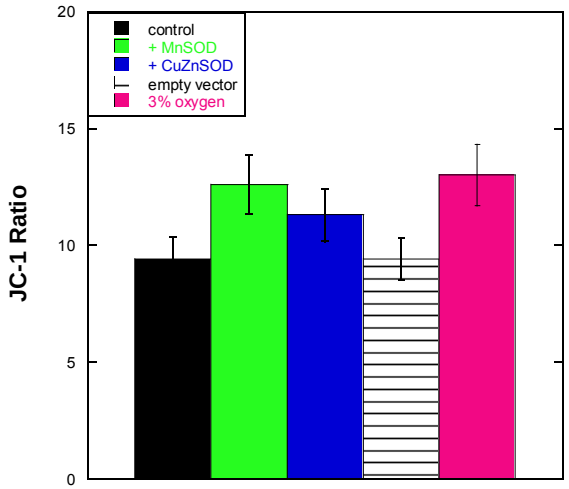

Figure 35. Oxidative stress in BPAEC at 20% oxygen is ameliorated by over-expression of MnSOD and CuZnSOD, or lowering the oxygen level (3%).

BPAEC were grown in 5% CO_2 and in either 3% or 20% oxygen (for at least 48 hrs prior to other treatment). When required, BPAEC were transiently transfected with empty vector (pCA14, Microbix), MnSOD or CuZnSOD plasmids 24 hrs prior to each experiment. Results are expressed as means ± SE from 3-6 experiments (the 20% oxygen level experiments are taken to be the controls, to which all other results are compared). BPAEC were seeded at 5 x 10^4 cells per well (6 well plates), grown for 24 hrs and then assayed for mitochondrial function using JC-1. ANOVA with a Dunnett *post hoc* test was conducted and differences were deemed significant at $p < 0.05$ (*) when compared to the 20% oxygen group. [184]

Further understanding the biological effects of peroxynitrite is severely hampered by the unsuitability of the existing probes for quantitatively determining the relevant bioinorganic species (NO, superoxide, peroxyitrite itself and also, CO_2/bicarbonate) in mitochondria. For example, one can clearly demonstrate mitochondrial effects of superoxide without being able to directly detect it, much less determine the effective concentration (Chapter 4.0). Significant advances in this particular analytical area would be very helpful.

APPENDIX A

ANTAGONISM OF NITRIC OXIDE TOWARD THE INHIBITION OF CYTOCHROME *C* OXIDASE BY CARBON MONOXIDE AND CYANIDE

Linda L. Pearce [*], Elisenda Lopez Manzano[*], Sandra Martinez-Bosch[*], Jim Peterson[*]

[*]Department of Environmental and Occupational Health,

The University of Pittsburgh, Graduate School of Public Health,

130 DeSoto Street, Pittsburgh, PennsylVania 15261

Keywords: Antagonism; Nitric Oxide; Cytochrome; Oxidase; Carbon Monoxide; Cyanide

Published in: *Chem. Res. Toxicol.* **2008,** *21,* 2073–2081

doi: 10.1021/tx800140y

A.1 ABSTRACT

The principle mitochondrial target where the respiratory inhibitors CO, CN^-, and NO act in the execution of their acute toxic effects is complex IV of the electron-transport chain, cytochrome *c* oxidase. However, there is a paucity of studies in the literature regarding the concerted effects of such poisons. Accordingly, the combined inhibitory effects of CO + CN^-, NO + CN^-, and NO + CO on the activity of cytochrome *c* oxidase preparations are reported. Only in the case of CO + CN^- do the effects of the two inhibitors seem to be additive as expected. NO appears to be antagonistic toward the effects of the other two inhibitors; that is, the effects of both CO an CN^- on enzyme activity are ameliorated by NO when present. To further clarify these observations, the ligand substitutions of heme-bound CN^- by NO in cytochrome *c* oxidase and hemoglobin have also been briefly investigated. These results suggest that displacement of CN^- from the ferric hemoproteins by NO is rate-limited by heme reduction- and in the case of the enzyme, the presence of nonligand-binding electron-transfer centers facilitates the reaction. The findings are discussed in relation to the idea that NO does not behave as a classic reversible (by dissociation) inhibitor.

A.2 INTRODUCTION

It is undoubtedly the case that, due to the widespread use of materials such as acrylonitrile copolymers and polyurethanes, the toxic effects of HCN in concert with those of CO have become of increasing concern worldwide in relation to victims of smoke inhalation [185-190]. Furthermore, while the literature is not extensive, there are independent

reports that the acute toxic effects of these two respiratory poisons are not additive but synergistic [191-193]. The observed synergistic lethality seems to involve the metabolic consequences of tissue hypoxia [191-193] rather than changes in blood flow [191] or altered blood CO and CN^- concentrations [192]. It follows that the biochemistry underlying these findings is quite likely associated with the inhibition of oxygen turnover at cytochrome *c* oxidase [complex IV of the mitochondrial electron-transport chain (ETC)] since both CO and CN^- are generally accepted to rapidly bind and inactivate the enzyme. Interestingly, it has been shown in rat brain that one effect of CO in vivo is to elevate NO levels [194]. Paradoxically, however, NO has been shown to either exacerbate [195-196] or protect against [196-197] the toxic effects of CN^- depending upon the particular cell culture and/or conditions employed. As NO is yet another complex IV inhibitor, it is clearly anticipated that investigating the combined effects of these three inhibitory species on cytochrome *c* oxidase activity may very well provide some insight into the mechanism of the reported CO and CN^- synergistic toxicity.

The active (O_2-binding) site of cytochrome *c* oxidase is binuclear, consisting of haem a_3 and Cu_B [198]. The active-site pocket has long been known to be able to simultaneously accommodate more than one diatomic ligand, such as two NO molecules [199], or NO and CN^- [8], or CO and CN^- [200], hence, by implication, O_2 together with another diatomic species. Therefore, studying the interactions of dual inhibitors with this particular enzyme is of some unusual importance. Here, we report the results of a study concerning the combined effects of CO + CN^-, NO + CN^-, and NO + CO on the activity of isolated bovine cytochrome *c* oxidase (ferrocytochrome *c*:oxygen oxidoreductase EC 1.9.3.1) and submitochondrial particles. The results appear to clarify some confounding observations reported in studies employing cultured cells and in vivo systems.

A.3 EXPERIMENTAL PROCEDURES

Cytochrome *c* oxidase was prepared as previously described [201] from intact bovine heart mitochondria using a modified Harzell−Beinert procedure (without the preparation of Keilin−Hartree particles). The enzyme was determined to be spectroscopically pure if the 444 to 424 nm ratio for the reduced enzyme was 2.2 or higher [202]. Derivatives were prepared in 50 mM potassium phosphate, 1 mM in sodium EDTA, and 0.1% in lauryl maltoside, pH 7.4−7.8, to concentrations of 10−80 μM (in enzyme). Enzyme concentrations were determined as total heme *a* using the differential (absorption) extinction coefficient of $\Delta\varepsilon_{604} = 12\ mM^{-1}\ cm^{-1}$ for the reduced minus oxidized spectrum of the mammalian enzyme [203]. Concentrations throughout are given on a per enzyme concentration basis (NOT per [heme *a*]). When required, submitochondrial particles were prepared from intact mitochondria simply by dispersion in buffer; the resulting osmotic shock ruptured the mitochondrial membranes. Mild sonication of these preparations did not lead to any measurable changes in cytochrome *c* oxidase activity.

Ferrocytochrome *c*:O_2 oxidoreductase activity was determined spectrophotometrically employing the high ionic strength method of Sinjorgo et al. [204]. Using this assay, we routinely obtained a turnover number with respect to cytochrome *c* of 340 (±30) s^{-1} (260 μM O_2, 0.1 M sodium phosphate, and 0.1% lauryl maltoside, pH 7.4, 22 °C) similar to that of the bovine enzyme isolated from a variety of tissues by others [204]. Oxygen consumption kinetics were measured polarographically using a catalytic amount of cytochrome *c* (60 μM) and 5 mM sodium ascorbate as the reductant. Reactions were carried out at room temperature in 0.1 M potassium phosphate buffer and 0.1% lauryl maltoside, pH 7.4, 22 °C, at an initial oxygen concentration of ~130 μM. Nitric oxide decomposition is dependent upon oxygen concentration and governed by the equation $-d[NO]/dt = 4k[NO]^2[O_2]$ with $k = 2 \times 10^6\ M^{-2}\ s^{-1}$ [205-206].

Consequently, starting with an oxygen concentration of ~130 μM, the initial rate of uncatalysed degradation of a 10 μM NO solution will be ~ 6 μM per minute at room temperature, but this slows dramatically as the reaction proceeds. All kinetic time courses for oxygen consumption (and ferrocytochrome *c* oxidation) were essentially linear in the range 10−60 s. Where required, rates were estimated from the linear-region slopes of the oxygen (or ferrocytochrome *c*) concentration vs time plots without applying corrections.

Hemoglobin A was obtained from Sigma, oxidized by $K_3Fe(CN)_6$ to metHb, further purified on a G-25 column, and then dialyzed against high (100 mM) and low (10 mM) salt sequentially to rid the protein of excess $[Fe(CN)_6]^{3-}$ and $[Fe(CN)_6]^{4-}$ [45]. MetHbCN was formed by titrating purified metHb with KCN until the fully formed species was detected spectrophotometrically at 540 nm (ε_{540} = 12.5 cm^{-1} mM^{-1}) [207].

All reagents were ACS grade or better, were used without further purification, and, unless stated to the contrary, were purchased from Aldrich or Sigma. Sodium dithionite, 87% minimum assay (+H_2O), was obtained from EM Science. Carbon monoxide and nitric oxide gases were obtained from Matheson Inc. Carbon monoxide-saturated solutions were made by bubbling CO through buffer solution for 30 min. Nitric oxide was scrubbed with water and KOH pellets prior to use, bubbled through anaerobic buffer (prepared by bubbling argon through the solution), and added to enzyme samples volumetrically with gastight syringes. Buffered solutions never exhibited any significant change of pH (i.e., <0.05 pH units) following NO additions.

Electronic absorption spectra were measured, and photometric determinations were made using Shimadzu UV-1650PC and UV-2501PC spectrophotometers. Rates of electron transfer from reduced cytochrome *c* to cytochrome *c* oxidase under saturating [O_2] (260 μM at 22 °C) were followed at 550 nm. A Clark type electrode (Rank Brothers), calibrated using saturated

sodium bisulphate (0% calibration) and air-saturated buffer (100% calibration), was employed to carry out the oxygen uptake experiments. The oxygen-depletion experiments performed under a closed-system configuration of the Clark type electrode showed linearity from 100 to ~ 12% oxygen levels over a 3 min period.

Cultured sheep pulmonary artery endotheial cells (SPAEC) were a gift from Bruce Pitt, Department of Environmental & Occupational Health, University of Pittsburgh. The SPAEC were grown in OptiMEM supplemented with 10% fetal bovine serum, 15 μg/mL endothelial cell growth supplement, 100 U/mL penicillin, and 100 μg/mL streptomycin at 37 °C in a 5% CO_2 atmosphere. Cells were plated into 24 well plates to ~ 95% confluence. Just prior to cyanide addition, media was removed and replaced with PBS (phosphate-buffered saline) after washing the cells once with PBS. Sodium cyanide (0−1.2 mM, final concentration) was added, and cells were incubated for 1 h at 37 °C. Cells were then washed with PBS, and 10% AlamarBlue was added to the assay for cell viability. Fluorescence changes (535 nm excitation, 590 nm emission) were monitored using a BGM Fluostar Galaxy plate reader. In those experiments, where both L-NAME and sodium cyanide were added to cells, L-NAME was incubated with the SPAEC for 30 min in PBS before the addition of cyanide as described above.

A.4 RESULTS

A.4.1 Steady-State Inhibition Kinetics

To establish the effects of dual inhibitors on the activity of cytochrome *c* oxidase, the kinetics of both ferrocytochrome *c* oxidation and dioxygen depletion have been examined. It has been shown that incubation of cytochrome *c* oxidase with CO leads to deactivation of the

enzyme by loss of subunit I [208]. To avoid the possibility of such processes, unless explicitly stated to the contrary, samples of the enzyme were not preincubated with CO, CN^-, or NO, turnover always being initiated before the addition of any inhibitors. To be sure that significant differences between inhibited rates and control (uninhibited) rates could routinely be obtained, we opted so far as was possible to work at single inhibitor concentrations sufficient to lower the measured activity by 50−60% of the control (maximal) rate (see Table 4). This approach also ensured that when pairs of inhibitors were added together at these pre-established concentrations, either a net loss or a gain in activity could be detected with roughly equal sensitivity. Because published K_i values can be laboratory- and/or preparation-dependent, the precise quantities of inhibitor to be used were determined by a few trial measurements.

Within the limits of experimental uncertainty, the concerted inhibitory effects of CO + CN^- on the rate of ferrocytochrome *c* oxidation by the isolated enzyme could reasonably be approximated as the sum of the effects of these two inhibitors acting separately (Figure 36A). It should be noted that from a qualitative perspective, the addition of the two inhibitory effects gives essentially the same result as one could obtain by simply increasing the concentration of a single inhibitor. This, of course, is exactly the result expected if the two inhibitors both form inactive enzyme−inhibitor complexes, which upon dissociation lead to regeneration of the catalytically competent enzyme. Therefore, these findings are entirely in keeping with the widely held view [8, 209-211] that CO and CN^- reversibly associate with the haem a_3-Cu_B pair of cytochrome *c* oxidase, preventing reaction of the enzyme with substrate O_2 while either inhibitory species remains bound in the binuclear site.

Table 4. Comparison of Observed Cytochrome c Oxidase (Complex IV) Turnover Numbers during Single and Dual Inhibition by CO, KCN, NO, CO + KCN, NO + KCN, and NO + CO.

a Calculated from fits in Figure 36; quoted errors are standard deviations.

b A 1.2 nM concentration of enzyme, pH 7.4, in 0.1 M sodium phosphate buffer, 1 mM EDTA, and 0.05% lauryl maltoside, 22 °C.

inhibitor (concentration)	**turnover number (k_{cat}, s^{-1})[a]**
uninhibited control[b]	346 ± 28
CO (0.5 mM)	190 ± 21
KCN (50 nM)	136 ± 8
NO (0.5 μM)	184 ± 30
CO (0.5 mM) and KCN (50 nM)	109 ± 9
KCN (50 nM) and NO (0.5 μM)	176 ± 8
NO (0.5 μM) and CO (0.5 mM)	182 ± 11

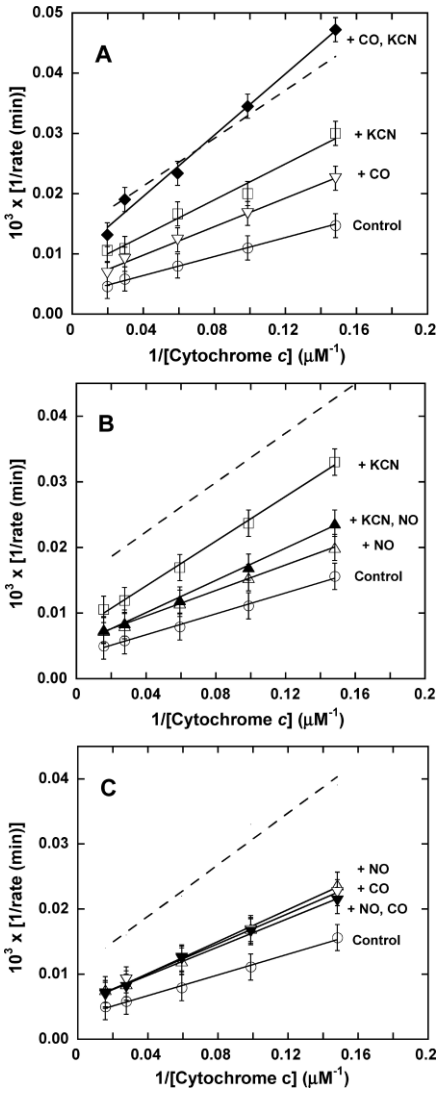

Figure 36. Dual inhibition of cytochrome *c* oxidase (complex IV) turnover (spectrophotometric measurements) by CO + CN−, NO + CN−, and NO + CO.

Lineweaver−Burk (double reciprocal) plots showing inhibition of ferrocytochrome *c* oxidation. Reaction conditions were 1.2 nM enzyme in 0.1 M aqueous potassium phosphate buffer, pH 7.4, 1.0 mM in EDTA, and 0.05% in lauryl maltoside, 22 °C. (A) Uninhibited control (○), 0.5 mM CO (▽), 50 nM KCN (□), and 0.5 mM in CO and 50 nM in KCN (♦). (B) Uninhibited (○), 0.5 μM NO (Δ), 50 nM KCN (□), and 50 nM in KCN and 0.5 μM in NO (▲). (C) Uninhibited (○), 0.5 mM CO (▽), 0.5 μM NO (Δ), and 0.5 μM in NO and 0.5 mM in CO (▼). In each panel, the broken line represents the combined effect of the two relevant inhibitors predicted by simple summation of their individual measured effects.

Unlike the CO + CN^- kinetics, the concerted inhibitory effects of NO + CN^- (Figure 1B) and NO + CO (Figure 1C) were clearly not additive. Remarkably, with NO in excess, the inhibition observed for NO + CN^- was actually less than that observed for the same concentration of CN^- alone (Figure 1B). The kinetics of cytochrome *c* oxidase inhibition by NO + CO were indistinguishable from those of either NO or CO alone in this particular set of experiments (Figure 1C). Other data sets (e.g., see Figure 3C below) suggested that, in fact, the NO + CO kinetics were dominated by the effect of NO alone. It does not appear that these qualitatively very different findings to those obtained for CO + CN^- (Figure 36A) can be explained by any straightforward considerations of relative affinities and mass action. Because the inhibition of cytochrome *c* oxidase by CO + CN^- yields simple additive results, it must be the NO that is principally responsible for the interesting nonadditive kinetics shown in Figure 1. More succinctly, the addition of NO (nominally ~~in~~hibitory") to the enzyme during turnover in the presence of either of the other two inhibitors did not lead to increased inhibition. It is to be stressed that in experiments where cytochrome *c* oxidase is inhibited by NO alone, there was no obvious indication in the kinetics of any unusual behavior. At [NO]:[O_2] ratios upward of 1:50, nonlinear kinetics were evident, but in the NO concentration range employed to obtain the data of Figure 1, linearity of double-reciprocal plots, with a straightforward (additive) dependence of the slope on NO concentration, was reproducibly observed (Figure 37). This is also the case for double-reciprocal plots of CO (only) and CN^- (only) at the concentrations employed here (not shown).

To verify that the unusual nonadditive kinetic behavior of mixed NO + CN^- and NO + CO inhibition were routinely to be observed irrespective of the procedure used, a more limited set of polarographic measurements was performed. Clark type oxygen electrodes are subject to

drift, and determinations made with these devices lack the sensitivity of the spectrophotometric method, which in practice requires that slightly different conditions be used in the two kinds of measurement. Here again, the inhibitory effects of CO and CN^- combined to yield increased inhibition when the two were present together (Figure 38A). However, at the individual inhibitory levels used in these experiments, the combined inhibition of NO + CN^- was less than that observed for CN^- alone (Figure 38B), and the combined inhibition of NO + CO was the same as that observed for NO alone (Figure 38C), in good qualitative agreement with the spectrophotometrically determined results of Figure 36.

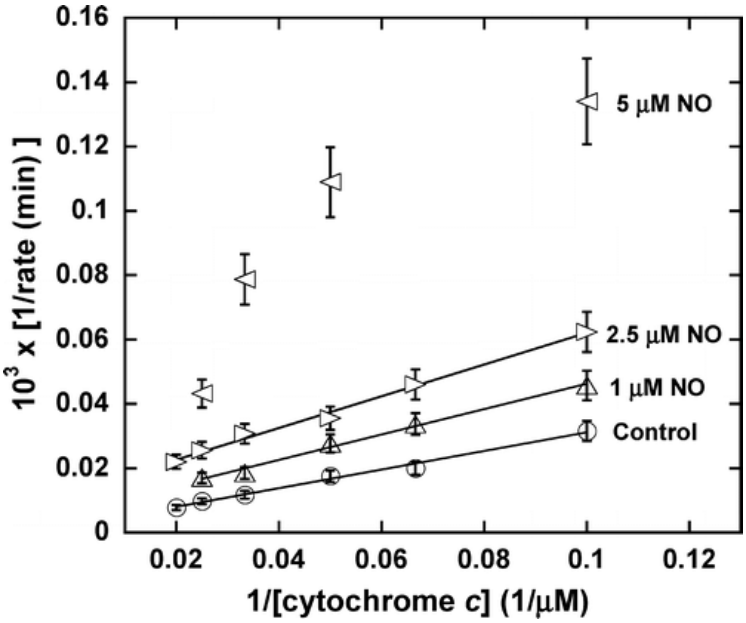

Figure 37. Lineweaver−Burk (double reciprocal) plot demonstrating inhibition of cytochrome *c* oxidase turnover by NO alone.

Measurements performed in 0.1 M aqueous potassium phosphate buffer, pH 7.4, 1.0 mM in EDTA, and 0.05% in lauryl maltoside, using samples that were 5.0 nM in enzyme at 37 °C.

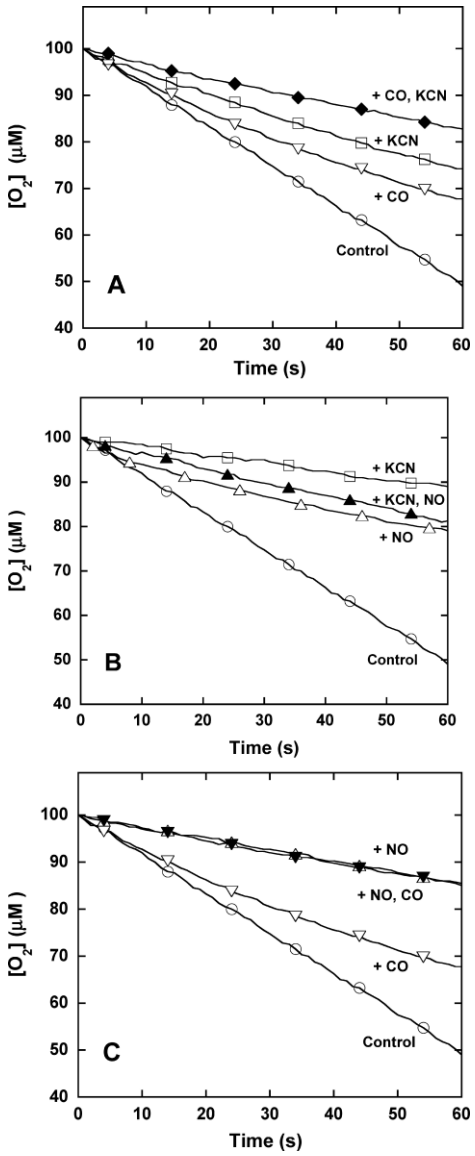

Figure 38. Dual inhibition of cytochrome *c* oxidase (complex IV) turnover (polarographic measurements) by CO + CN^-, NO + CN^-, and NO + CO.

Clark type oxygen electrode traces showing inhibition of O_2 consumption, 500 nM enzyme, 60 μM ferrocytochrome *c* in 0.1 M aqueous potassium phosphate buffer, pH 7.4, 1.0 mM in EDTA, and 0.05% in lauryl maltoside, 22 °C. Small adjustments to the locations of the traces relative to the ordinate axes have been made to assist with visual comparison. (A) Uninhibited control (○), 1.0 mM CO (▽), 1.0 μM KCN (□), and 1.0 mM in CO and 1.0 μM in KCN (◆). (B) Uninhibited (○), 8 μM NO (Δ), 2 μM KCN (□), and 2 μM in KCN and 8 μM in NO (▲). (C) Uninhibited (○), 10 μM NO (Δ), 1.0 mM CO (▽), and 10 μM in NO and 1.0 mM in CO (▼).

The ability of NO to counteract the inhibition of cytochrome *c* oxidase by CN^- was further investigated by varying the CN^- concentration at fixed [NO] (Figure 39A) and by varying the NO concentration at fixed [CN^-] (Figure 39B). The most interesting feature of these data is that, at all ratios of [NO]:[CN^-] examined, the inhibitory effects were never found to be quantitatively additive. That is, the combined inhibition observed for NO + CN^- was always found to be significantly less than one would estimate by summation of the inhibition measured for NO alone and CN^- alone at the same individual concentrations. NO appeared to dominate the inhibition kinetics only when present in greater than 4- (Figure 39B) to 7-fold (Figure 39A) excess. The difference between these estimates is not significant given the likely volumetric uncertainty involved in the assay procedures, where transfers of microliter quantities of gaseous reagents have been made with gastight syringes to reaction vessels closed with rubber septa. In measurements of cytochrome *c* oxidase activity in the presence of individual inhibitors, we typically find it necessary to add 5−10 times the concentration of NO as compared with CN^- to reaction mixtures to achieve the same degree of enzyme inhibition (e.g., see Table 4). Thus, when both were present, the ratio of [NO]:[CN^-] at which neither NO, nor CN^-, inhibition was dominant (i.e., 4−7) corresponded well to the concentration ratio at which the degree of inhibition due to each inhibitor should be equal (i.e., 5−10). In situations where both inhibitors were present, the effect of NO was dominant when it was in greater than several-fold excess ([CN^-] < 150 nM in Figure 39A), whereas the effect of CN^- was dominant if NO was present at less than several-fold excess ([NO] < 400 nM in Figure 39B). At the higher inhibitor levels, where total inhibiton of the enzyme was >60%, the differences between the results for NO + CN^- and CN^- only (Figure 39A) or NO + CN^- and NO only (Figure 39B) were within the experimental uncertainty. In summary, so far as these data are able to discriminate, the

mechanisms by which the two inhibitors function are apparently mutually exclusive (not additive). Consequently, under conditions where the inhibitory capacity of NO exceeds that of CN^- (corresponding to a greater than ~4-fold concentration excess), NO inhibition will dominate and CN^- inhibition will effectively be decreased.

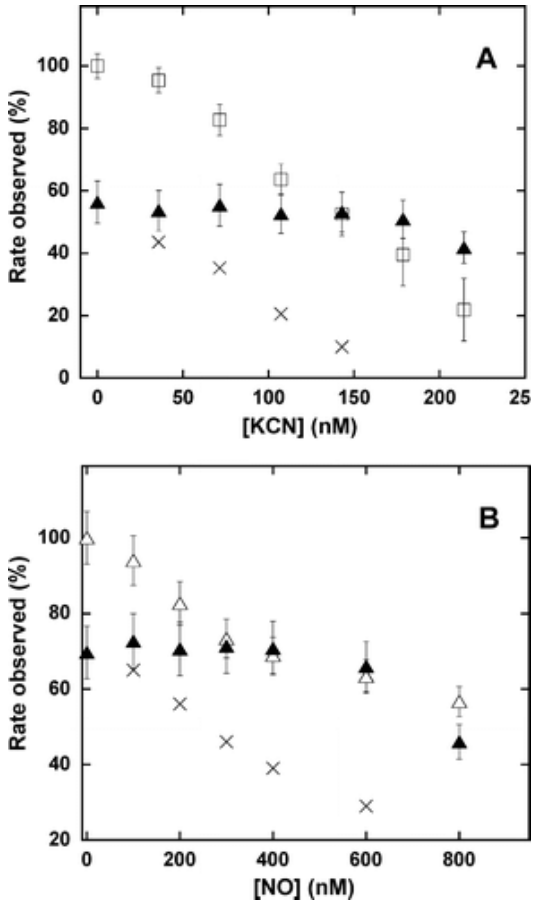

Figure 39. Dependence of cytochrome *c* oxidase turnover on the relative concentrations of NO and CN^- during mixed inhibition.

Measurements performed in 0.1 M aqueous potassium phosphate buffer, pH 7.4, 1.0 mM in EDTA, and 0.05% in lauryl maltoside, 22 °C, 2.4 nM enzyme concentration. (A) Variable [KCN], without NO (), NO added to 1.0 μM (▲). (B) Variable [NO], without KCN (Δ), KCN added to 80 nM (▲). Each point is the mean of 3−6 measurements, and error bars represent standard deviations. Total inhibition predicted (assuming no interaction) by simple summation of the individual effects due to NO plus CN^- (×).

A.4.2 Characterization of the Inhibited Forms

In the presence of an electron source, the cyanide-inhibited cytochrome *c* oxidase exists as a partially reduced derivative in which CN^- is bound to heme a_3 in its ferric form, Cu_B (and the other centers) being reduced [8, 209]. This species, which exhibits a well-known broad electron paramagnetic resonance (EPR) spectrum (Figure 40, broken trace) attributed to cyanoferriheme a_3, has also been detected during enzyme turnover in the presence of CN^-, although it was apparently not the major inhibited form [210]. Upon exposure to NO, the broad EPR signal was rapidly converted to a much sharper spectrum exhibiting a three-line hyperfine structure around $g = 2$ (Figure 40, solid trace). This signal has been unambiguously shown to derive from a five-coordinate nitrosylferroheme species [201]. That is, NO displaces CN^- from heme a_3 with near-concomitant reduction of the heme from the ferric to ferrous oxidation level. Given the similarity in the ligand properties of NO and CO, it was to be expected that the latter would also undergo an analogous substitution reaction with the partially reduced cyanide-inhibited cytochrome *c* oxidase, but this cannot be so convincingly demonstrated by EPR spectroscopy as the carbonmonoxyferroheme a_3 final product is EPR silent.

The displacement of CN^- from heme a_3 in cytochrome *c* oxidase by CO can be conveniently followed by electronic absorption spectroscopy. The partially reduced cyanide-inhibited enzyme exhibited a 428 nm Soret absorption band (Figure 41, broken trace) that was shifted to 433 nm following the introduction of CO (Figure 41, dotted trace) with an accompanying increase in the intensity of the visible region (α) band at 604 nm (not shown). These electronic absorption changes, which were complete by the time the sample could be returned to the spectrophotometer following addition of CO, are strong indicators of CO binding to heme a_3 in the ferrous state, confirming the expected reaction to have taken place.

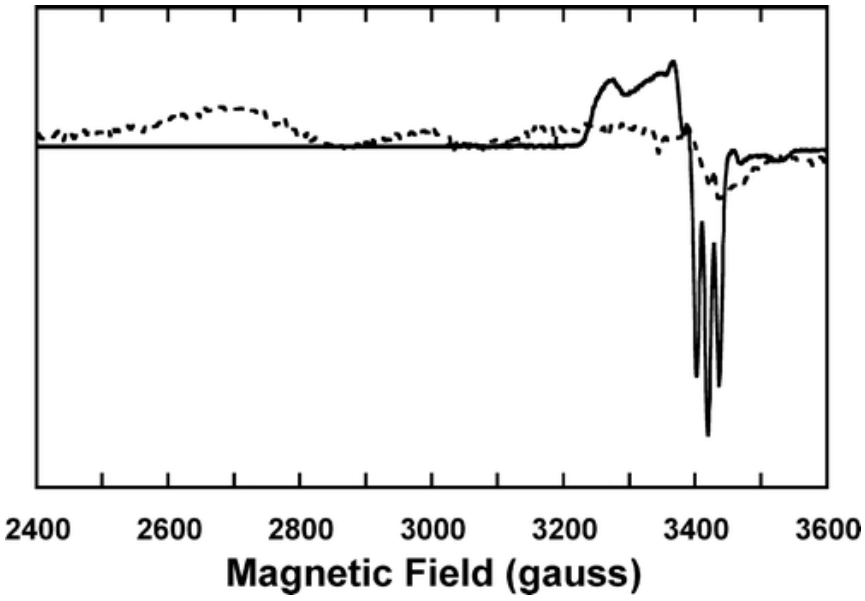

Figure 40. X-band EPR spectra showing displacement of CN− by NO at heme a3 of cytochrome *c* oxidase. Sample preparations were carried out in 0.1 M aqueous potassium phosphate buffer, pH 7.4, 1.0 mM in EDTA, and 0.05% in lauryl maltoside, 22 °C, prior to freezing in EPR tubes. Recording conditions: 0.2 mW microwave power, 4 G modulation amplitude, 1×10^4 amplifier gain, and 15 K sample temperature. Broken trace: partially reduced cyanide adduct, 60 μM in enzyme, 1.0 mM in KCN, ~1 mM in $Na_2S_2O_4$. Solid trace: partially reduced cyanide adduct plus NO, 60 μM in enzyme, 1.0 mM in KCN, ~1 mM in $Na_2S_2O_4$, and 1.9 mM (1.0 atm) NO.

Interestingly, following NO addition to the partially reduced cyanide-inhibited enzyme, a more complicated envelope with two maxima at 430 and 442 nm was obtained (Figure 41, solid trace). In fact, these two features were slightly variable in relative intensity between samples (not shown), demonstrating that they represent two distinct chemical species rather than being two bands in the spectrum of a single derivative. Because Soret features at >440 nm are associated with exogenous ligand-free ferrous heme a_3, this spectrum provides evidence that once NO has displaced CN^-, the NO itself may then be lost from the ferrous heme. This does not necessarily

mean, however, that the NO dissociates, it may be lost by conversion to some other species that is not a good ligand. In summary, both CO and NO are seemingly able to rapidly displace CN^- from ferric haem a_3 to form, respectively, ferrous CO and ferrous NO adducts, presumably with the acquisition of the necessary electron from a reduced center nearby, such as Cu_B. In the case of the NO adduct, there is some indication in the absorption spectrum for subsequent partial loss of bound NO.

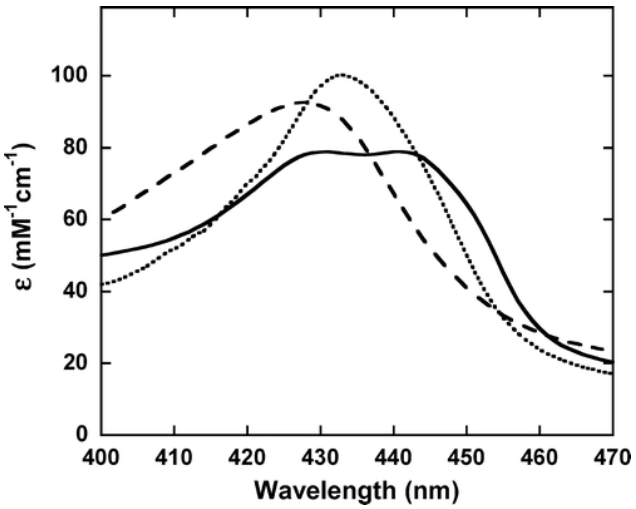

Figure 41. Electronic absorption spectra of cytochrome *c* oxidase derivatives showing displacement of CN^- by both NO and CO.

Samples were prepared in 100 mM aqueous potassium phosphate buffer, pH 7.4, and 0.05% lauryl maltoside, 22 °C, 1.00 cm pathlengths. Broken trace: partially reduced cyanide adduct, 12 μM in enzyme, 0.2 mM in KCN, and ~1 mM in $Na_2S_2O_4$; dotted trace: partially reduced cyanide adduct plus CO, 12 μM in enzyme, 0.2 mM in KCN, ~1 mM in $Na_2S_2O_4$, and ~1 mM (1.0 atm) CO; solid trace: partially reduced cyanide adduct plus NO, 12 μM in enzyme, 0.2 mM in KCN, ~1 mM in $Na_2S_2O_4$, and 1.9 mM (1.0 atm) NO.

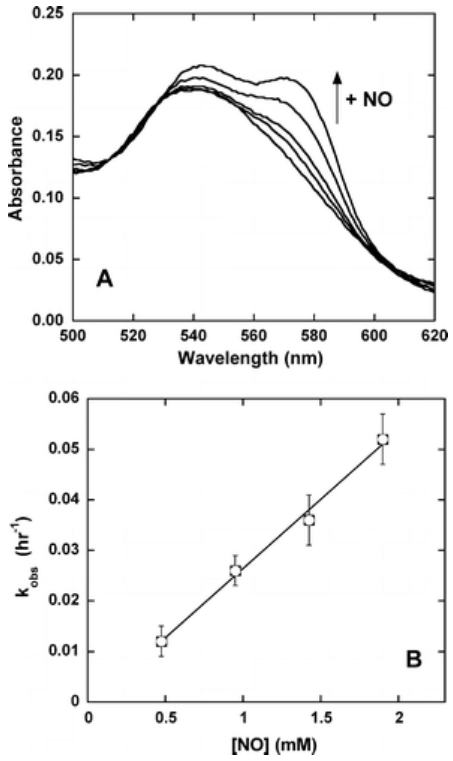

Figure 42. Reaction of NO with cyanomethemoglobin (metHbCN).

Samples were prepared in 100 mM aqueous potassium phosphate buffer, pH 7.4, 22 °C, 1.00 cm pathlengths. (A) Electronic absorption spectral changes (500−620 nm range) over time (~1 h) of 14 μM metHbCN plus 0.95 mM (0.5 atm) NO. (B) Linear dependence of the rate of reaction on the NO concentration.

In an effort to better understand the general features of a reaction where CN^- attached to a ferric heme is displaced by ligands having a marked preference for ferrous heme (namely, NO and CO), we performed a limited set of experiments with hemoglobin. Following the admission of NO gas to an anaerobic sample of cyanomethemoglobin, the visible region absorption spectrum slowly (k_{obs} ~0.5 h^{-1}) changed from that of the ferric heme-CN^- derivative to that of a mixture [212] of five- (minor component) and six-coordinate ferrous heme-NO adducts (Figure 42A). Significantly, when the analogous substitution was attempted with CO (not shown), there

was no detectable reaction after several hours. The rate of the overall reaction with NO was found to be independent of pH (one pH unit either side of 7.4, not shown) but linearly dependent upon [NO] (Figure 42B). The obvious reasonable interpretation of these observations is that reduction of the heme is rate limiting, and also, while NO may act as the necessary reducing agent, CO cannot. This supports the idea that reaction of the partially reduced cyanide adduct of cytochrome *c* oxidase is possible with CO and faster in the case of NO because of the proximity of reduced centers in the enzyme that are able to act as electron sources.

A.4.3 Biological Significance

To evaluate the possible biological significance of the present findings, we undertook a brief investigation of the effects of added KCN on endothelial cells. It is most convenient to investigate the effects of varying near-physiological NO levels by addition of nitric oxide synthase (NOS) inhibitors to endothelial cells since these are net producers of NO. The addition of the NOS inhibitor N_{ω}-nitro-l-arginine methyl ester (L-NAME) to SPAEC has no measurable effect on metabolic activity (Figure 43, broken line) for several hours. However, the SPAEC undergo a significantly increased loss of metabolic activity in the presence of L-NAME + KCN (Figure 43, ●) as compared to KCN alone (Figure 43, ■). These findings clearly indicate that NO, at endogenously generated levels in SPAEC, is an antagonist of KCN toxicity. There is also a limited amount of supporting data from other laboratories. Baskin et al. [213] have reported a protective effect of NO donors against the effects of NaCN in mice. Leavesley et al. [196] similarly found a protective effect of NO donors in cultured cells exposed to KCN, but surprisingly, these same authors report apparent enhancement of CN^- toxicity by low level NO production (see the Section 1.01(a)(i)A.5A.5).

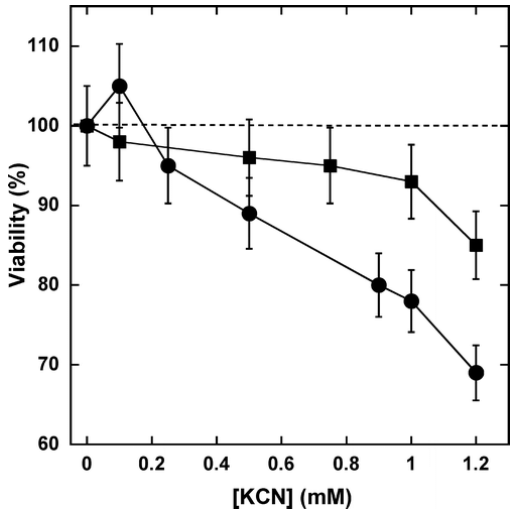

Figure 43. Resistance of sheep pulmonary artery endothelial cells (SPAEC) to CN− is suppressed in the presence of a nitric oxide synthase (NOS) inhibitor.

Viability was determined 2 h after exposures to KCN by AlamarBlue (see the section A.3 for details). Variable KCN (■) and variable KCN plus 0.5 mM L-NAME (●). The broken line indicates the effect of the NOS inhibitor L-NAME on the SPAEC in the absence of KCN (by extrapolation from the point where [KCN] = 0).

A.5 DISCUSSION

A.5.1 Functional Reserve of Cytochrome *c* Oxidase Activity?

On a per molar basis, the rate of ferrocytochrome *c* oxidation by its oxidase is expected to be four times the rate of oxygen removal, since four electrons are required for the conversion of one dioxygen to two water molecules during the enzyme-catalyzed reaction. However, even using samples of the purified enzyme, it can be very difficult in practice to straightforwardly compare kinetic determinations performed spectrophotometrically and polarographically. The two sets of measurements are optimally made under rather different sets of conditions (see the

section A.3) where the principal sources of error are not the same. Furthermore, there is typically some variation in the specific activity of different enzyme preparations and a loss in activity of individual preparations upon storage, which are important considerations given that the two procedures can seldom be performed at the same time. Thus, if a spectrophotometrically determined specific activity for cytochrome *c* oxidase is found to differ somewhat from four times the polarographically determined rate on a per molar basis, this need not necessarily be significant. The situation is even more problematic if all of the components of the ETC are present under partially inhibitory conditions. For example, inhibition of the cytochrome *c* oxidase (complex IV) by CN^- will result in accumulation of electrons in complexes I, II, and III; this, in turn, leads to an increase in superoxide (O_2^-) generation. Under spectrophotometric assay conditions, some of the electron accumulation in complexes I, II, and III could, conceivably, be due to back-flow from ferrocytochrome *c*, and conversely, O_2^- reacts with ferricytochrome *c* to regenerate the starting form of the cytochrome. That is, there are complex IV-independent reactions that can both oxidize and reduce cytochrome *c*. Consequently, any spectrophotometric measurement of cytochrome *c* oxidase activity under cyanide-inhibited conditions where other ETC components are present could be erroneously elevated or lowered depending upon the relative rates of such interfering reactions. When working with purified preparations of the enzyme, back-flow of electrons is of no concern, but we did verify that interference from O_2^- generation was insignificant in the present studies by observing that the addition of cyanide-insensitive manganese superoxide dismutase had no effect on the measured activity (not shown).

It has been reported that exposure to KCN of mouse brain in vivo [214] and rat mesencephalic cells in culture [196] requires >50% inhibition of cytochrome *c* oxidase before the rate of O_2 consumption is decreased. If not an experimental artifact, this is a potentially very

interesting observation indeed because it suggests the presence of some additional critical site(s) other than the terminal oxidase where the acute effects of CN^- toxicity are expressed. However, the "threshold effect" analysis [215-216] adopted to generate these results is subject to the interference and consequent interpretational difficulties that we have just described. So, at the level of the intact respiratory chain, there may be some threshold of cytochrome *c* oxidase inhibition by CN^- below which O_2 consumption is not decreased, but this remains to be verified unambiguously.

A.5.2 Inhibition by Nitric Oxide

We have shown that under appropriate turnover conditions, where NO is one of a pair of dual inhibitors, the measured cytochrome *c* oxidase inhibition kinetics essentially represent the effects of NO alone (Figure 36B,C and Figure 38B,C). That is, intriguingly, NO appears able to act as an antagonist of both CO and CN^- inhibition of the enzyme. As the inhibition kinetics of CO + CN^- (in the absence of NO) are additive in the expected manner (Figure 36A and Figure 38A), one is drawn to the conclusion that it is the behavior of NO that is in some way significantly different to that of these other two inhibitors. More specifically, the mechanism of NO inhibition cannot simply involve the reversible formation of an inactive enzyme−inhibitor complex; because if it did, the measured kinetic effects of NO + CN^- would be qualitatively similar to those exhibited by CO + CN^-, which is clearly not the case. Further to this point, the affinity of CN^- for cytochrome *c* oxidase (K_D = 20 nM, $k_2 \sim 10^6$ M^{-1} s^{-1}) [90, 196] is about 2 orders of magnitude less than that of NO (K_D = 0.1 nM, $k_2 \sim 10^8$ M^{-1} s^{-1}) [196, 217] when these parameters are determined for each inhibitory species in the absence of the other. Consequently, when both inhibitors are present, from consideration of mass action alone, it appears as though

NO should influence the measured rate of cytochrome *c* oxidase turnover even if CN^- is in 100-fold excess. That this is clearly not the case in turnover experiments (Figure 39B) casts additional doubt on the notion that NO behaves as a classic reversible (by dissociation) inhibitor and argues that the reported affinity parameters cannot all be physically meaningful in the present context of mixed (NO + CN^-) inhibition.

It has been suggested that NO be considered a substrate of cytochrome *c* oxidase [201, 218] as the enzyme is known to catalyze the oxidation of NO to NO_2^- under a variety of conditions [219]. This observation conveniently facilitates an explanation of the antagonistic effect of NO on the CO and CN^- inhibition of the enzyme. The conventional reaction catalyzed by cytochrome *c* oxidase is the four-electron reduction of molecular oxygen to water:

$$O_2 + 4e^- + 4H^+ \rightarrow 2H_2O \quad \textbf{[8]}$$

Equation 8. Reaction for the reduction of molecular oxygen to water by cytochrome *c* oxidase.

With CO or CN^- bound in the active site, this reaction cannot take place and, apparently, neither can any other O_2-consuming reaction. However, with NO occupying the active site, we propose that an alternative reaction is possible, in which NO can be considered an auxiliary substrate:

$$O_2 + 3e^- + 2H^+ + NO \rightarrow NO_2^- + H_2O \quad \textbf{[9]}$$

Equation 9. Reaction for the conversion of NO to NO_2^- by cytochrome *c* oxidase.

The conditions and mechanism by which the conversion of NO to NO_2^- might occur have been controversial; most other authors favor Cu_B as the site of NO oxidation. However, as NO has recently been shown to undergo what seems to be the same reaction with a bacterial terminal

oxidase lacking Cu_B [220], the favored view is probably erroneous. Fortunately, the only features of the reaction of cytochrome *c* oxidase with NO needed to explain the present results are that (i) NO becomes oxidized to nitrite in a process consuming O_2 (i.e., NO does not behave as a reversibly bound competitive inhibitor) [105, 220]; (ii) the rate of the reaction expressed in Equation 9 must be slower than the conventional reaction of Equation 8 as NO certainly does have a readily detected inhibitory effect on the enzyme (Figure 37); and (iii) the affinity of NO (taking into account mass action) for the enzyme must be greater than those of both CO and CN^-, so that NO effectively outcompetes the other two inhibitors for occupation of the active site, rendering their contributions to the overall kinetics negligible (Figure 36B,C and Figure 38B,C). Given the above three stipulations, NO can dominate the observed inhibition when CO or CN^- are also present because displacement of CO or CN^- by NO is facile and the subsequent conversion of NO to NO_2^- is slow in comparison. In other words, the observed kinetics are rate-limited by the NO-consuming reaction in Equation 9 (or some similar process), irrespective of whether or not CO and CN^- are also present.

Intriguingly, while finding exogenously administered NO donors to antagonize CN^- inhibition, the same group of authors also reports that endogenous (low level) NO production enhanced CN^- inhibition in mesencephalic cells [196]. No plausible biochemical explanation for these findings was offered. Mechanistically, it is not at all obvious how the action of NO could change from being toxic at low concentrations to protective at higher concentrations, and this is contrary to the current results where endogenous levels of NO were found to ameliorate CN^- toxicity in endothelial cells (Figure 43). Conflicting views concerning the effect of low NO levels toward cyanide toxicity could reflect differences in behavior of particular cell lines, properties of end points observed, or other experimental variables between laboratories.

However, resolution of this paradox is beyond the scope of the present work and must await further studies.

A.5.3 Supplemental Oxygen Therapy

An unexpected beneficial effect of supplemental O_2 delivery in the amelioration of cyanide toxicity has been the subject of dozens of experimental investigations and clinical case reports [221]. There has been no rational basis for this particular treatment as cyanide-inhibited cytochrome *c* oxidase cannot be reactivated by O_2 [222]. However, O_2 is also a substrate for nitric oxide synthase (NOS), and so, we can at least now postulate that supplemental O_2 leads to increased NO, which, as we show here, is an antagonist of CN^- inhibition of cytochrome *c* oxidase. Unfortunately, this explanation cannot be complete as supplemental O_2 is most effective when delivered in addition to nitrite and thiosulphate [223]. Nitrite is another potential source of NO [224], suggesting that constituent NOS alone might not be able to generate enough NO. Thiosulfate, a substrate for the enzyme rhodanese, promotes the conversion of CN^- to the less toxic thiocyanate ion (SCN^-). Conceivably, some portion of the supplemental O_2 may become diverted into O_2^- production. Subsequently generated derivatives of O_2^- (e.g., hydrogen peroxide and peroxynitrite) could then, perhaps, start oxidizing CN^- to less toxic species by means of reactions catalyzed by the numerous peroxidatic hemoproteins present in biological systems [225-226]. Again, however, examining such possibilities is outside the focus of the present investigation.

A.5.4 Inhibition by Carbon Monoxide

So far as the isolated enzyme is concerned, as compared with NO and CN^-, CO is a relatively poor inhibitor of cytochrome *c* oxidase (Figure 36 and Figure 38). There are those who suggest that the observed toxicity can stem from direct inhibition of cytochrome *c* oxidase by CO [227-228] and others who have argued that all of the cellular toxic effects of CO are likely due to the elevation of the steady-state NO levels mediated by competition between CO and endogenous NO for the same preferred locations [229-230]. However, the ~50% inhibition of cytochrome *c* oxidase reported [228] following exposure of mitochondrial preparations to 0.05% CO cannot be readily explained by either mechanism. The matter has recently been clarified by Iheagwara et al. [208]who showed that exposure of mice to low levels of CO led to substantial loss of cytochrome *c* oxidase activity in conjunction with decreased mitochondrial content of total heme *a* and the associated subunit I. This recently identified signaling process almost certainly provides a much more significant contribution to the net toxicity observed (in all experiments with viable mitochondria, cultured cells, excised tissues, and in vivo) than competitive binding of CO to the active site of the enzyme. Finally, we note that the reported synergism in the toxicity of CO + HCN is thought to be primarily associated with hypoxia at the cellular level [191-193]. Cleary, however, the present study suggests that this does not arise through any interaction at the oxygen-binding site of cytochrome *c* oxidase, since inhibition by CO + CN^- is the one simple additive case that we observed (Figure 36A and Figure 38A).

A.6 ACKNOWLEDGEMENTS

This work was supported by the National Institutes of Health (HL61411 to J.P. and L.L.P.).

APPENDIX B

THE RESISTANCE OF ELECTRON-TRANSPORT CHAIN FE–S CLUSTERS TO OXIDATIVE DAMAGE DURING THE REACTION OF PEROXYNITRITE WITH MITOCHONDRIAL COMPLEX II AND RAT-HEART PERICARDIUM

Linda L. Pearce [a,*], Sandra Martinez-Bosch[a], Elisenda Lopez Manzano[a], Daniel E. Winnica[a], Michael W. Epperly[b], Jim Peterson[a]

[a]Department of Environmental and Occupational Health

University of Pittsburgh Graduate School of Public Health

100 Technology Drive, Pittsburgh, PA 15219 USA

[b] Department of Radiation Oncology, University of Pittsburgh, USA

*Corresponding Authors: lip10@pitt.edu;

Keywords: Aconitase, Mitochondria, Cardiomyocytes, Complex II, EPR, Iron–sulfur clusters, Succinate dehydrogenase, Nitric oxide, Peroxynitrite

Published in: Nitric Oxide 20 (2009) 135–142

doi:10.1016/j.niox.2008.12.001

B.1 ABSTRACT

The effects of peroxynitrite and nitric oxide on the iron–sulfur clusters in complex II (succinate dehydrogenase) isolated from bovine heart have been studied primarily by EPR spectroscopy and no measurable damage to the constitutive 2Fe–2S, 3Fe–4S, or 4Fe–4S clusters was observed. The enzyme can be repeatedly oxidized with a slight excess of peroxynitrite and then quantitatively re-reduced with succinate. When added in large excess, peroxynitrite reacted with at least one tyrosine in each subunit of complex II to form 3-nitrotyrosines, but activity was barely compromised. Examination of rat-heart pericardium subjected to conditions leading to peroxynitrite production showed a small inhibition of complex II (16%) and a greater inhibition of aconitase (77%). In addition, experiments performed with excesses of sodium citrate and sodium succinate on rat-heart pericardium indicated that the "g = 2.01" EPR signal observed immediately following the beginning of conditions modeling oxidative/nitrosative stress, could be a consequence of both reversible oxidation of the constitutive 3Fe–4S cluster in complex II and degradation of the 4Fe–4S cluster in aconitase. However, the net signal envelope, which becomes apparent in less than 1 min following the start of oxidative/nitrosative conditions, is dominated by the component arising from complex II. Taking into account the findings of a previous study concerning complexes I and III [84] it is now apparent that, with the exception of the cofactor in aconitase, mammalian (mitochondrial) iron–sulfur clusters are surprisingly resistant to degradation stemming from oxidative/nitrosative stress.

B.2 INTRODUCTION

Iron–sulfur proteins have periodically been suggested to be critical targets of oxidative/nitrosative stress [231-233]. In mammals, these proteins are predominately found in mitochondria, with the exception of aconitase (containing a 4Fe–4S cluster) which is present in both mitochondrial and cytosolic forms [234]. Mitochondria have also been implicated in the production of oxidative/nitrosative stress via the formation of peroxynitrite [235-237] generated from the precursors superoxide and nitric oxide at diffusion-controlled rates [24]. Either directly, or through the action of one of its derivatives, the powerful oxidant peroxynitrite is known to modify biomolecules in several ways, including oxidizing iron–sulfur centers, generating thiyl radicals (which can decay to sulfenic acids) and reacting with protein tyrosines to form 3-nitrotyrosine [236, 238-240]. The peroxynitrite anion (ONO_2^-) is actually quite stable in aqueous media, but will tend to become protonated at neutral pH forming peroxynitrous acid ($HONO_2$). It is almost certainly this more reactive molecular entity, or some other derivative such as carboxylate radical (CO_3^-) formed in the reaction between peroxynitrite and dissolved carbon dioxide, which are responsible for most reactions with biomolecules [24]. Herein, we do not attempt to distinguish between these possibilities and use the term "peroxynitrite" to describe the anion and its immediate short-lived derivatives, but specifically not the precursor nitric oxide.

Recent analysis of complex I (NADH dehydrogenase) and complex III (cytochrome *c* reductase) from bovine heart mitochondria showed that the cofactors contained in these enzymes, including the iron–sulfur centers, were quite resistant to oxidative/nitrosative stress [84]. Complex III contains only one 2Fe–2S center [241-242], while complex I contains multiple 2Fe–2S and 4Fe–4S clusters [243]. Oxidative damage to iron–sulfur proteins commonly involves loss of one iron atom from a 4Fe–4S core, leading to production of a 3Fe–4S cluster [244]. The

fully oxidized forms of such products, $[3Fe–4S]^{+}$, formally containing 3 ferric ions, exhibit unique EPR signals with crossover g-values of 2.01–2.02 (the "g = 2.01 signal") observable at liquid helium temperatures; whereas, the single-electron reduced forms $[3Fe–4S]^{0}$ are typically EPR silent [244]. We have previously observed loss of complex I and complex III activity in conjunction with the appearance of a g~2.01 EPR signal in cultured cells and isolated mitochondria under conditions leading to the generation of peroxynitrite [84, 245]. However, we subsequently showed that the addition of bona fide peroxynitrite to isolated complex I (and complex III), while clearly leading to loss of activity, does not result in the appearance of any g~2.01 EPR signals. Thus, the origin of the oxidized $[3Fe–4S]^{+}$ cluster(s) responsible for this rapidly-developing (1 min) signal in mitochondria remains in doubt.

Two other mitochondrial enzymes are good candidates for this particular indicator of oxidative/nitrosative stress, aconitase and complex II (succinate dehydrogenase). Aconitase has been very carefully examined and shown to develop the 3Fe–4S center under a variety of conditions [246], but typically more slowly than the signals we describe here. Complex II contains a constitutive 3Fe–4S center which upon oxidation has an associated EPR g-value of 2.01 [241, 247]. Either, or both, of these enzymes could be responsible for this type of EPR signal that may be detected in mammalian tissues, cultured cells and isolated mitochondria under conditions of oxidative/nitrosative stress. We report here the results of an investigation into the identity of the particular $[3Fe–4S]^{+}$ cluster(s) responsible for the rapidly observed g~2.01 signal in mitochondria-rich heart tissue.

B.3 MATERIALS AND METHODS

B.3.1 Chemical reagents

Bovine cytochrome *c* (type III), dichloroindophenol, sodium cholate, ubiquinone-2 and sodium deoxycholate were obtained from Sigma/Aldrich. $NaONO_2$ was prepared according to the method of Beckman et al. [58], using manganese dioxide to eliminate excess hydrogen peroxide. Sodium lauryl maltoside was obtained from Anatrace, sodium dithionite (87%) from E.M. Science, nitric oxide gas (99.5%) from Matheson, and all other reagents used were ACS grade and purchased from Sigma/Aldrich or Fisher.

B.3.2 Enzyme purification

Complex II (EC 1.3.5.1., succinate dehydrogenase) was isolated from beef hearts (15 hearts per preparation) obtained from a local slaughterhouse using the slightly modified method of Ragan et al [60]. Briefly, mitochondria were first extracted from the hearts in the presence of 10 μM $CaCl_2$ and then frozen at −20 °C for no longer than 2 weeks before the complex II was isolated. A series of ammonium sulfate cuts in the presence of cholic acid, followed by ethanol and cyclohexane extractions to eliminate contamination by complex III, were used to purify the required complex II. The purity of the final product was determined by establishing the FAD content (5 nmol/mg protein) and by SDS–polyacrylamide gel electrophoresis. Porcine heart aconitase (EC 4.2.1.3., aconitate hydratase; isocitrate hydrolyase) was obtained from Sigma/Aldrich and used without further purification since it was found to exhibit the EPR signal of interest (Figure 48).

B.3.3 Enzyme assays

Complex II activity was determined by the method of Hatefi and Stiggall using 20 mM sodium succinate, 50 μM (oxidized) ubiquinone-2, 75 μM 2,6-dichloroindophenol (DCIP) and 0.5 ng complex II in 50 mM potassium phosphate, pH 7.4, 1 mM EDTA [60]. The reaction was followed by monitoring the decrease in absorbance at 600 nm after first pre-incubating for 5 min at 37 °C. Succinate dehydrogenase activity was calculated using the extinction coefficient ε_{600}= 21 $mM^{-1}cm^{-1}$ and expressed as μmol succinate/min/mg protein. Sodium cyanide was added (10 mM final concentration) to complex II assay mixtures in the case of tissue samples to inhibit Complex IV. Aconitase activity was assayed at 30°C in 50 mM Tris–HCl, pH~7.4, 30 mM sodium citrate, 0.6 mM $MnCl_2$, 0.2 mM $NADP^+$, and 1 unit of isocitrate dehydrogenase. The reaction was followed by measuring the increase in absorbance at 340 nm and the activity calculated as μmol citrate/min/mg protein using the extinction coefficient ε_{340}= 6.22 $mM^{-1}cm^{-1}$.

B.3.4 Nitric oxide and peroxynitrite additions

Protein samples were prepared in strongly buffered solution (M/10 sodium phosphate, 0.05% lauryl maltoside, pH 7.4). Nitric oxide gas (99.5%) was bubbled through water and then passed over potassium hydroxide pellets to remove any acidic impurities before further experimental use. Nitric oxide additions to samples were made with gas-tight Hamilton syringes. Stock solutions of $NaONO_2$ in aqueous NaOH were further diluted in water to a final [OH^-] of 1 mM or lower before addition to protein solutions. Additions of $NaONO_2$ solutions to protein samples were made by quick expulsion through " Teflon" needles from gas-tight Hamilton syringes with agitation to ensure rapid mixing. We have previously shown that, unlike slower

"bolus" additions, this rapid-mixing approach results in quantitative reduction of peroxynitrite by metalloenzymes that are able to donate at least two electrons [33]. Concentrations of $NaONO_2$ solutions were determined spectrophotometrically (ε_{302} = 1.67 mM^{-1} cm^{-1}) [248]. Following addition of nitric oxide gas, or peroxynitrite solution, to protein samples the measured pH change was always <0.05.

B.3.5 Electrophoresis and blots

Dot and Western blots were carried out using 15% pre-cast acrylamide gels, nitrocellulose membranes and electrophoresis/blotting apparatus from Bio-Rad, Richmond, CA and Chemiluminescence Reagent Plus from Perkin–Elmer Life Science, Boston, MA. Primary rabbit anti-3-nitrotyrosine antibodies and secondary antibodies of goat anti-rabbit IgG conjugated with alkaline phosphatase (AP) from Upstate Biotechnology, Lake Placid, NY were used. Antiserum was diluted in 1% bovine serum albumin in 10 mM Tris–HCl, pH 7.4 and 0.9% NaCl (TBS). Bound conjugates were visualized by staining for enzymatic activity with 5-bromo-4-chloro-3-indolyl phosphate p-toluidine salt and nitro-blue tetrazolium (NBT) for alkaline phosphatase. Protein samples were denatured in 2% SDS at room temperature prior to electrophoresis.

B.3.6 Preparations of cardiac tissue

Rat-heart pericardium was minced and homogenized in an equal volume of buffer (5 mM potassium phosphate, 0.25 M sucrose, 5 mM KCl, pH 7.4) using a hand-held homogenizer just enough to enable introduction of the tissue slurry into EPR tubes. Previously, we have sectioned

pericardium at 300 μm intervals in two crossed directions using a tissue chopper [245] to ensure that the majority of cardiomyocytes in the samples remained uncut. However, as the results of EPR experiments using samples prepared by either method were essentially identical, we dispensed with the latter more time-consuming procedure. The pericardial tissue was used to prepare all samples within 10 min of sacrificing the animal. All samples were preserved by immersion in liquid nitrogen within 2 min of their rapid mixing and introduction to the EPR sample tubes. EPR spectra were subsequently recorded without the samples ever being thawed. Parallel samples for use in subsequent enzyme activity assays were cryogenically preserved at the same time. For purposes of the activity assays, it was convenient to use sub-cellular fractions concentrated in mitochondria. The cryogenically stored homogenized tissue samples were thawed and centrifuged at 500 g for 5 min, the supernatant decanted and, subsequently, spun at 10,000 g for 10 min. The mitochondria-enriched pellets were then re-suspended in 5 mM potassium phosphate, 0.25 M sucrose, 5 mM KCl, pH 7.4 buffer to 10 mg/mL for activity measurements. Protein determinations were made using the BCA method kit from Pierce, Rockford, IL.

B.3.7 Instrumental methods

X-band (9.65 GHz) EPR spectra were recorded on a Bruker ESP 300 spectrometer equipped with a Bruker B-E 25 electromagnet and Bruker ER4116DM resonant cavity. Cryogenic temperatures were maintained with an Oxford Instruments ESR 910 cryostat in conjunction with a VC30 controller. Frequency calibration was with a microwave frequency counter and the magnetic field was calibrated with an NMR gaussmeter. The sample temperature was measured by means of a thermocouple calibrated using a Lakeshore carbon-glass resistor

(CGR-1-1000). A modulation frequency of 100 kHz was used throughout and, except for the data of Figure 49, all EPR spectra were recorded under non-saturating conditions. Electronic absorption measurements were performed with a Shimadzu UV-2501PC spectrophotometer and fluorescence spectra were recorded with a Shimadzu RF-5301 PC spectrofluorophotometer.

B.4 RESULTS

B.4.1 Reaction of isolated complex II with peroxynitrite

Complex II of the electron-transport chain contains one b-type cytochrome, one 2Fe–2S, one 4Fe–4S, one 3Fe–4S and one flavin per enzyme [241]. While 3Fe–4S moieties are often formed as artifacts during the isolation of bacterial iron–sulfur proteins, the 3Fe–4S cluster of complex II is unusual since it is constitutive to the enzyme and functionally required [249-250]. The 15 K EPR spectra of isolated preparations of the bovine enzyme (fully oxidized form) exhibited a sharp signal centered at 3430 gauss ($g \sim 2.01$) attributable to the $[3Fe–4S]^{+}$ core (Figure 44. X-band EPR spectra of isolated bovine complex II, demonstrating reversible oxidation and reduction of iron–sulfur clusters. Following reduction of the enzyme with succinate, the initial EPR signal was found to have disappeared and another broader signal due to the $[2Fe–2S]^{+}$ center was observed (Figure 44B). A small additional feature at 3450 gauss ($g = 2.00$) superimposed on the $[2Fe–2S]^{+}$ signal is due to a free radical, probably ubisemiquinone, which essentially disappeared upon further reduction of the enzyme with sodium dithionite (Figure 44C). At higher gain (Figure 44D) signals arising from the $[4Fe–4S]^{+}$ cluster were observed in the EPR spectra of dithionite-reduced samples. These findings are fully in keeping

with the reported EPR characteristics of complex II [241] and thus verify the overall similarity of our preparations to those of other authors. Upon reaction of the succinate-reduced enzyme with excess peroxynitrite, the signals of the $[2Fe–2S]^{+}$ and $[4Fe–4S]^{+}$ centers vanished and the g ~ 2.01 EPR signal of the $[3Fe–4S]^{+}$ cluster reappeared (Figure 36E). As oxidized $[2Fe–2S]^{2+}$ and $[4Fe–4S]^{2+}$ cores are diamagnetic, they do not exhibit any EPR signals and, consequently, these results show that peroxynitrite was able to extract electrons from the iron–sulfur clusters with the cores changing between their normally accessible oxidation states. Re-oxidation of complex II by peroxynitrite, even at 1000-fold excess, did not result in any change in the magnitude of the g ~ 2.01 signal compared to that obtained with the isolated enzyme, indicating that there was no decay of 3Fe–4S clusters, nor conversion of 4Fe–4S to 3Fe–4S. Furthermore, upon re-reduction of the enzyme with succinate, the EPR spectrum of the reduced $[2Fe–2S]^{+}$ core was found to quantitatively reappear along with the free radical signal at g = 2.00 (Figure 44F). This redox cycling of complex II with succinate and peroxynitrite could be repeated several times without either loss of activity, or the appearance of any additional EPR signals such as "free" ferric species (g = 4.3). Consequently, the spectra of Figure 44 clearly demonstrate that the iron–sulfur clusters of bovine complex II are able to undergo facile redox chemistry with peroxynitrite without any apparent core degradation.

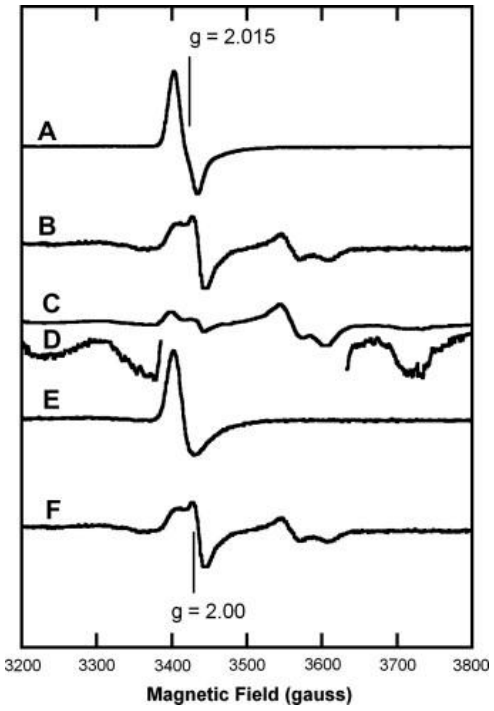

Figure 44. X-band EPR spectra of isolated bovine complex II, demonstrating reversible oxidation and reduction of iron–sulfur clusters.

Recording conditions: 15 K sample temperature; 4 mm OD sample tubes; 9.96 GHz frequency; 40 μW power; 10 G modulation amplitude; 100 kHz modulation frequency). Dispersions of 20 μM complex II in 0.1 M potassium phosphate buffer, 0.05% (w/v) in lauryl maltoside, pH 7.4. (A) Enzyme as isolated showing the signal arising from the oxidized [3Fe–4S] cluster at crossover g-value of 2.015. (B) Enzyme following addition of sodium succinate to 50 μM, frozen after 10 min incubation. The main features have associated g-values of 2.01 and 1.94 and arise from the reduced [2Fe–2S] cluster. (C) Enzyme frozen immediately following the addition of sodium dithionite to 100 μM. The main EPR features have g-values of 2.01 and 1.94 arising from the reduced [2Fe–2S] cluster and a sharp signal at g = 2.00 due to a free radical. (D) Sample as in C, power 600 μW, ×10 gain increase. The central signals have been removed to highlight the outer g-values of 2.08 and 1.85 associated with the signal of the reduced [4Fe–4S] cluster. (E) Sample as in B thawed, then re-frozen immediately following the addition of sodium peroxynitrite to 20 μM. (F) Sample as in E thawed, then re-frozen 10 min after the addition of sodium succinate to 50 μM.

B.4.2 Functional studies of complex II

Neither excess nitric oxide (2 μM nitric oxide, 2 nM enzyme, 20 min at 22 °C) nor excess peroxynitrite (20 μM $NaONO_2$, 2 nM enzyme, 22 °C) had any significant effect on the measured activity of purified complex II. In contrast, similar treatment with H_2O_2 was found to inhibit the enzyme by 50% (Table 1). This inhibitory reaction of H_2O_2 will be the subject of future studies—the result is included here to show that our failure to detect loss of complex II activity following exposure of the enzyme to nitric oxide and peroxynitrite was not simply due to a faulty activity assay. The lack of any significant reaction after exposure to 1000-fold excesses of nitric oxide and peroxynitrite, was additionally confirmed by the observation that there were no apparent changes in the EPR spectra of either oxidized or reduced complex II samples. Furthermore, no changes in the oxidized heme, or in the FAD, were detected by electronic absorption spectroscopy following exposure of the enzyme to 1000-fold excesses of nitric oxide, H_2O_2, or peroxynitrite. The absence of any measurable activity loss and/or cofactor modification following the addition of 1000-fold excess peroxynitrite to complex II is noteworthy because the protein is undoubtedly modified by this treatment, since 3-nitrotyrosine formation can readily be observed by Western blot and all four subunits of the enzyme contain tyrosine residues that are nitrated. In order to further verify the reliability of the sample manipulation procedures, we also examined the effects of nitric oxide, H_2O_2 and peroxynitrite on mitochondrial aconitase, which is known to be deactivated by oxidative degradation of its constitutive 4Fe–4S cluster to an inactive 3Fe–4S form. In keeping with the findings of others [177, 246, 251-252] we found that nitric oxide had negligible effect on aconitase activity at pH 7.4, while exposure to H_2O_2 and peroxynitrite clearly resulted in significant activity loss (Table 5).

Table 5. Effects of oxidative/nitrosative stress on the enzymatic activities of isolated complex II and aconitase. Data are expressed as % relative to controls, numbers in parentheses are standard errors derived from at least six replicate measurements. a Reagents added to enzyme solutions 20 min before dilution into assay mixtures containing substrates. NO exposure performed anaerobically. b Twenty five micromolar DCIP/min/mg protein (isolated from bovine heart). c Five micromolar citrate/min/mg protein (porcine, Sigma).

Conditions[a]	Complex II	Aconitase
Control	100 (±11)[b]	100 (±10)[c]
Nitric oxide (2 μM)	90 (±8)	92 (±7)
H_2O_2 (2 μM)	48 (±6)	70 (±6)
Peroxynitrite (20 μM)	95 (±8)	65 (±6)

In order to compare these functional characteristics of isolated complex II with those of the in situ enzyme, we also undertook a set of activity assays on freshly excised and homogenized rat-heart pericardium (Table 6). Endogenous generators of nitric oxide and superoxide were stimulated to release the reactive species to avoid working at high levels in the tissue that would be physiologically unreasonable. It has previously been shown that topical application of norepinephrine to cardiomyocytes elicits the intracellular production of nitric oxide, transiently (~ 1 s) reaching concentrations of several hundred nanomolar [161-162]. Inhibition of complex III with antimycin A is a convenient way of producing superoxide inside mitochondria of all cells—that is, significant levels result within the 2 min exposure time required in the present experiments. Note that alternate procedures such as the xanthine/xanthine oxidase method generate superoxide that does not efficiently enter the mitochondria of intact

cells [253] and may only produce detectable effects in isolated mitochondria following incubation times in excess of 10 min [254]. Interestingly, the same barely significant degree of complex II inhibition in the cardiac tissue was observed whether nitric oxide production was stimulated by norepinephrine, superoxide generation was stimulated by antimycin A, or both norepinephrine and antimycin A were used together to give elevated peroxynitrite (Table 6). Probably, one cannot avoid partial inhibition of the electron-transport chain at complex IV during elevated nitric oxide production, which will lead to some elevation in superoxide and H_2O_2 levels. Therefore, a plausible explanation for the just-detectable deactivation of complex II in the tissue is that it was due to inhibition of the enzyme by small amounts of H_2O_2 unavoidably formed in all three cases. Compared with the control, there was clearly significant loss of aconitase activity in the rat-heart pericardium following elevation of nitric oxide, superoxide and peroxynitrite (Table 6) as is to be expected [252-253].

Table 6. Effects of oxidative/nitrosative stress on the enzymatic activities of complex II and aconitase in rat-heart pericardium

Data are expressed as % relative to controls, numbers in parentheses are standard errors derived from at least six replicate measurements. a Reagents added to homogenized tissue 2 min before freezing for storage prior to assay (see text). b Nine micromolar DCIP/min/mg protein. c 0.6 micromolar citrate/min/mg protein.

Conditions[a]	Complex II	Aconitase
Control	100 (±12)[b]	100 (±8)[c]
+ Norepinephrine	86 (±3)	72 (±7)
+ Antimycin A	84 (±4)	31 (±2)
+ Norepinephrine and Antimycin A	84 (±3)	23 (±3)

B.4.3 Studies with rat-heart pericardium under oxidative/nitrosative stress

We have previously reported the appearance of a g 2.01 EPR signal in mitochondria-rich tissue under conditions where endogenous sources of superoxide and nitric oxide were stimulated to mimic oxidative/nitrosative stress. Compared to other cell types in the pericardium, the mitochondrial content of cardiomyocytes is very high, guaranteeing that the detected EPR signal arose from the latter only, any contributions from other sources being below the detection limit. The intensity of the EPR signal, indicating $[3Fe–4S]^{+}$ cores, was greatest under those conditions where the production of peroxynitrite was maximized and, indeed, the addition of bona fide peroxynitrite to isolated mitochondria or tissue also leads to production of the same signal. It was further shown that the signal(s) in question were not associated with any cluster reorganization in complexes I or III [84]. In the present study, the 15 K EPR spectrum of minced rat-heart pericardium contains signals with average g-value below 2.0 (Figure 45A, solid trace) in keeping with the presence of one-electron reduced 2Fe–2S and 4Fe–4S clusters ($[2Fe–2S]^{+}$ and $[4Fe–4S]^{+}$ cores). Stimulation of the endogenous production of nitric oxide (see at Figure 45B, solid trace) superoxide (Figure 45C, solid trace) or both (Figure 45D, solid trace) led to the production of another EPR signal centered at g~2.01 demonstrating the presence of a [3Fe–4S]+ core. The appearance of this signal unambiguously represents an oxidation of the center(s) in question and cannot be explained, for example, by stimulation of the citric acid cycle enzymes as this would result in a flux of reductants.

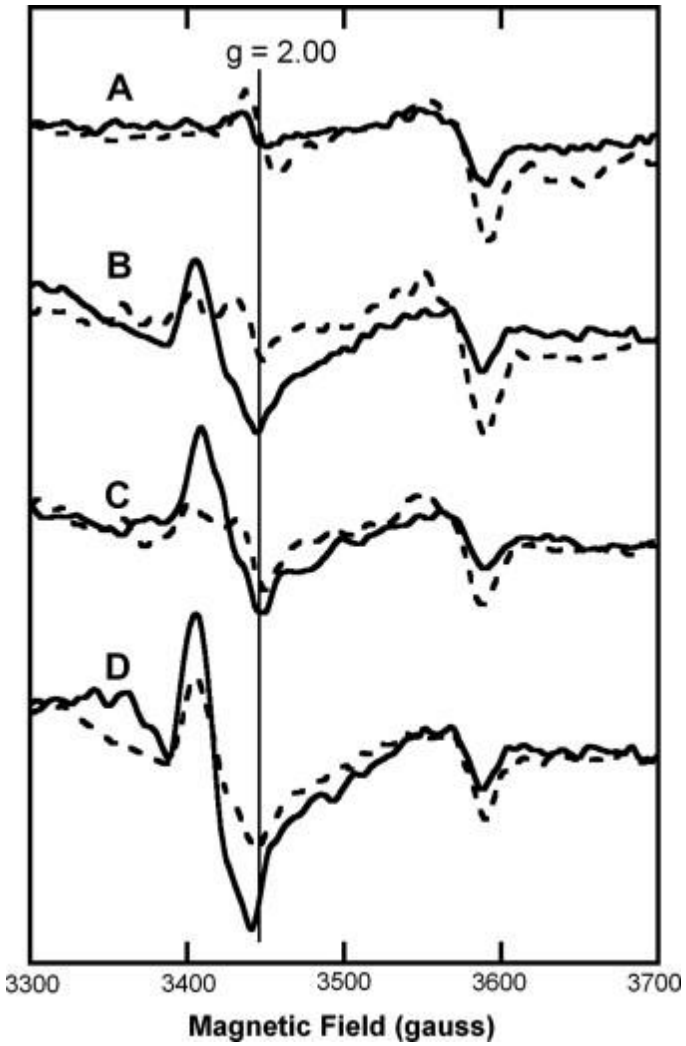

Figure 45. X-band EPR spectra of minced rat-heart pericardium demonstrating the effects of antimycin A, norepinephrine and succinate.

(Recording conditions: 15 K sample temperature; 4 mm OD sample tubes; 9.96 GHz frequency; 40 μW power; 10 G modulation amplitude; 100 kHz modulation frequency). Pericardium was prepared as described in Materials and methods. All samples were frozen within 2 min of reagent additions and cryogenically preserved for subsequent introduction to the spectrometer without thawing. Solid traces: (A) Control sample. (B) Norepinephrine (cardiomyocyte stimulant for nitric oxide production) added to 1 μM. (C) Antimycin A (specific complex III inhibitor leading to mitochondrial superoxide production) added to 100 μM. (D) Antimycin A and norepinephrin added to 100 and 1 μM, respectively. Dashed traces: As above, but samples pre-incubated with sodium succinate (added to 100 μM) for 5 min prior to other additions.

It should also be noted that following introduction to the bottom of an EPR tube, the finely divided pericardium becomes anaerobic within about 30 s — conversion of oxymyoglobin to deoxymyoglobin being readily apparent by observation of the color change from red-brown to darker red. The sample can be reoxygenated by inverting the tube and the change from aerobic to anaerobic conditions observed again — this process being routinely repeatable several times. Since the EPR samples, having undergone the color change described, were then aerated/mixed once in the tube before being cryogenically preserved, it is quite clear that all were prepared under conditions where reductive nutrients were not depleted. It has previously been shown that at the levels of NO achieved by stimulation of endogenous sources in pericardial tissue there is no measurable reaction with deoxymyoglobin and/or oxymyoglobin; that is, any signals arising from, respectively, formation of metmyoglobin and/or nitrosylmyoglobin remain below detection by EPR [255]. For example, in the present data set this is confirmed by the absence of any positive features arising from nitrosylmyoglobin at <3300 gauss in the spectra of Figure 45 and Figure 46. Similarly, there was no increase in the intensity of any metmyoglobin signals 1200 gauss following stimulation of the pericardial tissue to release NO (not shown). Therefore, as deoxymyoglobin and oxymyoglobin are themselves EPR silent, the presence of myoglobin in the tissue does not interfere with observation of the mitochondrial events of interest. Further to this point, at endogenously-generated levels of NO, the major product of NO catabolism in cardiomyocytes is nitrite, whereas reaction of NO with oxymyoglobin produces nitrate [162].

When the set of experiments mimicking oxidative/nitrosative stress was repeated in the presence of added succinate, the appearance of the g~2.01 signal was suppressed (Figure 45B–D, broken traces) strongly suggesting the $[3Fe–4S]^{+}$ core in question to arise from reversible redox chemistry of the constitutive $[3Fe–4S]^{0,+-}$ core cluster in complex II (succinate dehydrogenase).

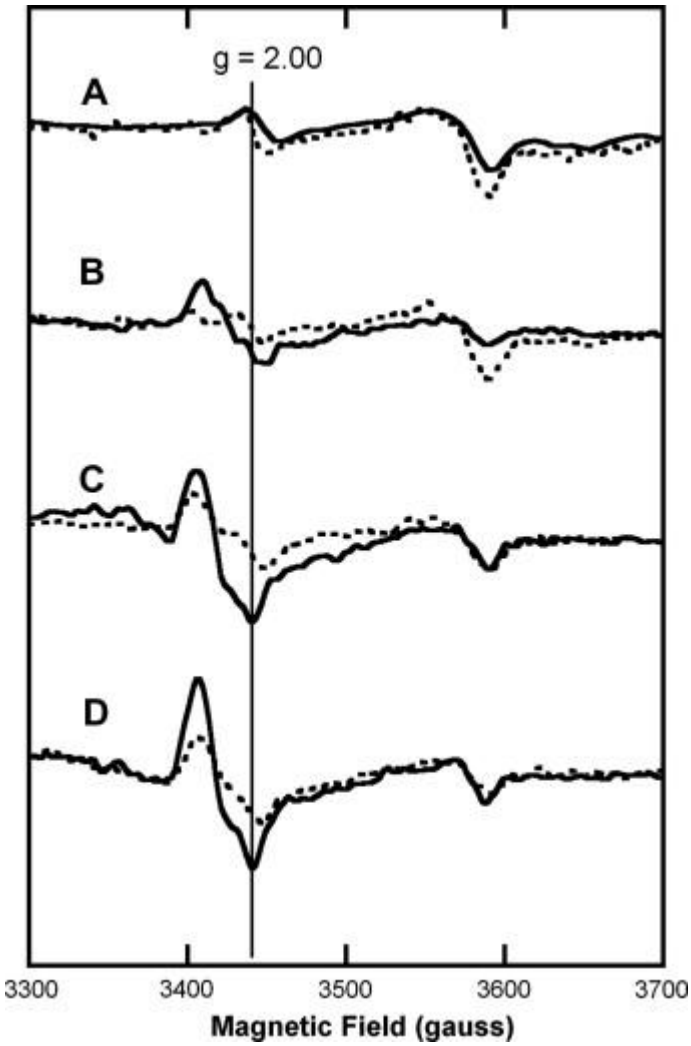

Figure 46. X-band EPR spectra of minced rat-heart pericardium demonstrating the effects of antimycin A, norepinephrine and citrate.

(Recording conditions: 15 K sample temperature; 4 mm OD sample tubes; 9.96 GHz frequency; 40 μW power; 10 G modulation amplitude; 100 kHz modulation frequency). Pericardium was prepared as described in the Materials and methods, frozen within 2 min of additions and then transferred to the spectrometer. Solid traces: (A) Control sample. (B) Norepinephrine (cardiomyocyte stimulant for nitric oxide production) added to 1 μM. (C) Antimycin A (specific complex III inhibitor leading to mitochondrial superoxide production) added to 100 μM. (D) Antimycin A and norepinephrin added to 100 and 1 μM, respectively. Dotted traces: As above, but samples pre-incubated with sodium citrate (added to 1 mM) for 5 min prior to other additions.

Confoundingly, however, the g ~ 2.01 EPR signal was also suppressed by the addition of citrate (Figure 46) in keeping with the findings of others working with isolated mitochondria [256]. The $[3Fe–4S]^{0,+-}$ core cluster in aconitase is known to undergo reconstitution into the active 4Fe–4S form upon turnover with substrate citrate [257]. Consequently, the g~2.01 signal that develops under these conditions modeling oxidative/nitrosative stress may, in principle, be partly due to aconitase as well as complex II. Not surprisingly, the addition of both citrate and succinate concomitantly to minced pericardium suppressed the EPR signal obtained following treatment with norepinephrine + antimycin A to a greater extent than either citrate or succinate alone, but we were unable to eliminate the g~2.01 signal entirely (Figure 47, black dashes). Addition of bona fide peroxynitrite (in the form of pre-synthesized $NaONO_2$) to minced pericardium also resulted in the appearance of a g~2.01 EPR signal (Figure 47, solid red trace) but at lower intensity than if peroxynitrite were generated inside the mitochondria using the norepinephrine + antimycin A procedure (Figure 47, solid black trace). Prior addition of citrate together with succinate lowered the intensity of the g~2.01 signal obtained following the addition of peroxynitrite to minced pericardium, but again, the suppression was partial (Figure 47, red dots). In general, it was observed that pre-incubation of pericardial tissue with both citrate and succinate together (before treatment with either peroxynitrite, or norepinephrine + antimycin A) always suppressed the development of any g~2.01 signal to a greater extent than either citrate, or succinate, alone (not shown). In the absence of peroxynitrite and/or norepinephrine + antimycin A, the addition of succinate and/or citrate led, as expected, to the appearance of characteristic signals of reduced iron–sulfur clusters only (Figure 47, blue trace). Unfortunately, these results remain equivocal, because as citrate is a precursor for succinate in the citric acid cycle, the addition of citrate must necessarily increase reduction of complex II in addition to turning over

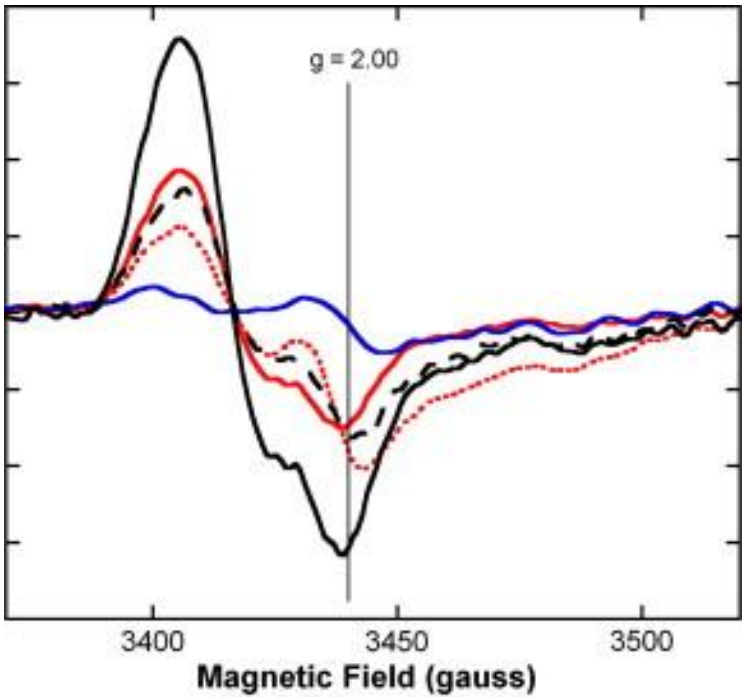

Figure 47. X-band EPR spectra of minced rat-heart pericardium demonstrating the additive, but still partial, protective effects against peroxynitrite of both citrate and succinate.

(Recording conditions: 15 K sample temperature; 4 mm OD sample tubes; 9.96 GHz frequency; 40 μW power; 10 G modulation amplitude; 100 kHz modulation frequency. Rat-heart pericardium stimulated with antimycin A and norepinephrine added to 100 and 1 μM final concentrations, respectively, then frozen within 2 min (solid black trace); pre-incubated with sodium citrate (1 mM in the medium) plus sodium succinate (100 μM in the medium) before stimulation with antimycin A and norepinephrine (black dashes); following addition of sodium peroxynitrite to 1 mM in the medium (solid red trace); pre-incubated with sodium citrate (1 mM in the medium) plus sodium succinate (100 μM in the medium) before addition of peroxynitrite (red dots); pre-incubated with sodium succinate only (100 μM in the medium) for 5 min prior to freezing (blue trace). The signals due to any [2Fe–2S]+ and [4Fe–4S]+ reduced clusters present in complex II at >3700 gauss have been truncated to provide an expanded view in the region of most interest.

aconitase. That is, while the data clearly confirm that the g 2.01 signal, a signature for the [3Fe–4S]+-core cluster, is formed in similar fashion either by the addition of bona fide peroxynitrite, or by norepinephrine + antimycin A, it does not reveal whether the signal arises principally from complex II, or it is derived from both aconitase and complex II. However, it should be noted that the sensitivity of the g 2.01 signal to succinate does strongly suggest that the signature cannot be associated with aconitase alone.

In an effort to quantify the two potential contributions to the g~2.01 in rat-heart pericardium (Figure 48, solid trace) we have additionally studied the characteristics of this signal in isolated (air-oxidized) aconitase (Figure 48, dotted trace) and isolated (air-oxidized) complex II (Figure 48, broken trace). Upon comparing the temperature dependence of the rat pericardium, porcine aconitase and bovine complex II signals, we found there to be no significant difference between them under non-saturating conditions (Figure 48, inset). (Note that much of the relevant early literature describes temperature-dependent EPR measurements performed under conditions of partially saturating power to distinguish between cluster types). However, there was a readily detectable, difference between the power-saturation characteristics of the g ~2.01 in aconitase and complex II at constant temperature (Figure 49, open squares and open triangles, respectively). Moreover, the power-saturation characteristics of the rat pericardium (Figure 49, filled circles) could essentially be superimposed on the data obtained from complex II, indicating the signal to arise predominantly from this enzyme rather than aconitase.

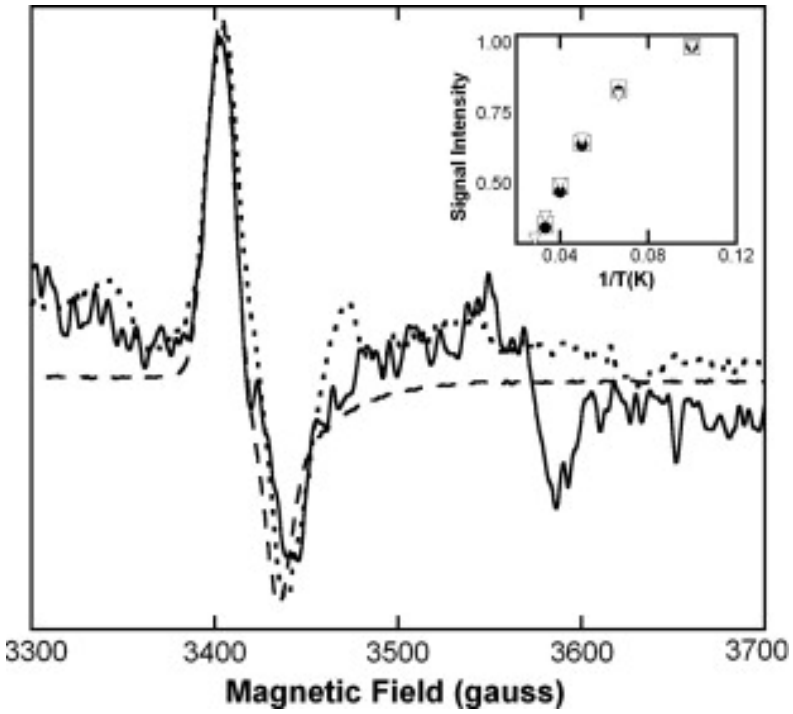

Figure 48. Comparison of the X-band EPR spectra of rat-heart pericardium (black trace), isolated porcine aconitase (dotted trace) and isolated bovine complex II (dashed trace).

Recording conditions: 15 K sample temperature; 4 mm OD sample tubes; 9.96 GHz frequency; 40 μW power; 10 G modulation amplitude; 100 kHz modulation frequency). The minced rat-heart pericardium was treated with antimycin A (to 100 μM in the medium) and norepinephrine (to 1 μM in the medium) for 2 min at 22 °C prior to freezing in the EPR tube. The other samples were taken from preparations of the enzymes as isolated for introduction into EPR tubes. For ease of visual comparison, the intensities of the data sets have been arbitrarily scaled to match. Inset: temperature dependence of the g 2.01 components. Intensity taken as the product of the peak height by its squared width. Aconitase (□), complex II (∇) and rat-heart pericardium (●). See Materials and methods for further details.

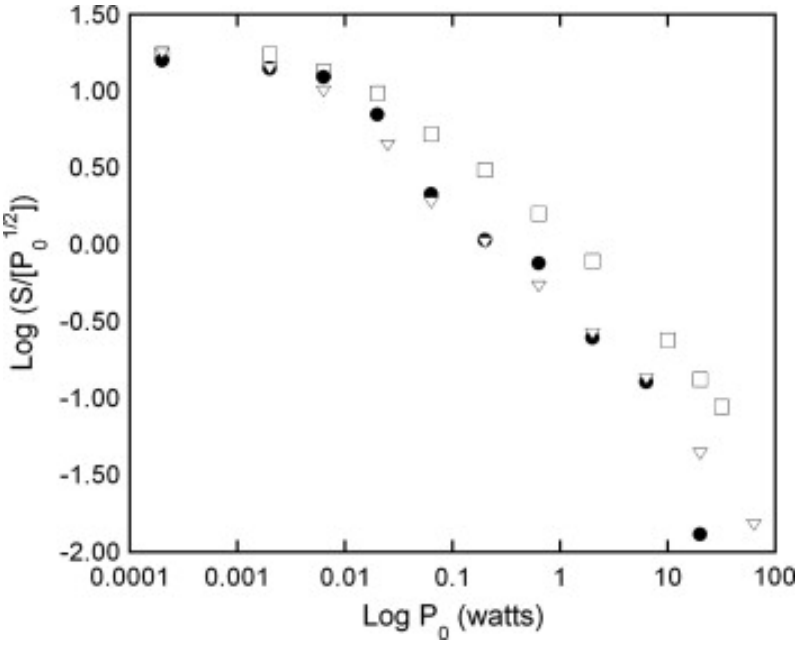

Figure 49. Power saturation curves of the g 2.01 components of the X-band EPR spectra at 20 K of aconitase, complex II and rat-heart pericardium demonstrating that the signal arising from intact mitochondria is like that of complex II.

(Recording conditions: 10 G modulation amplitude; 4 mm OD sample tubes; 9.96 GHz frequency; 100 kHz modulation frequency. The magnitude of the instrument noise during these measurements was within the vertical dimensions of the symbols). Same samples as for Figure 48. Isolated porcine aconitase (□), isolated bovine complex II (∇) and minced rat-heart pericardium treated with antimycin A and norepinephrine, added to 100 and 1 μM in the medium, respectively (●).

B.5 DISCUSSION

It is sometimes argued that the breakdown of certain biological macromolecules such as iron–sulfur proteins, can lead to the liberation of ~~"~~free iron" and subsequent problems associated with Fenton/Haber-Weiss chemistry. In order to obtain ~~"~~free iron" from iron–sulfur clusters, 4Fe–4S, 3Fe–4S and/or 2Fe–2S must first be cleaved in some manner. The first step in degradation of many 4Fe–4S clusters has been shown to be the production of an oxidized [3Fe–4S]$^{+}$ core with concomitant loss of labile iron [258]. In addition to our own group, others have shown that mitochondria, or mitochondria-rich cells, experiencing oxidative/nitrosative stress often exhibit an EPR signal with an associated g-value of 2.01 [233, 259] . This was once identified as stemming from a HiPiP-type iron–sulfur cluster but has more recently been shown to be a [3Fe–4S]$^{+}$ center. Previously, we have demonstrated that exposure of complex I to near physiological levels of either peroxynitrite or nitric oxide does not result in formation of any [3Fe–4S]$^{+}$ cores or appearance of detectable "labile iron" [84]. In this work we show that complex II, which contains a constitutive 3Fe–4S cluster, can be oxidized by peroxynitrite and subsequently re-reduced by succinate without any apparent cofactor degradation (Figure 44): that is, all three of the iron–sulfur cluster types (2Fe–2S, 3Fe–4S or 4Fe–4S) are resistant to oxidative damage. The results of further experiments with rat-heart pericardium experiencing oxidative/nitrosative stress clearly demonstrate that the production of an oxidized [3Fe–4S]$^{+}$-core cluster is significantly prevented by the pre-addition of succinate (Figure 45). We suggest that under physiological and non-inflammatory pathophysiological conditions, the iron–sulfur clusters of complexes I, II and III can be reversibly oxidized by peroxynitrite—that is, routinely be re-reduced without degradation and loss of labile iron.

While our work continues to suggest that low-level peroxynitrite generation (by implication, either in short bursts, or chronically) is of little consequence to mitochondria where the electron-transport chain is functioning and anti-oxidant metabolites such as glutathione are not depleted, this does not necessarily mean that peroxynitrite is never harmful. For example, in any situation where upregulation of inducible nitric oxide synthase accompanying inflammation is present, the resulting elevated level of peroxynitrite may be enough to overwhelm the capability of the (possibly impaired) electron-transport-chain complexes to deal with it. Work by Cammack et al. [233] showed that relatively high levels of authentic peroxynitrite (1 mM) added to rat liver mitochondria diminished the amount of oxidized g ~ 2.01 EPR signal observed, suggesting 3Fe–4S cluster degradation. Also, the studies of Han et al. [256] clearly showed that very high levels of peroxynitrite resulted in destruction of the 3Fe–4S clusters in damaged aconitase. These results indicate that sufficiently elevated (extreme pathophysiological) peroxynitrite levels can damage and degrade the iron–sulfur cluster in aconitase at least. However, even at 1000-fold excesses of peroxynitrite over enzyme, we observed no convincing evidence for this type of cluster destruction in complex II (Figure 44 and Table 5).

It is now clear that, unlike their bacterial counterparts, mammalian iron–sulfur clusters are stable to oxidative degradation. The exception to this appears to be aconitase, the activity of which requires the presence of its constitutive 4Fe–4S cluster. The work of several other groups has clearly demonstrated that this enzyme is particularly vulnerable to oxidative/nitrosative stress, but inactivation of aconitase by formation of the 3Fe–4Fe cluster is entirely reversible provided the cysteine ligand to the fourth iron in the cluster is not derivatized [256, 259]. We have confirmed that aconitase becomes inhibited under the particular conditions modeling oxidative/nitrosative stress we employ here (Table 6), but this does not necessarily involve the

obligatory formation of a 3Fe–4S cluster [252]. However, we can only, with confidence, assert the g 2.01 EPR signal to originate from complex II (Figure 45 and Figure 49)—the argument that aconitase contributes at all being entirely circumstantial. In summary, we conclude that the oxidized $[3Fe–4S]^{+}$-core cluster exhibiting the g ~ 2.01 EPR signal, formed rapidly following transient oxidant production, is the result of the reaction of the oxidant (most likely peroxynitrite) predominantly with complex II.

A remaining question is the connection between markers of oxidative stress, such as the oxidized 3Fe–4S clusters of complex II and aconitase, and cell injury or death. It would seem, based on this study, that complex II is not much compromised by the direct action of near physiological levels of nitric oxide or peroxynitrite (although irreversible damage by H_2O_2 is still possible). The observed reversible and succinate-dependent redox chemistry of the 3Fe–4S cluster in rat-heart pericardial tissue (Figure 45) without significant loss of activity (Table 6) provides further confirmation that the unusual 3Fe–4S center is constitutive in complex II [250, 260]. While the g ~2.01 EPR signal is clearly a marker of oxidative/nitrosative stress, it is probably only an indirect indicator of compromised protein function under near physiological conditions. That is, other enzymes present in the mitochondria may be irreversibly damaged while complex II (and perhaps, aconitase) can remain active for some period of time during which a g~2.01 signal may be evident. As further evidence that the iron–sulfur clusters in the complexes of the mammalian mitochondrial electron-transport chain are resistant to oxidative damage, we note that these enzymes can be isolated aerobically without degradation of their constitutive clusters. In our laboratory, the sensitivity of the purified respiratory complexes containing iron–sulfur clusters to functional damage from peroxynitrite increases in the order: complex II < complex I < complex III. Consequently, as the most sensitive of these enzymes has

the lowest iron–sulfur content (a single two-iron cluster in complex III) it is entirely reasonable that the mechanism(s) of irreversible inactivation must involve components other than the iron–sulfur clusters.

B.6 ACKNOWLEDGEMENTS

The authors would like to thank Michael P. Hendrich for access to the EPR facility in the Department of Chemistry at Carnegie Mellon University. This work was supported by a grant from the National Institute of Health (HL61411 to LLP & JP).

BIBLIOGRAPHY

1. Adams, P.L. and D.M. Turnbull, *Disorders of the electron transport chain.* J Inherit Metab Dis, 1996. **19**(4): p. 463-9.

2. Kerr, D.S., *Treatment of mitochondrial electron transport chain disorders: a review of clinical trials over the past decade.* Mol Genet Metab. **99**(3): p. 246-55.

3. MacMunn, The Journal of Physiology, 1886. **7**: p. 246-255.

4. Keilin, D., Proc. R. Soc. Lond. B., 1920. **98**: p. 354-372.

5. Margoliash, E., *Primary Structure and Evolution of Cytochrome C.* Proc Natl Acad Sci U S A, 1963. **50**: p. 672-9.

6. Sharpe, M.A., et al., *EPR evidence of cyanide binding to the Mn(Mg) center of cytochrome c oxidase: support for Cu(A)-Mg involvement in proton pumping.* Biochemistry, 2009. **48**(2): p. 328-35.

7. Peisach, J., W.E. Blumberg, and A. Adler, *ELECTRON PARAMAGNETIC RESONANCE STUDIES OF IRON PORPHIN AND CHLORIN SYSTEMS*.* Annals of the New York Academy of Sciences, 1973. **206**(The Chemical and Physical Behavior of Porphyrin Compounds and Related Structures): p. 310-327.

8. Hill, B.C., et al., *Low-spin ferric forms of cytochrome a3 in mixed-ligand and partially reduced cyanide-bound derivatives of cytochrome c oxidase.* Biochem J, 1983. **215**(1): p. 57-66.

9. Cammack, R., *Electron Paramagnetic Resonance Spectroscopy of Metalloproteins* in *Spectroscopic Methods and Analyses*. 1993, Humana Press. p. 327-344.

10. Otsuka, M., *Characterization of the reactivity of nitrihemoglobin*, in *Chemistry*. 2007, Carnegie Mellon University: Pittsburgh.

11. Carraway, A.D., *N-acetylated heme peptides: models for hemoproteins*, in *chemistry*. 1995, University of Alabama: Tuscaloosa. p. 105.

12. Palmer, G., *The electron paramagnetic resonance of metalloproteins.* Biochem Soc Trans, 1985. **13**(3): p. 548-60.

13. Reedy, C.J. and B.R. Gibney, *Heme protein assemblies.* Chem Rev, 2004. **104**(2): p. 617-49.

14. Cooper, C.E.W., M.T., *Haemoglobin: From Romans in Britain to Carry On up the Amazon* in *The Biochemist*. 1996. p. 7-11.

15. Radi, R., A. Cassina, and R. Hodara, *Nitric Oxide and Peroxynitrite Interactions with Mitochondria.* Biological Chemistry, 2005. **383**(3-4): p. 401-409.

16. Drose, S. and U. Brandt, *The mechanism of mitochondrial superoxide production by the cytochrome bc1 complex.* J Biol Chem, 2008. **283**(31): p. 21649-54.

17. Huie, R.E.P., S, *Reaction of nitric oxide with superoxide.* Free Radic Res Commun, 1993. **18**: p. 195-199.

18. Radi, R., *Peroxynitrite reactions and diffusion in biology.* Chemical Research In Toxicology, 1998. **11**(7): p. 720-721.

19. Szabo, C., H. Ischiropoulos, and R. Radi, *Peroxynitrite: biochemistry, pathophysiology and development of therapeutics.* Nat Rev Drug Discov, 2007. **6**(8): p. 662-80.

20. Tretyakova, N.Y., J.S. Wishnok, and S.R. Tannenbaum, *Peroxynitrite-induced secondary oxidative lesions at guanine nucleobases: chemical stability and recognition by the Fpg DNA repair enzyme.* Chem Res Toxicol, 2000. **13**(7): p. 658-64.

21. Rubbo, H., A. Trostchansky, and V.B. O'Donnell, *Peroxynitrite-mediated lipid oxidation and nitration: mechanisms and consequences.* Arch Biochem Biophys, 2009. **484**(2): p. 167-72.

22. Radi, R., et al., *Peroxynitrite-induced membrane lipid peroxidation: the cytotoxic potential of superoxide and nitric oxide.* Arch Biochem Biophys, 1991. **288**(2): p. 481-7.

23. Viner, R.I., T.D. Williams, and C. Schoneich, *Peroxynitrite modification of protein thiols: oxidation, nitrosylation, and S-glutathiolation of functionally important cysteine residue(s) in the sarcoplasmic reticulum Ca-ATPase.* Biochemistry, 1999. **38**(38): p. 12408-15.

24. Pacher, P., J.S. Beckman, and L. Liaudet, *Nitric oxide and peroxynitrite in health and disease.* Physiol Rev, 2007. **87**(1): p. 315-424.

25. Radi, R., et al., *Inhibition of mitochondrial electron transport by peroxynitrite.* Arch Biochem Biophys, 1994. **308**(1): p. 89-95.

26. Nalwaya, N. and W.M. Deen, *Analysis of Cellular Exposure to Peroxynitrite in Suspension Cultures.* Chemical Research in Toxicology, 2003. **16**(7): p. 920-932.

27. Merenyi, G., et al., *Mechanism and Thermochemistry of Peroxynitrite Decomposition in Water.* The Journal of Physical Chemistry A, 1999. **103**(29): p. 5685-5691.

28. Pfeiffer, S., et al., *Metabolic fate of peroxynitrite in aqueous solution. Reaction with nitric oxide and pH-dependent decomposition to nitrite and oxygen in a 2:1 stoichiometry.* J Biol Chem, 1997. **272**(6): p. 3465-70.

29. Goldstein, S., et al., *Effect of *NO on the decomposition of peroxynitrite: reaction of N2O3 with ONOO.* Chem Res Toxicol, 1999. **12**(2): p. 132-6.

30. Goldstein S., M.G., *The Chemistry of Peroxynitrite: Implications for Biological Activity.* Methods in Enzymology, 2008. **436**: p. 49-61.

31. Lobachev, V.L., *The chemistry of peroxynitrite. Reaction mechanisms and kinetics.* Russ. Chem. Rev., 2006. **75**(5): p. 375-396.

32. Thomson, L., et al., *Kinetics of cytochrome c2+ oxidation by peroxynitrite: implications for superoxide measurements in nitric oxide-producing biological systems.* Arch Biochem Biophys, 1995. **319**(2): p. 491-7.

33. Pearce, L.L., B.R. Pitt, and J. Peterson, *The peroxynitrite reductase activity of cytochrome c oxidase involves a two-electron redox reaction at the heme a(3)-Cu(B) site.* J Biol Chem, 1999. **274**(50): p. 35763-7.

34. Sharpe, M.A. and C.E. Cooper, *Interaction of peroxynitrite with mitochondrial cytochrome oxidase. Catalytic production of nitric oxide and irreversible inhibition of enzyme activity.* J Biol Chem, 1998. **273**(47): p. 30961-72.

35. Denicola, A., et al., *Peroxynitrite reaction with carbon dioxide/bicarbonate: kinetics and influence on peroxynitrite-mediated oxidations.* Arch Biochem Biophys, 1996. **333**(1): p. 49-58.

36. Eiserich, J.P., et al., *Formation of nitric oxide-derived inflammatory oxidants by myeloperoxidase in neutrophils.* Nature, 1998. **391**(6665): p. 393-7.

37. Perrin, D. and W.H. Koppenol, *The quantitative oxidation of methionine to methionine sulfoxide by peroxynitrite.* Arch Biochem Biophys, 2000. **377**(2): p. 266-72.

38. Cassina, A.M., et al., *Cytochrome c nitration by peroxynitrite.* J Biol Chem, 2000. **275**(28): p. 21409-15.

39. Jin, F., *The superoxide radical reacts with tyrosine-derived phenoxyl radicals by addition rather than by electron transfer.* J. Chem. Soc., Perkin Trans. 2, 1993(9): p. 1583-1588.

40. Guidarelli, A., L. Cerioni, and O. Cantoni, *Inhibition of complex III promotes loss of Ca^{2+} dependence for mitochondrial superoxide formation and permeability transition evoked by peroxynitrite.* J Cell Sci, 2007. **120**(Pt 11): p. 1908-14.

41. Pearce, L.L., et al., *The resistance of electron-transport chain Fe-S clusters to oxidative damage during the reaction of peroxynitrite with mitochondrial complex II and rat-heart pericardium.* Nitric Oxide, 2009. **20**(3): p. 135-42.

42. Murray, M., *Drug-mediated inactivation of cytochrome P450.* Clin Exp Pharmacol Physiol, 1997. **24**(7): p. 465-70.

43. Garcia-Ruiz, I., et al., *Mitochondrial complex I subunits are decreased in murine nonalcoholic fatty liver disease: implication of peroxynitrite.* J Proteome Res.

44. Barone, M.C., V.M. Darley-Usmar, and P.S. Brookes, *Reversible inhibition of cytochrome c oxidase by peroxynitrite proceeds through ascorbate-dependent generation of nitric oxide.* J Biol Chem, 2003. **278**(30): p. 27520-4.

45. Bonaventura, C., et al., *Internal electron transfer between hemes and Cu(II) bound at cysteine beta93 promotes methemoglobin reduction by carbon monoxide.* J Biol Chem, 1999. **274**(9): p. 5499-507.

46. Yamamoto, T., et al., *Selective nitration of mitochondrial complex I by peroxynitrite: involvement in mitochondria dysfunction and cell death of dopaminergic SH-SY5Y cells.* J Neural Transm, 2002. **109**(1): p. 1-13.

47. Radi, R., *Nitric oxide, oxidants, and protein tyrosine nitration.* Proc Natl Acad Sci U S A, 2004. **101**(12): p. 4003-8.

48. Gebicka, L. and J. Didik, *Mechanism of peroxynitrite interaction with cytochrome c.* Acta Biochim Pol, 2003. **50**(3): p. 815-23.

49. Turrens, J.F. and A. Boveris, *Generation of superoxide anion by the NADH dehydrogenase of bovine heart mitochondria.* Biochem J, 1980. **191**(2): p. 421-7.

50. Turrens, J.F., A. Alexandre, and A.L. Lehninger, *Ubisemiquinone is the electron donor for superoxide formation by complex III of heart mitochondria.* Arch Biochem Biophys, 1985. **237**(2): p. 408-14.

51. Kussmaul, L. and J. Hirst, *The mechanism of superoxide production by NADH:ubiquinone oxidoreductase (complex I) from bovine heart mitochondria.* Proc Natl Acad Sci U S A, 2006. **103**(20): p. 7607-12.

52. Robinson, K.M., et al., *Selective fluorescent imaging of superoxide in vivo using ethidium-based probes.* Proc Natl Acad Sci U S A, 2006. **103**(41): p. 15038-43.

53. Zielonka, J., et al., *Cytochrome c-mediated oxidation of hydroethidine and mito-hydroethidine in mitochondria: identification of homo- and heterodimers.* Free Radic Biol Med, 2008. **44**(5): p. 835-46.

54. Benov, L., L. Sztejnberg, and I. Fridovich, *Critical evaluation of the use of hydroethidine as a measure of superoxide anion radical.* Free Radical Biology and Medicine, 1998. **25**(7): p. 826-831.

55. Crow, J.P., *Dichlorodihydrofluorescein and dihydrorhodamine 123 are sensitive indicators of peroxynitrite in vitro: implications for intracellular measurement of reactive nitrogen and oxygen species.* Nitric Oxide, 1997. **1**(2): p. 145-57.

56. Interchim, *Probes for Mitochondria and endoplasmic reticulum (ER)*, in *Cell biology - study probes*. p. 129-135.

57. Glebska, J. and W.H. Koppenol, *Peroxynitrite-mediated oxidation of dichlorodihydrofluorescein and dihydrorhodamine.* Free Radic Biol Med, 2003. **35**(6): p. 676-82.

58. Beckman, J.S., et al., *Oxidative chemistry of peroxynitrite.* Methods Enzymol, 1994. **233**: p. 229-40.

59. Abriata, L.A., et al., *Nitration of solvent-exposed tyrosine 74 on cytochrome c triggers heme iron-methionine 80 bond disruption. Nuclear magnetic resonance and optical spectroscopy studies.* J Biol Chem, 2009. **284**(1): p. 17-26.

60. Ragan, C.I., et al., *Sub-fractionation of mitochondria and isolation of the proteins of oxidative phosphorylation*, in *Mitochondria: A Practical Approach*, V. Darley-Usmar, D. Rickwood, and M.T. Wilson, Editors. 1987, IRL Press: Oxford. p. 79-112.

61. Hartzell, C.R. and H. Beinert, *Components of cytochrome c oxidase detectable by EPR spectroscopy.* Biochim Biophys Acta, 1974. **368**(3): p. 318-38.

62. Hatefi, Y.a.R., J.S. , *Preparation and Properties of DPNH-Cytochrome c Reductase (Complex I-III of the Respiratory Chain).* Methods in Enzymology, 1967. **X**(Estabrook R.W. and Pullman, M.E., eds.): p. 225-231.

63. Hatefi, Y., *The mitochondrial electron transport and oxidative phosphorylation system.* Annu Rev Biochem, 1985. **54**: p. 1015-69.

64. Sharpley, M.S., et al., *Interactions between phospholipids and NADH:ubiquinone oxidoreductase (complex I) from bovine mitochondria.* Biochemistry, 2006. **45**(1): p. 241-8.

65. Sinjorgo, K.M., et al., *Bovine cytochrome c oxidases, purified from heart, skeletal muscle, liver and kidney, differ in the small subunits but show the same reaction kinetics with cytochrome c.* Biochim Biophys Acta, 1987. **893**(2): p. 251-8.

66. Griess, P., *Bemerkungen zu der Abhandlung der HH. Weselsky und Benedikt Ueber einige Azoverbindungen. Ber. Deutsch Chem Ges.*, 1879. **12**: p. 426-428.

67. Epperly, M.W., et al., *Mitochondrial localization of superoxide dismutase is required for decreasing radiation-induced cellular damage.* Radiat Res, 2003. **160**(5): p. 568-78.

68. Epperly, M.W., et al., *Mitochondrial targeting of a catalase transgene product by plasmid liposomes increases radioresistance in vitro and in vivo.* Radiat Res, 2009. **171**: p. 588-595.

69. Villeneuve, L., et al., *Spectroscopic and photophysical investigations on the nature of localization of rhodamine-123 and its dibromo derivative in different cell lines.* Journal of Fluorescence, 1996. **6**(4): p. 209-219.

70. Pastorino, J.G., et al., *The cytotoxicity of tumor necrosis factor depends on induction of the mitochondrial permeability transition.* J Biol Chem, 1996. **271**(47): p. 29792-8.

71. Robinson, K.M., M.S. Janes, and J.S. Beckman, *The selective detection of mitochondrial superoxide by live cell imaging.* Nat Protoc, 2008. **3**(6): p. 941-7.

72. Margoliash, E. and N. Frohwirt, *Spectrum of horse-heart cytochrome c.* Biochem J, 1959. **71**(3): p. 570-2.

73. Sun, J.Z., X.; Broderick, M.; Fein, H., *Measurement of Nitric Oxide Production in Biological Systems by Using Griess Reaction Assay* Sensors, 2003. **3**: p. 276-284.

74. Bartsch, R.G., *Cytochromes: Bacterial.* Methods in Enzymology, 1971. **23**: p. 344-363.

75. Jin, W.J., et al., *Fluorescence quenching of ethidium ion by porphyrin cations and quaternary ammonium surfactants in the presence of DNA.* Spectrochim Acta A Mol Biomol Spectrosc, 1997. **53A**(14): p. 2701-7.

76. Balaban, R.S., S. Nemoto, and T. Finkel, *Mitochondria, oxidants, and aging.* Cell, 2005. **120**(4): p. 483-95.

77. Lambert, A.J. and M.D. Brand, *Reactive oxygen species production by mitochondria.* Methods Mol Biol, 2009. **554**: p. 165-81.

78. Wang, D., H. Masutani, and J. Yodoi, *Are the properties of mitochondrial membranes redox regulated?* IUBMB Life, 2006. **58**(11): p. 670-3.

79. Wu, Z., J. Zhang, and B. Zhao, *Superoxide anion regulates the mitochondrial free Ca2+ through uncoupling proteins.* Antioxid Redox Signal, 2009. **11**(8): p. 1805-1818.

80. Kozlov, A.V., et al., *Different effects of endotoxic shock on the respiratory function of liver and heart mitochondria in rats.* Am J Physiol Gastrointest Liver Physiol, 2006. **290**(3): p. G543-9.

81. Staniek, K. and H. Nohl, *Are mitochondria a permanent source of reactive oxygen species?* Biochim Biophys Acta, 2000. **1460**(2-3): p. 268-75.

82. Kanai, A., et al., *Differing roles of mitochondrial nitric oxide synthase in cardiomyocytes and urothelial cells.* Am J Physiol Heart Circ Physiol, 2004. **286**(1): p. H13-21.

83. Goldstein, S. and G. Merenyi, *The chemistry of peroxynitrite: implications for biological activity.* Methods Enzymol, 2008. **436**: p. 49-61.

84. Pearce, L.L., et al., *Nitrosative stress results in irreversible inhibition of purified mitochondrial complexes I and III without modification of cofactors.* Nitric Oxide, 2005. **13**(4): p. 254-63.

85. Borutaite, V., et al., *Reversible inhibition of cellular respiration by nitric oxide in vascular inflammation.* Am J Physiol Heart Circ Physiol, 2001. **281**(6): p. H2256-60.

86. Berman, M.C., et al., *Autoxidation of soluble trypsin-cleaved microsomal ferrocytochrome b5 and formation of superoxide radicals.* Biochem J, 1976. **157**(1): p. 237-46.

87. Cassell, R.H. and I. Fridovich, *The role of superoxide radical in the autoxidation of cytochrome c.* Biochemistry, 1975. **14**(9): p. 1866-8.

88. Wallace, W.J., et al., *Mechanism of autooxidation for hemoglobins and myoglobins. Promotion of superoxide production by protons and anions.* J Biol Chem, 1982. **257**(9): p. 4966-77.

89. Mugnol, K.C., et al., *Spectroscopic, structural, and functional characterization of the alternative low-spin state of horse heart cytochrome C.* Biophys J, 2008. **94**(10): p. 4066-77.

90. Jones, M.G., et al., *A re-examination of the reactions of cyanide with cytochrome c oxidase.* Biochem J, 1984. **220**(1): p. 57-66.

91. Wilson, M.T., et al., *A plausible two-state model for cytochrome c oxidase.* Proc Natl Acad Sci U S A, 1981. **78**(11): p. 7115-8.

92. Carraway, A.D., M.G. McCollum, and J. Peterson, *Characterization of N-Acetylated Heme Undecapeptide and Some of Its Derivatives in Aqueous Media: Monomeric Model Systems for Hemoproteinss.* Inorganic Chemistry, 1996. **35**(23): p. 6885-6891.

93. Carraway, A.D., et al., *The Alkaline Transition of Bis(N-acetylated) Heme Undecapeptide.* Inorg Chem, 1998. **37**(18): p. 4654-4661.

94. Carraway, A.D., et al., *Monomeric ferric heme peptide derivatives: model systems for hemoproteins.* J Inorg Biochem, 1995. **60**(4): p. 267-76.

95. Rosell, F.R., J.C. Ferrer, and A.G. Mauk, *Proton-linked protein conformational switching: definition of the alkaline conformational transition of yeast iso-1-ferricytochrome c.* J Am Chem Soc, 1998. **120**: p. 11234-11245.

96. Cheesman, M.R., C. Greenwood, and A.J. Thomson, *Magnetic circular dichroism of hemoproteins.* Adv. Inorg. Chem., 1991. **36**: p. 201-55.

97. Gadsby, P.M.A. and A.J. Thomson, *Assignment of the axial ligands of ferric ion in low-spin hemoproteins by near-infrared magnetic circular dichroism and electron paramagnetic resonance spectroscopy.* Journal of the American Chemical Society, 1990. **112**: p. 5003-5011.

98. Gadsby, P.M., et al., *Identification of the ligand-exchange process in the alkaline transition of horse heart cytochrome c.* Biochem J, 1987. **246**(1): p. 43-54.

99. Rafferty, S.P., et al., *Electrochemical, kinetic, and circular dichroic consequences of mutations at position 82 of yeast iso-1-cytochrome c.* Biochemistry, 1990. **29**(40): p. 9365-9.

100. Orii, Y. and H. Shimada, *Reaction of cytochrome c with nitrite and nitric oxide. A model of dissimilatory nitrite reductase.* J Biochem, 1978. **84**(6): p. 1542-52.

101. Carraway, A.D., et al., *Characterization of heme c peptides by mass spectrometry.* J Inorg Biochem, 1993. **52**(3): p. 201-7.

102. Battistuzzi, G., et al., *Thermodynamics of the alkaline transition of cytochrome c.* Biochemistry, 1999. **38**(25): p. 7900-7.

103. Ferguson-Miller, S., D.L. Brautigan, and E. Margoliash, *Correlation of the kinetics of electron transfer activity of various eukaryotic cytochromes c with binding to mitochondrial cytochrome c oxidase.* J Biol Chem, 1976. **251**(4): p. 1104-15.

104. Sinjorgo, K.M., et al., *The effects of pH and ionic strength on cytochrome c oxidase steady-state kinetics reveal a catalytic and a non-catalytic interaction domain for cytochrome c.* Biochim Biophys Acta, 1986. **850**(1): p. 108-15.

105. Pearce, L.L., et al., *The catabolic fate of nitric oxide: the nitric oxide oxidase and peroxynitrite reductase activities of cytochrome oxidase.* J Biol Chem, 2002. **277**(16): p. 13556-62.

106. Sarti, P., et al., *Nitric oxide and cytochrome c oxidase: mechanisms of inhibition and NO degradation.* Biochem Biophys Res Commun, 2000. **274**(1): p. 183-7.

107. Feinberg, B.A., J.E. Bedore, Jr., and S. Ferguson-Miller, *Methionine-80-sulfoxide cytochrome c: preparation, purification and electron-transfer capabilities.* Biochim Biophys Acta, 1986. **851**(2): p. 157-65.

108. Ivanetich, K.M., J.J. Bradshaw, and G.V. Fazakerley, *Identification of the sixth ligand of methionine sulfoxide cytochrome c.* Biochem Biophys Res Commun, 1976. **72**(2): p. 433-9.

109. Berlett, B.S., R.L. Levine, and E.R. Stadtman, *Carbon dioxide stimulates peroxynitrite-mediated nitration of tyrosine residues and inhibits oxidation of methionine residues of glutamine synthetase: both modifications mimic effects of adenylylation.* Proc Natl Acad Sci U S A, 1998. **95**(6): p. 2784-9.

110. Hansel, A., et al., *Mitochondrial targeting of the human peptide methionine sulfoxide reductase (MSRA), an enzyme involved in the repair of oxidized proteins.* Faseb J, 2002. **16**(8): p. 911-3.

111. Rosell, F.I., et al., *Characterization of an alkaline transition intermediate stabilized in the Phe82Trp variant of yeast iso-1-cytochrome c.* Biochemistry, 2000. **39**(30): p. 9047-54.

112. Schonhoff, C.M., B. Gaston, and J.B. Mannick, *Nitrosylation of cytochrome c during apoptosis.* J Biol Chem, 2003. **278**(20): p. 18265-70.

113. Nakagawa, H., et al., *Nitration of specific tyrosine residues of cytochrome C is associated with caspase-cascade inactivation.* Biol Pharm Bull, 2007. **30**(1): p. 15-20.

114. Wang, W., et al., *Superoxide flashes in single mitochondria.* Cell, 2008. **134**(2): p. 279-90.

115. Hoffman, D.L., J.D. Salter, and P.S. Brookes, *Response of mitochondrial reactive oxygen species generation to steady-state oxygen tension: implications for hypoxic cell signaling.* Am J Physiol Heart Circ Physiol, 2007. **292**(1): p. H101-8.

116. Zielonka, J. and B. Kalyanaraman, *Hydroethidine- and MitoSOX-derived red fluorescence is not a reliable indicator of intracellular superoxide formation: another inconvenient truth.* Free Radic Biol Med, 2010. **48**(8): p. 983-1001.

117. Nohl, H., L. Gille, and K. Staniek, *Intracellular generation of reactive oxygen species by mitochondria.* Biochem Pharmacol, 2005. **69**(5): p. 719-23.

118. Baymann, F., et al., *Electrochemical and spectroscopic investigations of the cytochrome bc1 complex from Rhodobacter capsulatus.* Biochemistry, 1999. **38**(40): p. 13188-99.

119. Phillips, J.D., L.A. Graham, and B.L. Trumpower, *Subunit 9 of the Saccharomyces cerevisiae cytochrome bc1 complex is required for insertion of EPR-detectable iron-sulfur cluster into the Rieske iron-sulfur protein.* J Biol Chem, 1993. **268**(16): p. 11727-36.

120. Zhang, H., et al., *Exposing the complex III Qo semiquinone radical.* Biochim Biophys Acta, 2007. **1767**(7): p. 883-7.

121. Dopner, S., et al., *The structural and functional role of lysine residues in the binding domain of cytochrome c in the electron transfer to cytochrome c oxidase.* Eur J Biochem, 1999. **261**(2): p. 379-91.

122. Zielonka, J., M. Hardy, and B. Kalyanaraman, *HPLC study of oxidation products of hydroethidine in chemical and biological systems: ramifications in superoxide measurements.* Free Radic Biol Med, 2009. **46**(3): p. 329-38.

123. Cai, J. and D.P. Jones, *Superoxide in apoptosis. Mitochondrial generation triggered by cytochrome c loss.* J Biol Chem, 1998. **273**(19): p. 11401-4.

124. Harman, D., *Aging: a theory based on free radical and radiation chemistry.* J Gerontol, 1956. **11**(3): p. 298-300.

125. Rattan, S.I.S., *Theories of biological aging: Genes, proteins, and free radicals doi:10.1080/10715760600911303.* Free Radical Research, 2006. **40**(12): p. 1230-1238.

126. Valko, M., et al., *Free radicals and antioxidants in normal physiological functions and human disease.* The International Journal of Biochemistry & Cell Biology, 2007. **39**(1): p. 44-84.

127. Lu, C., et al., *Is Antioxidant Potential of the Mitochondrial Targeted Ubiquinone Derivative MitoQ Conserved in Cells Lacking mtDNA?* Antioxid Redox Signal, 2008. **10**(3): p. 651-660.

128. Abdollahi, M., et al., *Pesticides and oxidative stress: a review.* Med Sci Monit, 2004. **10**(6): p. RA141-7.

129. Moller, P., et al., *Air pollution, oxidative damage to DNA, and carcinogenesis.* Cancer Lett, 2008. **266**(1): p. 84-97.

130. Valavanidis, A., T. Vlachogianni, and K. Fiotakis, *Tobacco smoke: involvement of reactive oxygen species and stable free radicals in mechanisms of oxidative damage, carcinogenesis and synergistic effects with other respirable particles.* Int J Environ Res Public Health, 2009. **6**(2): p. 445-62.

131. Sun, J., et al., *Role of antioxidant enzymes on ionizing radiation resistance.* Free Radic Biol Med, 1998. **24**(4): p. 586-93.

132. Esterbauer, H., G. Wag, and H. Puhl, *Lipid peroxidation and its role in atherosclerosis.* Br Med Bull, 1993. **49**(3): p. 566-76.

133. Salonen, J.T., *The role of lipid peroxidation, antioxidants and pro-oxidants in atherosclerosis.* Acta Cardiol, 1993. **48**(5): p. 457-9.

134. Moreira, P.I., et al., *Oxidative stress mechanisms and potential therapeutics in Alzheimer disease.* J Neural Transm, 2005. **112**(7): p. 921-32.

135. Poulos, T.L., et al., *The crystal structure of cytochrome c peroxidase.* . Journal of Biological Chemistry 1980 **255** (2): p. 575-580

136. English, A.M. and G. Tsaprailis, *Catalytic Structure-Function Relationships in Heme Peroxidases Advances in Inorganic Chemistry*, A.G. Sykes, Editor. 1995, Academic Press. p. 79-125.

137. Smith, A.T. and N.C. Veitch, *Substrate binding and catalysis in heme peroxidases.* Current Opinion in Chemical Biology, 1998. **2**(2): p. 269-278.

138. Bindoli, A., J.M. Fukuto, and H.J. Forman, *Thiol Chemistry in Peroxidase Catalysis and Redox Signaling doi:10.1089/ars.2008.2063. Antioxidants & Redox Signaling, 2008. 10(9):* p. 1549-1564.

139. Floris, R., et al., *Interaction of myeloperoxidase with peroxynitrite. A comparison with lactoperoxidase, horseradish peroxidase and catalase.* Eur J Biochem, 1993. **215**(3): p. 767-75.

140. Gebicka, L. and J. Didik, *Catalytic scavenging of peroxynitrite by catalase.* Journal of Inorganic Biochemistry Special Issue Containing Contributions from the First Latin Ame - rican Meeting on Biological Inorganic Chemistry - LABIC 2008, 2009. 103(10):p. 1375-1379.

141. Sampson, J.B., et al., *Myeloperoxidase and horseradish peroxidase catalyze tyrosine nitration in proteins from nitrite and hydrogen peroxide.* Arch Biochem Biophys, 1998. **356**(2): p. 207-13.

142. Sampson, J.B., H. Rosen, and J.S. Beckman, *Peroxynitrite-dependent tyrosine nitration catalyzed by superoxide dismutase, myeloperoxidase, and horseradish peroxidase.* Methods Enzymol, 1996. **269**: p. 210-18.

143. Alayash, A.I., B.A. Ryan, and R.E. Cashon, *Peroxynitrite-mediated heme oxidation and protein modification of native and chemically modified hemoglobins.* Arch Biochem Biophys, 1998. **349**(1): p. 65-73.

144. Herold, S. and K. Shivashankar, *Metmyoglobin and Methemoglobin Catalyze the Isomerization of Peroxynitrite to Nitrateâ€* Biochemistry, 2003. **42**(47): p. 14036-14046.

145. Su, J. and J.T. Groves, *Mechanisms of Peroxynitrite Interactions with Heme Proteins.* Inorganic Chemistry, 2010. **49**(14): p. 6317-6329.

146. Su, J. and J.T. Groves, *Mechanisms of peroxynitrite interactions with heme proteins.* Inorg Chem, 2010. **49**(14): p. 6317-29.

147. Padmaja, S., G.L. Squadrito, and W.A. Pryor, *Inactivation of Glutathione Peroxidase by Peroxynitrite.* Arch Biochem Biophys, 1998. **349**(1): p. 1-6.

148. Arteel, G.E. and H. Sies, *Protection against peroxynitrite by cocoa polyphenol oligomers.* FEBS Lett, 1999. **462**(1-2): p. 167-70.

149. Batthyany, C., et al., *Time course and site(s) of cytochrome c tyrosine nitration by peroxynitrite.* Biochemistry, 2005. **44**(22): p. 8038-46.

150. Jang, B. and S. Han, *Biochemical properties of cytochrome c nitrated by peroxynitrite.* Biochimie, 2006. **88**(1): p. 53-8.

151. Souza, J.M., et al., *Nitrocytochrome c: synthesis, purification, and functional studies.* Methods Enzymol, 2008. **441**: p. 197-215.

152. Ascenzi, P., et al., *Cardiolipin modulates allosterically peroxynitrite detoxification by horse heart cytochrome c.* Biochemical and Biophysical Research Communications, 2011. **404**(1): p. 190-194.

153. Radi, R., A. Denicola, and B.A. Freeman, *Peroxynitrite reactions with carbon dioxide-bicarbonate.* Methods Enzymol, 1999. **301**: p. 353-67.

154. Badyal, S.K., et al., *Iron oxidation state modulates active site structure in a heme peroxidase.* Biochemistry, 2008. **47**(15): p. 4403-9.

155. Carraway, A.D., M.G. McCollum, and J. Peterson, *Characterization of N-Acetylated Heme Undecapeptide and Some of Its Derivatives in Aqueous Media: Monomeric Model Systems for Hemoproteinss.* Inorg Chem, 1996. **35**(23): p. 6885-6891.

156. Carraway, A.D., M.G. McCollum, and J. Peterson, *Characterization of N-Acetylated Heme Undecapeptide and Some of Its Derivatives in Aqueous Media: Monomeric Model Systems for Hemoproteins.* Inorg Chem, 1996. **35**(23): p. 6885-6891.

157. Stuehr, D.J., et al., *Activated murine macrophages secrete a metabolite of arginine with the bioactivity of endothelium-derived relaxing factor and the chemical reactivity of nitric oxide.* J Exp Med, 1989. **169**(3): p. 1011-20.

158. Han, D., E. Williams, and E. Cadenas, *Mitochondrial respiratory chain-dependent generation of superoxide anion and its release into the intermembrane space.* Biochem J, 2001. **353**(Pt 2): p. 411-6.

159. Han, D., et al., *Voltage-dependent anion channels control the release of the superoxide anion from mitochondria to cytosol.* J Biol Chem, 2003. **278**(8): p. 5557-63.

160. Romero, N., et al., *Diffusion of peroxynitrite in the presence of carbon dioxide.* Arch Biochem Biophys, 1999. **368**(1): p. 23-30.

161. Kanai, A.J., et al., *Beta-adrenergic regulation of constitutive nitric oxide synthase in cardiac myocytes.* Am J Physiol, 1997. **273**(4 Pt 1): p. C1371-7.

162. Kanai, A.J., et al., *Identification of a neuronal nitric oxide synthase in isolated cardiac mitochondria using electrochemical detection.* Proc Natl Acad Sci U S A, 2001. **98**(24): p. 14126-31.

163. Boveris, A. and E. Cadenas, *Mitochondrial production of superoxide anions and its relationship to the antimycin insensitive respiration.* FEBS Lett, 1975. **54**(3): p. 311-4.

164. Radi, R., et al., *Peroxynitrite reactions and formation in mitochondria.* Free Radic Biol Med, 2002. **33**(11): p. 1451-64.

165. Linares, E., et al., *Role of peroxynitrite in macrophage microbicidal mechanisms in vivo revealed by protein nitration and hydroxylation.* Free Radic Biol Med, 2001. **30**(11): p. 1234-42.

166. McCord, J.M. and I. Fridovich, *Superoxide dismutase: the first twenty years (1968-1988).* Free Radic Biol Med, 1988. **5**(5-6): p. 363-9.

167. Borgstahl, G.E., et al., *The structure of human mitochondrial manganese superoxide dismutase reveals a novel tetrameric interface of two 4-helix bundles.* Cell, 1992. **71**(1): p. 107-18.

168. Keller, J.N., et al., *Mitochondrial manganese superoxide dismutase prevents neural apoptosis and reduces ischemic brain injury: suppression of peroxynitrite production, lipid peroxidation, and mitochondrial dysfunction.* J Neurosci, 1998. **18**(2): p. 687-97.

169. Filipovic, D., et al., *Acute and/or chronic stress models modulate CuZnSOD and MnSOD protein expression in rat liver.* Mol Cell Biochem, 2010. **338**(1-2): p. 167-74.

170. Gnaiger, E., *Oxygen conformance of cellular respiration. A perspective of mitochondrial physiology.* Adv Exp Med Biol, 2003. **543**: p. 39-55.

171. Goldstein, S., J. Lind, and G. Merenyi, *The reaction of ONOO- with carbonyls: Estimation of the half-lives of ONOOC(O)O- and O2NOOC(O)O.* Journal of the Chemical Society, Dalton Transactions, 2002(5): p. 808-810.

172. Xia, Y., *Superoxide Generation from Nitric Oxide Synthases.* Antioxid Redox Signal, 2007. **9**(10): p. 1773-1778.

173. Griffith, B., et al., *NOX enzymes and pulmonary disease.* Antioxid Redox Signal, 2009. **11**(10): p. 2505-16.

174. Tsan, M.F., et al., *Susceptibility of heterozygous MnSOD gene-knockout mice to oxygen toxicity.* Am J Respir Cell Mol Biol, 1998. **19**(1): p. 114-20.

175. Anderson, C.P., et al., *Depletion of glutathione by buthionine sulfoxine is cytotoxic for human neuroblastoma cell lines via apoptosis.* Exp Cell Res, 1999. **246**(1): p. 183-92.

176. Lee, K.E., R.D. Mayer, and A.T. Cockett, *Effect of systemic glutathione depletion by buthionine sulfoximine on sensitivity of murine bladder cancer to cytotoxic agents.* Urology, 1989. **34**(6): p. 376-80.

177. Gardner, P.R., *Aconitase: sensitive target and measure of superoxide.* Methods Enzymol, 2002. **349**: p. 9-23.

178. Nisoli, E., et al., *Mitochondrial biogenesis in mammals: the role of endogenous nitric oxide.* Science, 2003. **299**(5608): p. 896-9.

179. Nisoli, E., et al., *Mitochondrial biogenesis by NO yields functionally active mitochondria in mammals.* Proc Natl Acad Sci U S A, 2004. **101**(47): p. 16507-12.

180. Nisoli, E. and M.O. Carruba, *Nitric oxide and mitochondrial biogenesis.* J Cell Sci, 2006. **119**(Pt 14): p. 2855-62.

181. Modlinger, P.S., C.S. Wilcox, and S. Aslam, *Nitric oxide, oxidative stress, and progression of chronic renal failure.* Seminars in Nephrology, 2004. **24**(4): p. 354-365.

182. Jeremy, J.Y., et al., *Oxidative Stress, Nitric Oxide, and Vascular Disease.* Journal of Cardiac Surgery, 2001. **17**(4): p. 324-327.

183. Sergent, O., et al., *Effect of nitric oxide on iron-mediated oxidative stress in primary rat hepatocyte culture.* Hepatology, 1997. **25**(1): p. 122-127.

184. Stitt-Fischer, M.S., et al., *Manganese Superoxide Dismutase is not Protective in Bovine Pulmonary Artery Endothelial Cells at Systemic Oxygen Levels.* Radiat Res, 2010. **174**(6): p. 679-90.

185. Ferrari, L.A., et al., *Hydrogen cyanide and carbon monoxide in blood of convicted dead in a polyurethane combustion: a proposition for the data analysis.* Forensic Sci Int, 2001. **121**(1-2): p. 140-3.

186. Alarie, Y., *Toxicity of fire smoke.* Crit Rev Toxicol, 2002. **32**(4): p. 259-89.

187. Alcorta, R., *Smoke inhalation & acute cyanide poisoning. Hydrogen cyanide poisoning proves increasingly common in smoke-inhalation victims.* JEMS, 2004. **29**(8): p. suppl 6-15; quiz suppl 16-7.

188. Yeoh, M.J. and G. Braitberg, *Carbon monoxide and cyanide poisoning in fire related deaths in Victoria, Australia.* J Toxicol Clin Toxicol, 2004. **42**(6): p. 855-63.

189. Wardaszka, Z., et al., *[Levels of carbon monoxide and hydrogen cyanide in blood of fire victims in the autopsy material of the Department of Forensic Medicine, Medical University of Bialystok].* Arch Med Sadowej Kryminol, 2005. **55**(2): p. 130-3.

190. Eckstein, M. and P.M. Maniscalco, *Focus on smoke inhalation--the most common cause of acute cyanide poisoning.* Prehosp Disaster Med, 2006. **21**(2): p. s49-55.

191. Pitt, B.R., et al., *Interaction of carbon monoxide and cyanide on cerebral circulation and metabolism.* Arch Environ Health, 1979. **34**(5): p. 345-9.

192. Norris, J.C., S.J. Moore, and A.S. Hume, *Synergistic lethality induced by the combination of carbon monoxide and cyanide.* Toxicology, 1986. **40**(2): p. 121-9.

193. Moore, S.J., I.K. Ho, and A.S. Hume, *Severe hypoxia produced by concomitant intoxication with sublethal doses of carbon monoxide and cyanide.* Toxicol Appl Pharmacol, 1991. **109**(3): p. 412-20.

194. Mendelman, A., et al., *Blood flow and ionic responses in the awake brain due to carbon monoxide.* Neurol Res, 2002. **24**(8): p. 765-72.

195. Gunasekar, P.G., J.L. Borowitz, and G.E. Isom, *Cyanide-induced generation of oxidative species: involvement of nitric oxide synthase and cyclooxygenase-2.* J Pharmacol Exp Ther, 1998. **285**(1): p. 236-41.

196. Leavesley, H.B., et al., *Interaction of cyanide and nitric oxide with cytochrome c oxidase: implications for acute cyanide toxicity.* Toxicol Sci, 2008. **101**(1): p. 101-11.

197. Jensen, M.S., N.C. Nyborg, and E.S. Thomsen, *Various nitric oxide donors protect chick embryonic neurons from cyanide-induced apoptosis.* Toxicol Sci, 2000. **58**(1): p. 127-34.

198. Yoshikawa, S., K. Shinzawa-Itoh, and T. Tsukihara, *Crystal structure of bovine heart cytochrome c oxidase at 2.8 A resolution.* J Bioenerg Biomembr, 1998. **30**(1): p. 7-14.

199. Brudvig, G.W., T.H. Stevens, and S.I. Chan, *Reactions of nitric oxide with cytochrome c oxidase.* Biochemistry, 1980. **19**(23): p. 5275-85.

200. Hill, B.C., *The pathway of CO binding to cytochrome c oxidase. Can the gateway be closed?* FEBS Lett, 1994. **354**(3): p. 284-8.

201. Pearce, L.L., et al., *Reversal of cyanide inhibition of cytochrome c oxidase by the auxiliary substrate nitric oxide: an endogenous antidote to cyanide poisoning?* J Biol Chem, 2003. **278**(52): p. 52139-45.

202. Gibson, Q.H., G. Palmer, and D.C. Wharton, *The Binding of Carbon Monoxide by Cytochrome C Oxidase and the Ratio of the Cytochromes a and A3.* J Biol Chem, 1965. **240**: p. 915-20.

203. van Gelder, B.F., *On cytochrome c oxidase. I. The extinction coefficients of cytochrome a and cytochrome a3.* Biochim Biophys Acta, 1966. **118**(1): p. 36-46.

204. Sinjorgo, K.M., et al., *Bovine cytochrome c oxidases, purified from heart, skeletal muscle, liver and kidney, differ in the small subunits but show the same reaction kinetics with cytochrome c.* Biochim Biophys Acta, 1987. **893**(2): p. 251-8.

205. Ford, P.C., D.A. Wink, and D.M. Stanbury, *Autoxidation kinetics of aqueous nitric oxide.* FEBS Lett, 1993. **326**(1-3): p. 1-3.

206. Lewis, R.S. and W.M. Deen, *Kinetics of the reaction of nitric oxide with oxygen in aqueous solutions.* Chem Res Toxicol, 1994. **7**(4): p. 568-74.

207. Antonini, E. and M. Brunori, *Hemoglobin and Myoglobin in Their Reactions with Ligands*. 1971, NorthHolland Publishing Co.: Amsterdam. p. 40-54.

208. Iheagwara, K.N., et al., *Myocardial cytochrome oxidase activity is decreased following carbon monoxide exposure.* Biochim Biophys Acta, 2007. **1772**(9): p. 1112-6.

209. Eglinton, D.G., et al., *Near-infrared magnetic and natural circular dichroism of cytochrome c oxidase.* Biochem J, 1980. **191**(2): p. 319-31.

210. Jensen, P., et al., *Cyanide inhibition of cytochrome c oxidase. A rapid-freeze e.p.r. investigation.* Biochem J, 1984. **224**(3): p. 829-37.

211. Einarsdottir, O., et al., *Photodissociation and recombination of carbonmonoxy cytochrome oxidase: dynamics from picoseconds to kiloseconds.* Biochemistry, 1993. **32**(45): p. 12013-24.

212. Fago, A., et al., *The case of the missing NO-hemoglobin: spectral changes suggestive of heme redox reactions reflect changes in NO-heme geometry.* Proc Natl Acad Sci U S A, 2003. **100**(21): p. 12087-92.

213. Baskin, S.I., E.W. Nealley, and J.C. Lempka, *Cyanide toxicity in mice pretreated with diethylamine nitric oxide complex.* Hum Exp Toxicol, 1996. **15**(1): p. 13-18.

214. Pettersen, J.C. and S.D. Cohen, *The effects of cyanide on brain mitochondrial cytochrome oxidase and respiratory activities.* J Appl Toxicol, 1993. **13**(1): p. 9-14.

215. Davey, G.P., S. Peuchen, and J.B. Clark, *Energy thresholds in brain mitochondria. Potential involvement in neurodegeneration.* J Biol Chem, 1998. **273**(21): p. 12753-7.

216. Mazat, J.P., et al., *Metabolic control analysis and threshold effect in oxidative phosphorylation: implications for mitochondrial pathologies.* Mol Cell Biochem, 1997. **174**(1-2): p. 143-8.

217. Giuffre, A., et al., *Reaction of nitric oxide with the turnover intermediates of cytochrome c oxidase: reaction pathway and functional effects.* Biochemistry, 2000. **39**(50): p. 15446-53.

218. Cooper, C.E., *Nitric oxide and cytochrome oxidase: substrate, inhibitor or effector?* Trends Biochem Sci, 2002. **27**(1): p. 33-9.

219. Torres, J., et al., *Cytochrome c oxidase rapidly metabolises nitric oxide to nitrite.* FEBS Lett, 2000. **475**(3): p. 263-6.

220. Borisov, V.B., et al., *Nitric oxide reacts with the ferryl-oxo catalytic intermediate of the CuB-lacking cytochrome bd terminal oxidase.* FEBS Lett, 2006. **580**(20): p. 4823-6.

221. Litovitz, T., *The use of oxygen in the treatment of acute cyanide poisoning.*, in *In clinical and experimental toxicology of cyanides, B.B.T.C. Marrs, Editor. 1987, Wright Pub. :* Bristol. p. 467-472.

222. Isom, G.E. and J.L. Way, *Effects of oxygen on the antagonism of cyanide intoxication: cytochrome oxidase, in vitro.* Toxicol Appl Pharmacol, 1984. **74**(1): p. 57-62.

223. Way, J.L., et al., *The mechanism of cyanide intoxication and its antagonism.* Ciba Found Symp, 1988. **140**: p. 232-43.

224. Dejam, A., et al., *Emerging role of nitrite in human biology.* Blood Cells Mol Dis, 2004. **32**(3): p. 423-9.

225. Moreno, S.N., et al., *Oxidation of cyanide to the cyanyl radical by peroxidase/H2O2 systems as determined by spin trapping.* Arch Biochem Biophys, 1988. **265**(2): p. 267-71.

226. Stolze, K., S.N. Moreno, and R.P. Mason, *Free radical intermediates formed during the oxidation of cyanide by horseradish peroxidase/H2O2 as detected with nitroso spin traps.* J Inorg Biochem, 1989. **37**(1): p. 45-53.

227. Miro, O., et al., *Mitochondrial cytochrome c oxidase inhibition during acute carbon monoxide poisoning.* Pharmacol Toxicol, 1998. **82**(4): p. 199-202.

228. Alonso, J.R., et al., *Carbon monoxide specifically inhibits cytochrome c oxidase of human mitochondrial respiratory chain.* Pharmacol Toxicol, 2003. **93**(3): p. 142-6.

229. Thom, S.R. and H. Ischiropoulos, *Mechanism of oxidative stress from low levels of carbon monoxide.* Res Rep Health Eff Inst, 1997(80): p. 1-19; discussion 21-7.

230. Thom, S.R., et al., *Role of nitric oxide-derived oxidants in vascular injury from carbon monoxide in the rat.* Am J Physiol, 1999. **276**(3 Pt 2): p. H984-92.

231. Brown, G.C. and V. Borutaite, *Inhibition of mitochondrial respiratory complex I by nitric oxide, peroxynitrite and S-nitrosothiols.* Biochim Biophys Acta, 2004. **1658**(1-2): p. 44-9.

232. Panov, A., et al., *Rotenone model of Parkinson disease: multiple brain mitochondria dysfunctions after short term systemic rotenone intoxication.* J Biol Chem, 2005. **280**(51): p. 42026-35.

233. Cammack, R., et al., *Applications of electron paramagnetic resonance spectroscopy to study interactions of iron proteins in cells with nitric oxide.* Spectrochim Acta A Mol Biomol Spectrosc, 1998. **54A**(14): p. 2393-402.

234. Beinert, H. and M.C. Kennedy, *Aconitase, a two-faced protein: enzyme and iron regulatory factor.* Faseb J, 1993. **7**(15): p. 1442-9.

235. Shigenaga, M.K., T.M. Hagen, and B.N. Ames, *Oxidative damage and mitochondrial decay in aging.* Proc Natl Acad Sci U S A, 1994. **91**(23): p. 10771-8.

236. Berlett, B.S. and E.R. Stadtman, *Protein oxidation in aging, disease, and oxidative stress.* J Biol Chem, 1997. **272**(33): p. 20313-6.

237. Boczkowski, J., et al., *Peroxynitrite-mediated mitochondrial dysfunction.* Biol Signals Recept, 2001. **10**(1-2): p. 66-80.

238. Koppenol, W.H., et al., *Peroxynitrite, a cloaked oxidant formed by nitric oxide and superoxide.* Chem Res Toxicol, 1992. **5**(6): p. 834-42.

239. Radi, R., et al., *Peroxynitrite oxidation of sulfhydryls. The cytotoxic potential of superoxide and nitric oxide.* J Biol Chem, 1991. **266**(7): p. 4244-50.

240. Augusto, O., et al., *EPR detection of glutathiyl and hemoglobin-cysteinyl radicals during the interaction of peroxynitrite with human erythrocytes.* Biochemistry, 2002. **41**(48): p. 14323-8.

241. Beinert, H., *Spectroscopy of succinate dehydrogenases, a historical perspective.* Biochim Biophys Acta, 2002. **1553**(1-2): p. 7-22.

242. Singer, T.P. and M.K. Johnson, *The prosthetic groups of succinate dehydrogenase: 30 years from discovery to identification.* FEBS Lett, 1985. **190**(2): p. 189-98.

243. Chevallet, M., et al., *Two EPR-detectable [4Fe-4S] clusters, N2a and N2b, are bound to the NuoI (TYKY) subunit of NADH:ubiquinone oxidoreductase (Complex I) from Rhodobacter capsulatus.* Biochim Biophys Acta, 2003. **1557**(1-3): p. 51-66.

244. Beinert, H. and A.J. Thomson, *Three-iron clusters in iron-sulfur proteins.* Arch Biochem Biophys, 1983. **222**(2): p. 333-61.

245. Pearce, L.L., et al., *Identification of respiratory complexes I and III as mitochondrial sites of damage following exposure to ionizing radiation and nitric oxide.* Nitric Oxide, 2001. **5**(2): p. 128-36.

246. Castro, L., M. Rodriguez, and R. Radi, *Aconitase is readily inactivated by peroxynitrite, but not by its precursor, nitric oxide.* J Biol Chem, 1994. **269**(47): p. 29409-15.

247. Johnson, M.K., et al., *Magnetic circular dichroism studies of succinate dehydrogenase. Evidence for [2Fe-2S], [3Fe-xS], and [4Fe-4S] centers in reconstitutively active enzyme.* J Biol Chem, 1985. **260**(12): p. 7368-78.

248. Hughes, M.N. and H.G. Nicklin, *The chemistry of pernitrites. Part I. Kinetics of decomposition of pernitrous acid.* Journal of the Chemical Society A: Inorganic, Physical, Theoretical, 1968: p. 450-452.

249. Ackrell, B.A., *Progress in understanding structure-function relationships in respiratory chain complex II.* FEBS Lett, 2000. **466**(1): p. 1-5.

250. Cecchini, G., *Function and structure of complex II of the respiratory chain.* Annu Rev Biochem, 2003. **72**: p. 77-109.

251. Gardner, P.R., et al., *Nitric oxide sensitivity of the aconitases.* J Biol Chem, 1997. **272**(40): p. 25071-6.

252. Kennedy, M.C., W.E. Antholine, and H. Beinert, *An EPR investigation of the products of the reaction of cytosolic and mitochondrial aconitases with nitric oxide.* J Biol Chem, 1997. **272**(33): p. 20340-7.

253. Gardner, P.R., et al., *Superoxide radical and iron modulate aconitase activity in mammalian cells.* J Biol Chem, 1995. **270**(22): p. 13399-405.

254. Echtay, K.S., et al., *Superoxide activates mitochondrial uncoupling protein 2 from the matrix side. Studies using targeted antioxidants.* J Biol Chem, 2002. **277**(49): p. 47129-35.

255. Peterson, J., A.J. Kanai, and L.L. Pearce, *A mitochondrial role for catabolism of nitric oxide in cardiomyocytes not involving oxymyoglobin.* Am J Physiol Heart Circ Physiol, 2004. **286**(1): p. H55-8.

256. Han, D., et al., *Sites and mechanisms of aconitase inactivation by peroxynitrite: modulation by citrate and glutathione.* Biochemistry, 2005. **44**(36): p. 11986-96.

257. Beinert, H., M.C. Kennedy, and C.D. Stout, *Aconitase as Ironminus signSulfur Protein, Enzyme, and Iron-Regulatory Protein.* Chem Rev, 1996. **96**(7): p. 2335-2374.

258. Beinert, H., et al., *Iron-sulfur stoichiometry and structure of iron-sulfur clusters in three-iron proteins: evidence for [3Fe-4S] clusters.* Proc Natl Acad Sci U S A, 1983. **80**(2): p. 393-6.

259. Bulteau, A.L., M. Ikeda-Saito, and L.I. Szweda, *Redox-dependent modulation of aconitase activity in intact mitochondria.* Biochemistry, 2003. **42**(50): p. 14846-55.

260. Ackrell, B.A., *Cytopathies involving mitochondrial complex II.* Mol Aspects Med, 2002. **23**(5): p. 369-84.